# Balancing WNT signaling in early forebrain development

Inaugural-Dissertation

to obtain the academic degree
Doctor rerum naturalium (Dr. rer. nat.)

submitted to the Department of Biology, Chemistry, Pharmacy
of Freie Universität Berlin

by

**Shuang Geng**

Berlin, April 25th 2023

The work was carried under the supervision of Dr. rer. nat. Annette Hammes-Lewin, during the period from Aug 2018 to Dec 2022 at the Max Delbrück Center for Molecular Medicine in the Helmholtz Association, Berlin-Buch

1st reviewer: **Dr. Annette Hammes-Lewin**

Max Delbrück Center for Molecular Medicine

2nd reviewer: **Prof. Dr. Ursula Koch**

Department of Biology, Chemistry, Pharmacy

Freie Universität Berlin

Date of defense: 30th August 2023

**Acknowledgment**

I would like to express my deepest appreciation to Dr Annette Hammes for her inspiration, supervision and mentorship during my PhD work, which helped me to become an independent scientist. Special thanks to CSC council and MDC institute for providing me with funding and support necessary to pursue my PhD. I treasure this chance very much. I am also thankful to the Advanced Light Microscopy technology platform at the MDC, particularly Dr. Anje Sporbert and Dr. Sandra Raimundo, for their expert guidance and support with confocal microscopy.

I had the pleasure of working with all the colleagues from the Hammes, Lewin and Hörnberg groups, and I am grateful to all of them for their assistance and support throughout the years. Lastly, I'd like to say thanks to my friends and my family.

**Declaration of Independence:**

Herewith I certify that I have prepared and written my thesis independently and that I have not used any sources and aids other than those indicated by me.

**List of publications**

**Shuang Geng**[*], Fabian Paul[*], Izabela Kowalczyk, Sandra Raimundo, Anje Sporbert, Tamrat Meshka Mamo[#] and Annette Hammes[#] (2023). Balancing WNT signaling in early forebrain development: The role of LRP4 as a modulator of LRP6 function. Frontiers in Cell and Developmental Biology 11:1173688. DOI:10.3389/fcell.2023.1173688

* These authors contributed equally to this work and share first authorship

# Corresponding author

# Contents

**List of abbreviations**

| Abbreviations | Definition |
|---|---|
| AChR | Acetylcholine receptor |
| APC | Adenomatous polyposis coli |
| BMP | Bone morphogenetic protein |
| BSA | Bovine serum albumin |
| CNS | Central nervous system |
| Dkk1 | Dickkopf WNT signaling pathway inhibitor 1 |
| DMSO | Dimethyl sulfoxide |
| Dvl | Activating the disheveled proteins |
| EDTA | Ethylenediaminetetraacetic acid |
| EGF | Epidermal growth factor |
| FCS | Fetal Bovine Serum |
| FZD | Frizzled |
| GSK3 | Glycogen synthase kinase 3 |
| HBSS | Hank's Balanced Salt Solution |
| IHC | Immunohistochemistry |
| LDL | Low-density lipoprotein |
| LDLR | Low-density lipoprotein receptor |
| LEF1 | Lymphoid enhancer factor 1 |
| LRP | Low-density lipoprotein receptors |
| MPM-2 | Mitotic protein monoclonal 2 |
| MuSK | Muscle-specific kinase |
| NE | Neuroepithelia |
| NMJ | Neuromuscular junction |
| NPCs | Neural progenitor cells |
| NTC | Neural tube closure |
| NTD | Neural tube defect |
| PBS | Phosphate-buffered saline |
| PFA | Paraformaldehyde |

| | |
|---|---|
| pHH3 | phospho-histone-H3 |
| RIPA | Radioimmunoprecipitation assay |
| RNAi | RNA interference |
| RT | Room temperature |
| SHH | Sonic hedgehog |
| Sostdc1 | Sclerostin domain containing 1/Wise |
| SOX2 | SRY-box 2 |
| TCF/LEF | T-cell factor/lymphoid enhancer binding factor |
| WNT | Wingless-related integration site |

## Abstract

During early forebrain development, the establishment of the regional identity of neural progenitor cells (NPCs) relies on the integration of signals from multiple signaling centers, including the WNT signaling pathway. WNT pathway is essential for embryonic development and is regulated by LDL receptor related proteins (LRPs), which act as co-receptors of frizzled. While the LRP family member - LRP5 and LRP6 are well known as co-receptors of frizzled, acting as the main receptor of WNT3a. Recent evidence suggests that LRP4 also plays a role in the central nervous system.

My aim is to shed light on the common and distinct functions of LRP4 and LRP6 and the interactions between LRP4/6 linked to the WNT pathway during early forebrain development. To achieve this, a genetic approach was used to analyze the forebrain development of LRP4-, LRP6-deficient mouse embryos, as well as *Lrp4*$^{-/-}$; *Lrp6*$^{-/-}$ double mutant mouse embryos at E9.5. High-resolution immunofluorescence imaging, cell culture models and molecular biology approaches were employed to investigate the effects of genetic inactivation of LRP4 and LRP6 on canonical WNT activity, mitotic activity of forebrain neuronal precursors, and the development of NTDs.

The results of this study indicate that loss of LRP6 can lead to a developmental disorder in E9.5 embryos, such as caudal truncation, neural tube defects (NTDs) and forebrain hypoplasia. Importantly, loss of LRP4 can partially rescue these deficits in *Lrp6* null mutants. Specially, caudal truncation and impaired mitotic activity of forebrain neuronal precursors observed in *Lrp6*$^{-/-}$ mutants were rescued in *Lrp4*$^{-/-}$; *Lrp6*$^{-/-}$ double mutants. However, cranial NTDs in LRP6-deficient mice were not ameliorated by genetic ablation of *Lrp4*. Additionally, it was demonstrated that genetic inactivation of LRP4 rescued impaired canonical WNT activity and the downstream targets in *Lrp6*$^{-/-}$ mutants. Moreover, the data suggest that LRP4 and LRP6 also influence the proliferation of human retinal pigment epithelial (hTERT RPE-1) cells in cell culture, adding to their roles in embryonic development. Furthermore, the study revealed that LRP4 modulates LRP6-dependent WNT signaling in a more general context, as demonstrated in hTERT RPE-1 cells.

Overall, these results highlight the important and complex role of LRP4 and LRP6 in forebrain development and WNT signaling regulation. The findings suggest that LRP4

acts as a negative regulator of LRP6-mediated canonical WNT signaling and plays a critical role in the regulation of mitotic activity of neuronal precursors in the early developing forebrain. Additionally, the results suggest that LRP5 or an as-yet undetermined receptor can compensate for the loss of LRP6 as an FZD co-receptor in the absence of LRP4. These findings provide new insights into the molecular mechanisms that regulate forebrain development and may have implications for the understanding and treatment of developmental disorders.

**Zusammenfassung**

Um die regionale Identität neuraler Vorläuferzellen (NPCs) während der frühen Entwicklung des Vorderhirns festzulegen, ist die präzise Regulation von Signalwegen, einschließlich des WNT-Signalwegs, entscheidend. LRPs (LDL-Rezeptor-verwandte Proteine) sind essentiell für die WNT-Signalübertragung und spielen daher eine wichtige Rolle in der frühen Entwicklung des embryonalen Vorderhirns. LRP5 und LRP6 sind als Korezeptoren von Frizzled bekannt, die als Hauptrezeptoren von WNT3a fungieren. Jüngste Erkenntnisse deuten darauf hin, dass auch LRP4 im zentralen Nervensystem eine Rolle spielt. Mein Ziel ist es, die gemeinsamen und unterschiedlichen Funktionen von LRP4 und LRP6 und die Wechselwirkungen zwischen LRP4/6, die mit dem WNT-Weg während der frühen Entwicklung des Vorderhirns verbunden sind, zu untersuchen. In meinem Projekt habe ich einen genetischen Ansatz gewählt, um die Entwicklung des Vorderhirns von LRP4-, LRP6-defizienten Mausembryonen, sowie *Lrp4*$^{-/-}$; *Lrp6*$^{-/-}$ Doppelmutanten zu frühen Embryonalstadien kurz nach der Neurulation zu untersuchen. Unter Anwendung von Mausgenetik, hochauflösender Immunfluoreszenz-Bildgebung, Zellkulturmodellen und molekularbiologischen Ansätzen konnte ich folgende Ergebnisse zeigen: Der Verlust von LRP6 kann zu Entwicklungsstörungen bei E9.5-Embryonen führen, wie z.B. kaudale Verkürzung der Körperachse, Neuralrohrdefekte (NTDs) und Vorderhirnhypoplasie. Wichtig ist, dass der Verlust von LRP4 diese Defizite in *Lrp6*-Nullmutanten teilweise beheben kann. Insbesondere wurde die kaudale Verkürzung und beeinträchtigte mitotische Aktivität von neuronalen Vorläufern des Vorderhirns, die bei *Lrp6*$^{-/-}$ Mutanten beobachtet wurden, bei *Lrp4*$^{-/-}$; *Lrp6*$^{-/-}$ Doppelmutanten gerettet. Jedoch wurden kraniale NTDs in LRP6-defizienten Mäusen nicht durch genetische Ablation von Lrp4 beeinflusst. Weiterhin konnte ich zeigen, dass die genetische Inaktivierung von LRP4 die beeinträchtigte kanonische WNT-Aktivität in *Lrp6*$^{-/-}$ Mutanten rettete. Über den Kontext der Entwicklung des Vorderhirns hinaus konnte ich zeigen, dass LRP4 die LRP6-abhängige WNT-Signalübertragung in einem allgemeineren Kontext moduliert, d. h., in humanen pigmentierten Retina Epithelzellen (hTERT RPE-1).

Basierend auf den Ergebnissen dieser Studie schlussfolgere ich, dass LRP4 ein negativer Regulator der LRP6-vermittelten kanonischen WNT-Signalgebung ist, der die mitotische Aktivität von neuronalen Vorläufern im sich früh entwickelnden

Vorderhirn reguliert. Ferner schlussfolgern wir, dass LRP5 oder ein noch unbestimmter Rezeptor den Verlust von LRP6 als FZD-Korezeptor in Abwesenheit von LRP4 kompensieren kann.

# 1. Introduction

## 1.1 Early morphogenetic events during forebrain development

### 1.1.1 Neurulation processes during forebrain development

The adult mammalian forebrain is one of the most complex structures. The forebrain comprises the telencephalon and the diencephalon, which are the most anterior segments of the mammalian brain. This division of the brain is essential for processing sensory information, perception, memory, emotions, conscious thinking and controlling motor activity.

Neurulation is the process of forming the neural tube from the neural plate, which will eventually become the brain and spinal cord. During this process, neuroepithelial cells in the neural plate receive signals from the surrounding tissue to proliferate and to undergo cell shape changes. These early patterning and morphogenesis events allow the neural plate to invaginate and bend dorsally to form a U-shaped neural groove. Then the lateral borders of neural groove elevate into the neural folds. Finally, the neural folds are brought together at the dorsal midline to form the neural tube (Dennis et al., 2016; Sadler, 2005) (Figure 1). In mice embryo, neural tube closure (NTC) normally starts at around embryonic day E8.5, and at E10.5 the process is completed with the closure of the posterior neuropore (Mao et al., 2010). Neural tube closure progresses in a rostral direction to form the neural tube into the future brain, and simultaneously in a caudal direction along the future spinal cord (Copp & Greene, 2013). Neural progenitor cells (NPCs) in the developing neocortex are essential for this process (Da Silva et al., 2021). The NPCs constitute the predominant part of neural plate during neurulation. The proliferation, differentiation, and cell survival of NPCs need to be precisely controlled to coordinate the process of neural tube closure. Deregulation of these cell behaviors leads to disturbances such as open neural tube defects (S.-L. Yang et al., 2015). By E12.5, neuron differentiation begins in the cortex, and the progenitor cells, which are adjacent to the ventricles, are regionally specified. This process will produce excitatory neurons in the dorsal cortex, followed by with oligodendrocytes and astrocytes (Harrison-Uy & Pleasure, 2012).

There are three vesicles that raise from the early neural tube: the hindbrain derives from the rhombencephalon; the midbrain originates from the early mesencephalon; the forebrain encompasses the prosencephalon (Dennis et al., 2016). By the end of somitogenesis, forebrain comprises the dorsally positioned telencephalon and eyes, the ventrally positioned hypothalamus, and the more caudally located diencephalon (Wilson & Houart, 2009).

Despite its complexity, the forebrain is raised from a simple layer of neuroepithelial cells, which is derived from the anterior neuroectoderm (Wilson & Houart, 2009; Xing et al., 2021). Live imaging reveals that neuroepithelial cells organize into tetrads and multicellular rosettes as the anterior-posterior oriented junctions contract (Nikolopoulou et al., 2017). In the course of neuroepithelial cell cycle, the cell nuclei migrates along the apical-basal-axis (Wodarz & Huttner, 2003). The proliferation and differentiation of progenitor cells is regulated by multiple pathways, including receptor tyrosine kinases (RTKs), Notch, Hedgehog (HH), TGFβ and WNT signaling pathway (Guo & Xing, 2022).

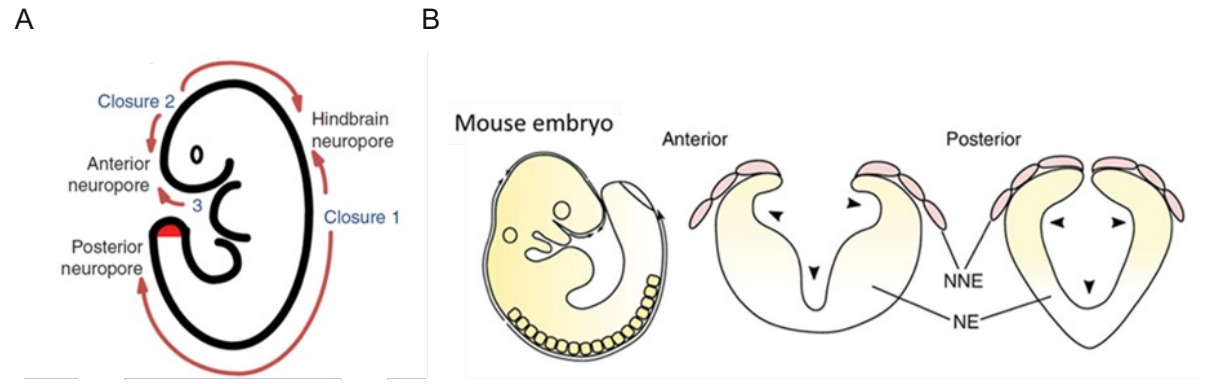


Figure 1: Schematic summary of neurulation and neural tube closure in mouse embryo.

(A) In mice, closure is completed sequentially at the anterior neuropore, hindbrain neuropore, and posterior neuropore. The initial neutral tube closure event (closure 1) starts at the hindbrain/cervical boundary and closure spreads bidirectionally from this site. Closure 2 begins at the forebrain/ midbrain boundary. Closure 3 occurs at the rostral end of the anterior neuropore, closure spreading caudally from here. (B) Key features of neurulation of mouse embryos. The arrows indicate the directions of closure. The arrows in indicate directions of closure. Arrowheads indicate hinge points. NE, neuroepithelium; NNE, non-neural ectoderm. Figure was adapted from *Andrew J. Copp and Nicholas D. E. Greene, 2013* (Copp & Greene, 2013) and *Evanthia Nikolopoulou, et al, 2017* (Nikolopoulou et al., 2017).

### 1.1.2 Signaling patterns during forebrain development

In the course of mammalian brain development, the central nervous system (CNS) undergoes growth that specifically meets the metabolic needs of neurons and glia (Rattner et al., 2022). Regional specification of the developing CNS is crucial in establishing various profiles of gene expression. This process can be divided into two main aspects: expansion, which involves the horizontal expansion of cells in the neuroepithelium that give rise to the neural tube (Falk et al., 2008); and cell differentiation, wherein the neuroepithelial cells differentiate to form the mature CNS (Zappone et al., 2000). The early developmental process in CNS patterning is largely conserved, and studies in chicks, fish, and mice begin to unravel the mechanisms of forebrain development (Wilson & Houart, 2009). During development, neuron and glia metabolisms request the precise vasculature growth in the CNS. The process of CNS development acquires a complicated series of molecular and cellular activities and multiple signaling pathways were required during the rapid growth of the CNS (Rattner et al., 2022). The morphogen signaling centers contribute to the regional patterning of NPCs. The expression of the morphogens WNT, Sonic hedgehog (SHH) and Bone morphogenetic protein (BMP) can be detected in the developing forebrain at an early stage (Marchini et al., 2021) (Figure 2).

The activity of Sonic hedgehog (SHH) in patterning the floor plate at the ventral midline of the neural tube was elegantly demonstrated (Brady & Vaccarino, 2021). In the ventral forebrain, SHH plays an important role in the generation and specification of cells of the medial and lateral ganglionic eminences, and is necessary to generate dopaminergic and serotonergic neurons in the midbrain (Ho & Scott, 2002; Nikolopoulou et al., 2017). In the midbrain and hindbrain, SHH is necessary for generation of neuronal cells; it also plays an important role in retinal development in vertebrates (Ho & Scott, 2002).

In frogs, fish, chicken and mouse, high expression levels of *Bmp* were found in anterior neural tube during development (Nikolopoulou et al., 2017). BMP activity is related to neural specification and early anterior to posterior patterning (Wilson & Houart, 2004). Some research suggested that BMP was involved in migration activity of cells in the

neural plate and promotes neurogenesis by pushing progenitors toward a neuronal fate and suppressing the oligodendroglia fate (Sadler, 2005; Wilson & Houart, 2004).

During early forebrain development, WNT signaling regulates the specification of cells in dorsal neural tube and is therefore involved in dorsal forebrain patterning. Ventral cell fate specification is controlled by the crosstalk between dorsal WNT signaling and SHH signaling, which takes place in the floor plate (Lian et al., 2019; Wilson & Houart, 2009) By the end of neural tube closure, WNT proteins can be detected in the dorsal midline of the forebrain (Harrison-Uy & Pleasure, 2012). Canonical WNT signaling is essential to cell fate determination, cell proliferation and cell differentiation during embryo development and has been demonstrated to play important roles in specific aspects of CNS formation (Harrison-Uy & Pleasure, 2012; J. E. Lee et al., 2006). In the mouse forebrain, several WNT ligands, such as WNT-2b, -3a, -5a, -7b and -8b, as well as BMP, are expressed in neuroepithelial cells (Machon et al., 2003; C. J. Zhou et al., 2006).

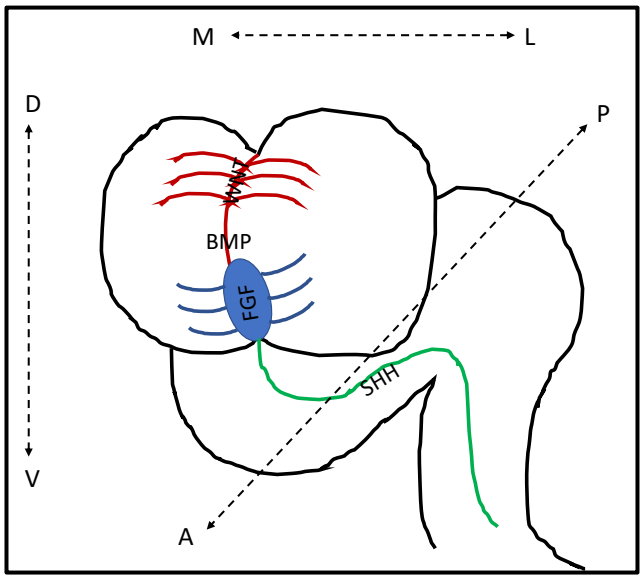


Figure 2: Signaling centers during early forebrain development

Schematic of the developing anterior neural tube at E9.5 showing the three signaling centers expressing. SHH, fibroblast growth factor (FGF), and WWNT/BMP family members from telencephalic signaling centers. FGF expresses at the rostral midline. BMP and WNT are expressed in the dorsal roof plate. SHH is expressed from floor plate cells in ventral midline.
A-P: Anterior - posterior, D-V: Dorsal - ventral, M- L: Medio - lateral.

## 1.2 Canonical WNT signaling pathway

### 1.2.1 Functions of the WNT pathway in health and diseases during development and postnatally

WNT morphogens are highly conserved lipid-modified secreted proteins that activate several signaling pathways, as described first in 1982 (Mehta et al., 2021; Liu et al., 2022). The WNT signaling pathway controls a multitude of processes during embryonic development and is involved in the regulation of fundamental mechanisms that include cell proliferation and determination of cell fate (Marchini et al., 2021). In addition to that, WNT signaling is also important for body axis patterning, cell migration, tissue maintenance, and tissue homeostasis regeneration (Liu et al., 2022). Impaired WNT signaling activity can lead to embryonic defects and developmental disorders; and abnormal WNT signaling activity in cancers is also found (Akiri et al., 2009).

The WNT signaling pathways include noncanonical and canonical pathways (Figure 3). The noncanonical WNT pathways, for example the Planar Cell Polarity and WNT/$Ca^{2+}$ pathways, is independent of T-cell factor/lymphoid enhancer binding factor (TCF/LEF) (Hayat et al., 2022) (Table 1). The canonical WNT pathway, which is also referred to the WNT/β-catenin pathway, involves the nuclear translocation of β-catenin and activation of target genes via TCF/LEF transcription factors (Liu et al., 2022). There are four segments comprising the WNT/β-catenin pathway: the extracellular signal, the membrane segment, the cytoplasmic segment, and the nuclear segment. The canonical WNT pathway is normally highly conserved and is activated by the binding of extracellular WNT ligands to the membrane receptors (Ferrer-Vaquer et al., 2010; Liu et al., 2022).

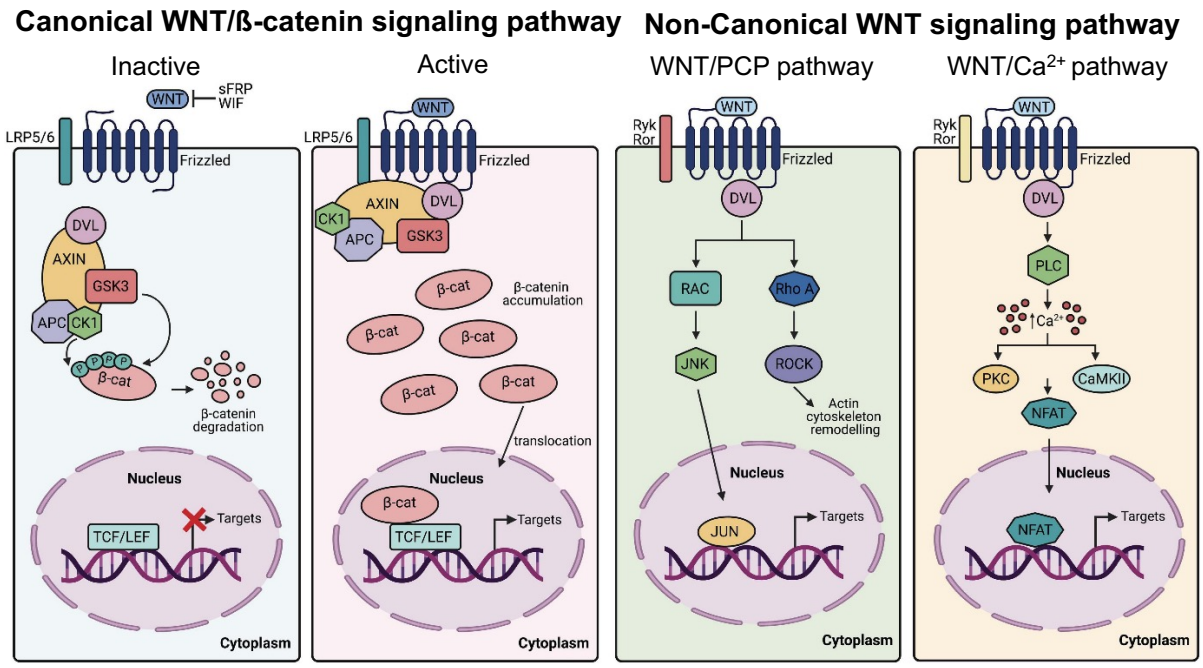


Figure 3: Schematics depicting canonical and non-canonical WNT signaling pathways.

**Canonical WNT pathways** (left panels): When WNT morphogens are not present, the ß-catenin degradation complex (Axin, GSK3, APC) prevents accumulation of ß-catenin in the cytosol. As a consequence, ß-catenin cannot enter the nucleus and WNT targets genes are not activated. When WNT proteins are present, LRP5/6 forms a complex with Frizzled (FZD). WNTs bind to the receptor complex and DVL recruits the ß-catenin degradation complex, which is no longer able to degrade ß-catenin. As a consequence, intracellular ß-catenin level rises, which enables ß-catenin to enter the nucleus, initiate T*cf/Lef* transcription and activate WNT target gene expression. **Non-canonical WNT pathways** (right panels). In the WNT/PCP pathway, non-canonical WNT ligands bind Ryk/Ror-Frizzled receptors and recruit Dvl leading to further activate RhoA/ROCK and RAC/JNK. In the WNT/$Ca^{2+}$ pathway, the non-canonical WNT pathway interacts with Ryk/Ror-Frizzled. This process increases the concentration of intracellular $Ca^{2+}$ and initiates the activation downstream kinases and components of the signaling cascade. Figure was adapted from *M.Caracci, et al, 2021* (Caracci et al., 2021).

Non-canonical WNT signals are also involved in neural development. For example, Vangl2 regulates asymmetric divisions of mouse subventricular zone progenitors (Bengoa-Vergniory et al., 2017).

| | **names** | **functions** | **reference** |
|---|---|---|---|
| **Main canonical pathway members** | β-catenin | association with cadherins and the actin cytoskeleton. | B.MacDonald, et al.,2009(MacDonald et al., 2009) |
| | E-cadherin | association with other co-receptors at the cell surface to influence signaling | *L.Santiago, et al.,2017*(Santiago et al., 2017) |
| | WNTs | activation signaling through the canonical pathway involving beta-catenin | *L.Albrecht, et al.,2021*(Albrecht et al., 2021) |
| | Frizzled receptors | Regulation of the response to WNT signaling. | *S.Teo, et al,.2021*(Teo & Salinas, 2021) |
| | Degradation complex | suppresses the canonical pathway | *C.Liu, et al., 1999*(Chunming Liu et al., 1999) |
| | Transcriptional activation TCF/LEF | Binding to β-catenin and activates downstream targets | *E.Jho, et al., 2002*(Jho et al., 2002) |
| **Main non-canonical pathway members** | Planar cell polarity-convergent extension | establishing cell polarity | *M.Wang, et al.,2019*(Wang et al., 2019) |
| | Calcium pathway | promote ventral fate and antagonize dorsal fate | *R.Hayat, et al.,2022*(Hayat et al., 2022) |
| | Atypical receptor tyrosine kinase pathway (RTK) | interact with the frizzled receptors to form a heteromeric ligand binding site, mediate WNT dependent effects upon axonal guidance | *R.Widelitz, et al., 2005*(Widelitz, 2005) |

Table 1: Main members of the canonical and non-canonical pathway and their function.

WNT proteins are a family of secreted lipoproteins and about 40 kDa in size. WNT ligands have been suggested to go through post-translational modification and they can activate different intracellular signaling pathways by binding to several receptors and co-receptors at the cell surface (Newmire & Willoughby, 2015; Palomer et al., 2019). So far, several different WNT factors have been identified that are involved in mammalian development (Kucukefe & Kaypmaz, 2009). For example, loss of WNT3a can cause severe developmental defects in the dorsolateral neural tube and disrupt somitogenesis that causes a tailbud defect, which is also called caudal truncation (Greco et al., 1996; Hayat et al., 2022). In addition, WNT3a is also important for supporting the growth of many different epithelial tissues (Sonnen & Janda, 2021). It has been shown that several WNT ligands are expressed in discrete and overlapping patterns in developing forebrain by embryonic day 9.5 (E9.5), such as WNT1, WNT3, WNT3a, WNT7b (Harrison-Uy & Pleasure, 2012).

WNT5a was reported as a factor that is supporting proliferation and migration of human fetal liver progenitor cells (Z. Liu et al., 2021). Another ligand, WNT7 is required in embryogenic CNS angiogenesis and the formation of the blood-brain barrier formation (Sonnen & Janda, 2021). Histological research in *Wnt5a*$^{-/-}$ mouse embryos showed that WNT5a signaling is also critical for insulin-positive cell migration during pancreas development (H. J. Kim et al., 2005). Interestingly, several WNT ligands such as WNT2, WNT2b, and WNT8a have a high expression level in early heart development (Guo & Xing, 2022).

Over the past decade, studies have shown that the WNT pathway is a key pathway required not only for blood brain barrier formation, integrity and function, but also for neuronal survival and neurogenesis (Jia et al., 2019). Dysregulation of WNT signaling is involved in a number of malignancies, suggesting that properly balanced WNT signaling is critical for normal cell proliferation and cell cycle (Houschyar et al., 2019). Research on WNT3a- and LEF1-deficient mouse embryos has shown that WNT signaling takes part in the development of the hippocampus (Clevers & Nusse, 2012; Santiago et al., 2017). In the absence of WNT3a, an abnormal morphology of the

choroid plexus can be observed in E12.5 embryos (Harrison-Uy & Pleasure, 2012). Previous studies in mouse models have considered WNT signaling as a factor of developmental cognitive disorders, such as autism disorders and Alzheimer's disease (Kwan et al., 2016; Palomer et al., 2019). Other researches have already shown that abnormal activity of the canonical WNT pathway could contribute to the risk of developing autism and lead a severe symptoms, such as intelligence disabilities and communication problem (Kalkman, 2012).

WNT signaling pathway also plays an important role in cell differentiation of developing mouse limbs and skeletal tissues, which are generated by an expanding population of multipotent mesenchymal cells (Narcisi et al., 2015). WNT signaling is also important to osteoblast cells and encourage their division and differentiation into mature osteoblasts (Hayat et al., 2022). It is also reported that the canonical WNT signaling pathway is involved in osteoarthritis. An increase of β-catenin in cartilage degeneration has been observed, suggesting that WNT activation contributes to osteoarthritis (Clevers, 2006; Fernández-Torres et al., 2018)

Furthermore, WNT signaling is also required for synaptic plasticity and synaptic maintenance (Marzo et al., 2016). Recently, it is also reported that WNT ligands and their receptors/co-receptors are altered during aging (Marzo et al., 2016; Palomer et al., 2019). Furthermore, it has been shown that upregulating WNT/β-catenin signaling can lead to increased tumor metastasis in human lung cancer (Nguyen et al., 2009; Pacheco-Pinedo et al., 2011). The decrease of WNT2 activity in non-small-cell lung cancer tissues can increase programmed cell death (You et al., 2004). The up-regulated expression of WNT2 has also been detected in human fibroadenomas, breast cancer, and pancreatic cancer (Yu et al., 2021).

### 1.2.2 WNT/β-catenin signaling receptor components

In recent decades, extensive research work has been dedicated to analyzing WNT signaling pathways and the processes that are involved in WNT signaling in development. It is already well known that the canonical WNT pathway is essential for the development process of organisms and repair of different tissue types, it can also regulate cell cycle and cell fate (Hayat et al., 2022).

In the canonical pathway, WNT transduction is activated by secreted extracellular WNT ligands and their binding to the transmembrane receptor Frizzled (FZD) and its co-receptors, the low-density lipoprotein receptors 5/6 (LRP5/6). Binding of WNT to its receptor complex results in β-catenin stabilization (C. Gao et al., 2014b; Hayat et al., 2022; Santiago et al., 2017). FZD receptors have the classic seven transmembrane domains of G-protein coupled receptors and are rich in cysteine in extracellular domains (Albrecht et al., 2021; C. Gao et al., 2014b). LRP5/6 are both transmembrane cell surface proteins and share approximately 71% homology in extracellular domain, which is responsible for binding WNT ligands and the inhibitors, such as Dkk1 and sclerostin (Ren et al., 2021). LRP5/6 are involved in receptor-mediated endocytosis of lipoproteins and protein ligand (Joiner et al., 2013) (Figure 3).

Phosphorylation and dephosphorylation acts as a key mechanism and is responsible for the control of β-catenin levels within cells and the activation and deactivation of the WNT/β-catenin pathway (C. Gao et al., 2014a). In the absence of WNT, β-catenin protein is constantly degraded by a degradation complex, which is composed of the scaffolding protein Axin, the tumor suppressor adenomatous polyposis coli gene product (APC), casein kinase 1 (CK1), and glycogen synthase kinase 3 (GSK3) (Jho et al., 2002; MacDonald et al., 2009). In the absence of WNT, the ubiquitin ligase β-Trcp will recognize phosphorylated β-catenin and target it for proteasomal degradation. However, by binding of the WNT ligands to the receptor complex formed by Frizzled-LRP5/6, disheveled proteins (Dvl) and Axin2 is recruited by LRP5/6 phosphorylation (Ferrer-Vaquer et al., 2010; *Wnt Stabilization of β-Catenin Reveals Principles for Morphogen.Pdf*, n.d.). Upon stimulation with WNT, the ligand forms a complex with FZD and LRP5/6 to initiate a series of molecular events that ultimately lead to the stabilization of β-catenin by suppressing the phosphorylation of β-catenin (Chunming Liu et al., 1999; *Wnt Stabilization of β-Catenin Reveals Principles for Morphogen.Pdf*, n.d.). Once the WNT signaling pathway has been activated, an intracellular signaling cascade is switched on by activating the disheveled proteins (Dvl) and heterotrimeric G-proteins, which are required for downstream targets (Newmire & Willoughby, 2015).

The LEF/TCF family transcription factors can mediate the nuclear response to canonical WNT signals, the LEF/TCF family includes lymphoid enhancer factor 1 (LEF1), which activates downstream genes by associating with β-catenin (J. E. Lee et

al., 2006). Research has confirmed that LEF1 functions only as a transcriptional activator in the presence of β-catenin (C. Gao et al., 2014b; J. E. Lee et al., 2006).

Axin is a direct target of WNT signaling pathway and acts usually as an inhibitor of the pathway. Axin is believed to function by promoting the phosphorylation and consequent degradation of β-catenin (Jho et al., 2002). Axin proteins, including Axin1 and Axin2, can inhibit WNT signaling pathways by assembling the degradation complex with Gsk3β, APC and Ck1 (de Almeida et al., 2020; Yu et al., 2021). *Axin2* expression is mediated through LEF/TCF factors, and is also highly expressed in a number of human tumor cell lines (Lustig et al., 2001; Yu et al., 2021).

β-catenin is a critical player in canonical WNT signaling pathway and works with co-factors to initiate WNT target gene transcription. Animal models also confirmed that β-catenin is an important modulator of neuronal differentiation and cerebral cortex development (Bae & Hong, 2018; Kwan et al., 2016).

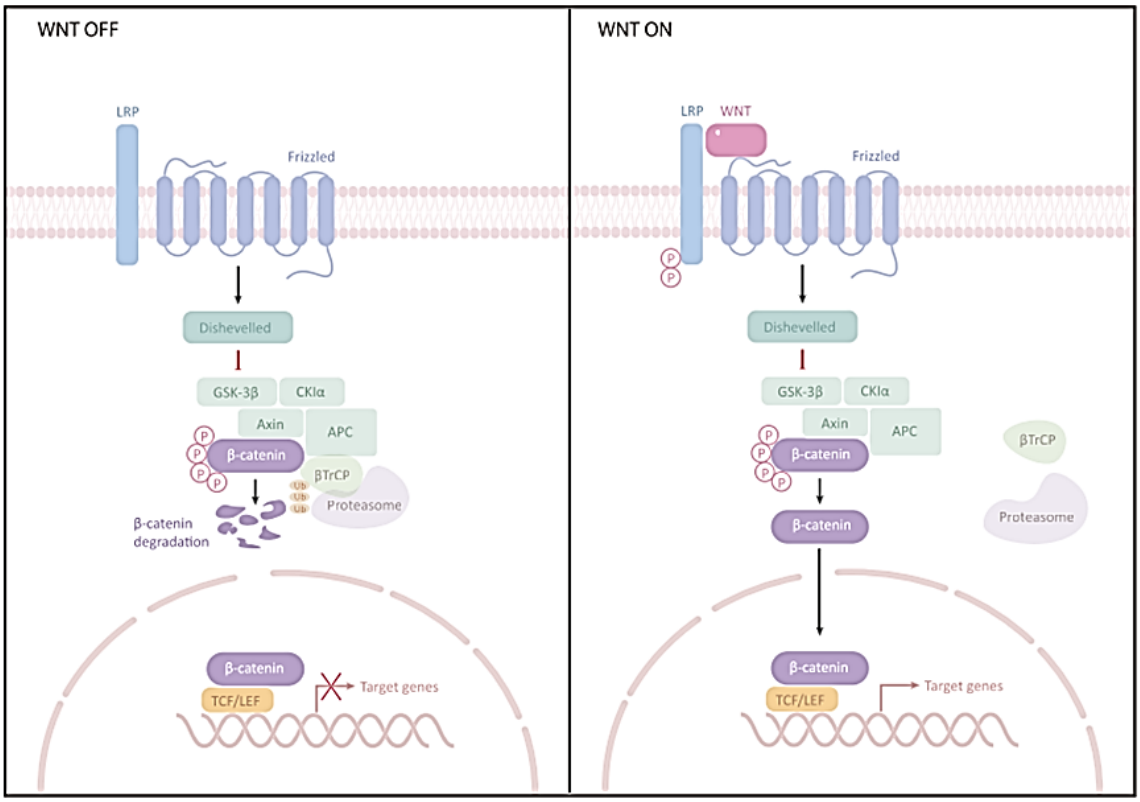


Figure 4: Canonical WNT/β-catenin signaling pathway and its components.

When WNT morphogens are not present, the ß-catenin degradation complex (Axin, GSK3, APC) prevents accumulation of β-catenin in the cytosol. As a consequence, β-catenin cannot enter the

nucleus and WNT targets genes are not activated. When WNT proteins are present, LRP5/6 forms a complex with FZD. WNTs bind to the receptor complex and DVL recruits the ß-catenin degradation complex, which is no longer able to degrade β-catenin. Consequently, intracellular β-catenin level rises, which enables β-catenin to enter the nucleus, initiate TCF/LEF transcription and activate WNT target gene expression. Figure was adapted from *Jiaqi Liu, et al, 2022* (Liu et al., 2022).

In WNT/β-catenin signaling pathway, β-catenin degradation is mediated by GSK3 that comprises a degradation complex (Albrecht et al., 2021; Yu et al., 2021). GSK3 can influence the differentiation and localization of neural cells (Rifes et al., 2020). Thus, there are also studies about cancers regulated by GSK3 with blocking WNT/β-catenin signaling pathway (Acebron & Niehrs, 2016). GSK3β, Dkk and Dvl are also important to chondral differentiation, hypertrophy and cartilage function (Fernández-Torres et al., 2018).

## 1.3 The low-density lipoprotein receptor-related proteins (LRPs) family

### 1.3.1 Structure and functions of LRP5 and LRP6

The low-density lipoprotein receptor (LDLR) is one of the most important proteins during development and in the adult organism (T. Yang & Williams, 2017). The LDL receptor is well known as an endocytic receptor that transports lipoproteins into cells by receptor-mediated endocytosis (Ohazama et al., 2010). Members of the low-density lipoprotein (LDL) receptor-related protein (LRP) family are an evolutionary well-conserved group of cell-surface receptors with multiple biological functions and are well known for their roles in lipid metabolism (Weatherbee et al., 2006). Several members of the LRP family are well studied and it is known that they have specific roles during embryonic development and also in the mammalian nervous system. For example, LRP2 is required for normal forebrain development and for neural tube closure (Mecklenburg et al., 2021; Willnow et al., 2007). LRP1 has been shown to influence skeletal development and postsynaptic specialization in the central nervous system. Moreover, LRP8 is also important for the normal layering of cortical neurons (Weatherbee et al., 2006; T. Yang & Williams, 2017).

There are a lot of biochemical and genetic studies on the LRP family members in vertebrates, specifically on LRP5 and LRP6, as they are coreceptors of the canonical

WNT signaling pathway. LRP5 and LRP6 are closely related and share a high degree of homology. They are transmembrane cell surface receptors involved in receptor-mediated endocytosis of lipoprotein and protein ligands (Joiner et al., 2013; C. J. Zhou et al., 2006). They contain large extracellular domains including four tandem YWTD-type-β-propeller domains, each followed by an epidermal growth factor (EGF)-like domain. These domains are followed by three type LDLR type A domains (Joiner et al., 2013). However, the LDLR repeats in LRP5 are not highly conserved to that in LRP6. The intracellular domain is rich in prolines and serines and contains a S/T cluster and downstream five reiterated PPP(S/T)PX(S/T) motifs (Chengcheng Liu et al., 2011). The cytoplasmic domain is 64% identical between LRP6 and LRP5 (Ren et al., 2021).

LRP5 and LRP6 play key roles in development, Lrp5/6 expression has been detected in different tissue types in various species, such as Xenopus, chicken and mouse, they are both important for embryonic development, glucose homeostasis, and bone cell metabolism (Alrefaei & Abu-Elmagd, 2022; Jin et al., 2022; Chengcheng Liu et al., 2011; Wei et al., 2006). LRP6 is essential for cardiac neural crest development; WNT/LRP6 interaction has been considered as a key regulator of axonal remodeling, synaptic plasticity and neurite outgrowth (Acebron & Niehrs, 2016; Makoto et al., 1997; Wu et al., 2021). In early stages of lung formation, *Lrp6* transcripts are detected in the border of lung and mesothelium. In the developing spinal cord, *Lrp6* was expressed in the ventricular zone along the dorsal–ventral side of the neural tube (Alrefaei & Abu-Elmagd, 2022). LRP5 was reported to be important to normal bone acquisition during growth and development (Sawakami et al., 2006). LRP5 was also identified as a regulator of adipose progenitor biology and regional adiposity (Loh et al., 2015).

Impaired LRP5 and LRP6 function, respectively, is also implicated in human disease, e.g., dysfunction of LRP6 has been related to coronary artery disease and fatal cardiac arrhythmia in adult patients (Wu et al., 2021). Researches have recently confirmed that *LRP5* gain-of-functions mutations lead to enhanced lower-body fat accumulation and can lead to osteoporosis in patients (Loh et al., 2015). Moreover, high expression of LRP6 has been detected in several types of cancers, including non-small-cell lung, bladder, breast, and colorectal cancers; there were three LRP6 missense variants found in patients with early colorectal cancer (Alrefaei & Abu-Elmagd, 2022). Additionally, previous studies have shown that LRP5 and LRP6 are involved in

diseases, such as Alzheimer's disease, degenerative joint disease and parathyroid tumors (Joiner et al., 2013).

In mice, *Lrp6*$^{-/-}$ embryos showed a loss of one or more posterior digits in forelimbs, and a reduction in size of tailbud at early embryonic stage, which will lead in loss of paraxial mesoderm and caudal somites at later stage (Pinson et al., 2000; Cheng Ji Zhou et al., 2004).The absence of LRP6 leads to very early embryonic lethality (Avilés & Stoeckli, 2016). LRP6, together with its co-receptor WNT, is also involved in neural tube defects (NTDs), which is the common and severe birth defects. Both gain-of-function and loss-of-function of *Lrp6* can cause NTDs in mice model (Zhao et al., 2022). In E9.5 *Lrp6*$^{-/-}$ embryos midbrain-hindbrain, the reduction of WNT activity could be detected. Furthermore, cell proliferation in neural folds was also decreased in *Lrp6*$^{-/-}$ embryos compared to wild types (Gray et al., 2010). LRP6 is also required to promote neurogenesis and cortical progenitor proliferation at later stages (C. J. Zhou et al., 2006). Recently, LRP6 was found to be involved not only in the canonical WNT pathway, but also in the non-canonical WNT pathway. LRP6 is associated with WNT/PCP signaling during axis elongation and gastrulation in *Xenopus* (Gray et al., 2013).

### 1.3.2 Structure and function of LRP4

LRP4 also belongs to the LDL receptor related protein family. LRP4 plays a pivotal role in the formation and the maintenance of the neuromuscular junction (NMJ), the synapse between a motor neuron and the skeletal muscle. LRP4 directly binds to Agrin on the myotube membrane to stimulate phosphorylation of muscle-specific kinase (MuSK) (Ohazama et al., 2010; Walker et al., 2021). In the absence of Agrin, LRP4 binds to MuSK to maintain a basal activity. By bridging Agrin and MuSK, LRP4 could transmit signal to MuSK and further activate intracellular cascades leading to muscle nicotinic acetylcholine receptor (AChR) clustering (Li et al., 2010). *Lrp4* null mice cannot form primitive neural AChR clusters normally, suggesting that LRP4 is requested for early postsynaptic differentiation in neuromuscular junctions (Jing et al., 2021). Agrin-Lrp4-MuSK signaling pathway engages in crosstalk with WNT signaling pathway. In the cytoplasm, the central effector of the WNT signaling pathway, Dvl1, interacts with MuSK to regulate AChR clustering (Ohkawara et al., 2021).

LRP4 has a large extracellular N-terminal region, a transmembrane domain, and a short C-terminal region without an identifiable catalytic motif (B. Zhang et al., 2008; Zong et al., 2012). The large extracellular region, like in other LRPs, contains EGF-like domains, and β-propeller domains (Depew & Mosca, 2021). The sequence and structure of LRP4 extracellular domain, which are similar to those of Lrp5 and Lrp6. LRP4 can bind to the ligands dickkopf WNT signaling pathway inhibitor 1 (Dkk1) and sclerostin domain containing 1 (Sostdc1), also known as Wise. Both ligands are regarded as modulators of the WNT signaling pathway (Ahn et al., 2013). The intracellular domain of LRP4 lacks some of the motifs present in LRP5 and LRP6 and known to be essential for WNT co-receptor function (Ahn et al., 2017; T. Yang & Williams, 2017). The intracellular portion of LRP4 is shorter compared to the LRP5/6 intracellular domain that contains an NPxY motif and a PDZ-binding motif, which are important for protein interactions and receptor endocytosis (Depew & Mosca, 2021) (Figure 5).

Besides playing a role in the formation of neuromuscular junctions, LRP4 has been shown to be involved in dendritic development and synaptogenesis in the central nervous system (Karakatsani et al., 2017). In addition to early neural system development, LRP4 is also critical in the adult CNS, such as maintenance of excitatory synaptic transmission, hippocampal synaptic plasticity, associative and spatial learning, and long-term potentiation (Pohlkamp et al., 2015). In addition, *LRP4* mutations are associated with limb, kidney and tooth malformations in the Cenani-Lenz syndrome, a congenital human disorder (Ahn et al., 2013; Karakatsani et al., 2017). In addition, findings showed that pathogenic variants of LRP4 are associated with diseases of the nervous system, including myasthenia gravis, amyotrophic lateral sclerosis, and Alzheimer's disease (Depew & Mosca, 2021). Besides the role in postsynaptic differentiation, LRP4 is important for initial steps of synapse development in early brain development as well as to instruct cellular events, including serving as an early signal to induce presynaptic differentiation (Depew & Mosca, 2021; Karakatsani et al., 2017). LRP4 expression is detected in embryonic cortical and hippocampal neurons, reduction of LRP4 expression decreased density of synapses and number of primary dendrites in these neurons (Karakatsani et al., 2017). Increased *Lrp4* expression in cultured CNS neurons resulted in an increase in the number of spines. *In vitro* experiments confirmed that decrease of *Lrp4* expression can change dendritic morphology in hippocampus and cortical neurons. On the

contrast, upregulated *Lrp4* expression in these neurons had the opposite effect (Karakatsani et al., 2017).

LRP4, together with Wise, provides extracellular communication between mesenchymal and epithelial cells by the integration of WNT signaling pathway, which controls processes of regulation during the development of craniofacial organs, especially teeth development (Ohazama et al., 2010). *Lrp4* mutants have supernumerary teeth in the diastema region, since apoptosis is reduced in the incisor region (Ahn et al., 2010). In addition, mice lacking LRP4 die at birth due to breathing deficits (Walker et al., 2021; B. Zhang et al., 2008; Zong et al., 2012).

It is well studied that LRP4 inhibits in the WNT signaling pathway by binding to extracellular molecules including WNT ligands, Dkk1, sclerostin (Sost) and Wise (Sostdc1) (Ahn et al., 2013, 2017; Jing et al., 2021; Ohkawara et al., 2021). Overexpression of *Lrp4* results in decreased WNT/β-catenin signaling activity *in vitro* (Ahn et al., 2017). *In vitro* studies have suggested that Wise, a potential physiological ligand of LRP4, can inhibit WNT/β-catenin signaling via the ability to bind to the extracellular domains of LRP5/6 (Ahn et al., 2017). Altogether, there is increasing evidence that LRP4 also acts as an important component in the WNT/β-catenin signaling pathway (Ahn et al., 2013; Ohkawara et al., 2021).

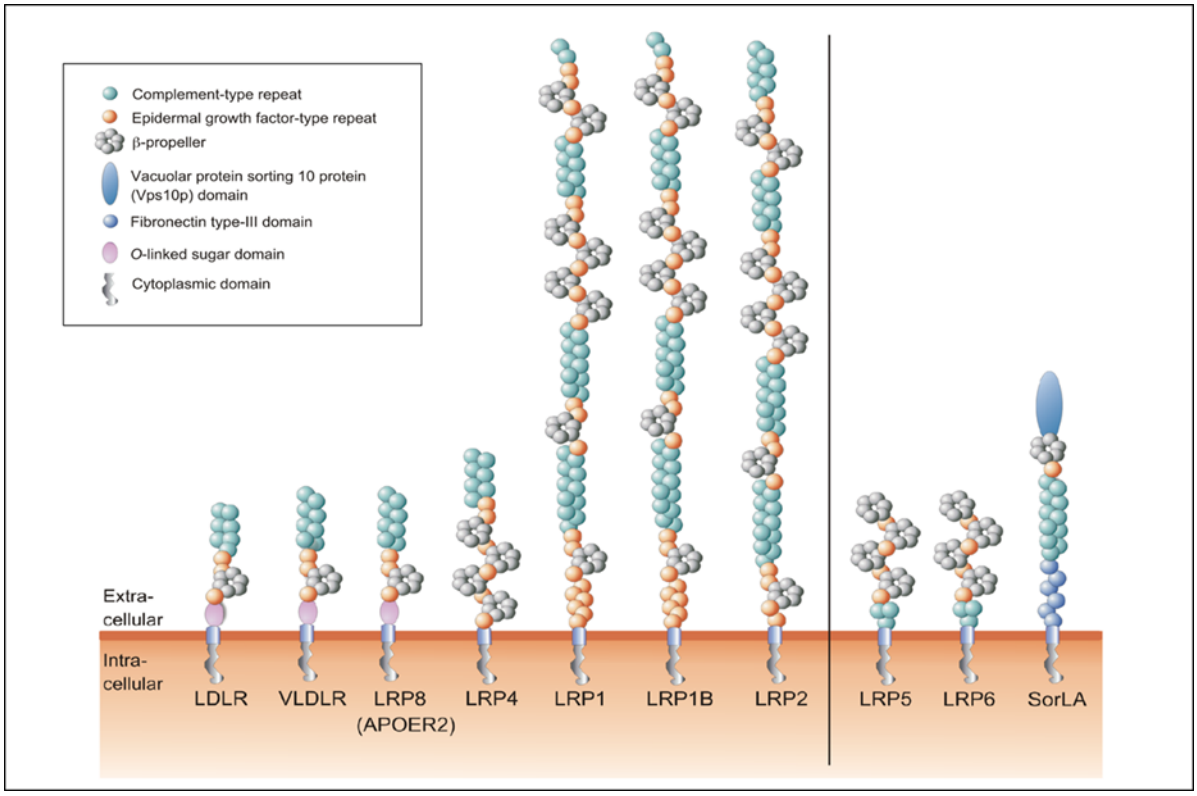


Figure 5: LDL receptor family.

Low-density lipoprotein receptor-related proteins (LRPs) are an evolutionary well-conserved group of cell-surface receptors with multiple biological functions. Figure was adapted from *Thomas E. Willnow, et al, 2007* (Willnow et al., 2007).

Modulation of WNT signaling is often mediated by secreted WNT antagonists, which interact with WNTs, FZD and its receptors LRP5/6. Dkk1 and Wise can bind to the extracellular domain of Lrp5/6 and inhibit WNT signaling by interrupting the formation of the FZD-LRP5/6 complex (Ahn et al., 2013). Since LRP4 is a co-receptor of Dkk1 and Wise, suggesting that LRP4 could be a negative factor of WNT signaling pathway and would interact with LRP5/6. Ahn and collogues have confirmed that LRP4 plays an important role in patterning and morphogenesis of the murine mammary glands, through modulating WNT pathway. Abnormal mammary glands could be found in *Lrp4* null mice (Ahn et al., 2013). Intriguingly, as shown by the laboratory of Rob Krumlauf, loss of LRP4 can partly rescue or compensate for developmental defects caused by loss of LRP6 (Ahn et al., 2013, 2017). Loss- and gain-of-function studies for LRP4 in mouse models and *in vitro* showed that LRP4 can modulate LRP6 function. In specific,

a hypomorph for LRP4 could rescue the abnormal limb and tooth development defects in *Lrp5/6* mutants (Ahn et al., 2017).

| **Gene** | **Species** | **Mutation** | **Phenotype** |
|---|---|---|---|
| LRP4 | Mouse | ENU mutagenesis, spontaneous mutant, targeted disruption | Impaired limb formation, renal agenesis, impaired orofacial development, reduced bone growth, neuromuscular junction defects |
| | Human | Loss-of-function | Cenani-Lenz syndrome |
| LRP6 (Arrow) | Mouse | Loss-of-function | Abnormal pattering of body axis, neural tube and limb defects, orofacial abnormalities, cardiac neural crest and outflow tract defects, hypoplasia of neocortex, ocular coloboma, neuroretinal patterning defect |
| | Human | Missense mutation | Autosomal dominant early Coronary artery disease |

Table 2: List of loss-of-function models of LRP4 and LRP6

Adapted from *Thomas.E.Willnow et al.,* 2012 (Willnow et al., 2012)

These studies focused on mammary gland, tooth and limb development but there were no studies on the role of LRP4 in early forebrain, and the interaction between LRP4 and LRP6 during early forebrain development remains to be revealed.

# 2. Aim and Hypothesis

## 2.1 Aim

The WNT signaling pathway is one of the most important signaling pathways in the process of neurulation. LRPs are crucial for WNT signaling and therefore involved in early embryonic forebrain development. LRP5 and LRP6 are well studied as co-receptors for frizzled, the main WNT receptor.

LRP4 has emerged as an important component of the WNT/ß-catenin signaling pathway. The LRP4 intracellular domain lacks some of the motifs that are present in LRP5 and LRP6 and are known to be essential for WNT co-receptor function, therefore LRP4 may act in a different mechanistic way on WNT signaling pathway compared to LRP5/6. Previous work in the field suggests that LRP4 could be an inhibitor of the WNT pathway. Overexpression of *Lrp4* results in decreased WNT/β-catenin signaling activity *in vivo*. This indicates that LRP4 may have a different impact on WNT signaling pathway compared with LRP5/6. However, little is known about the function of LRP4 as a potential modulator of LRP6 in the central nervous system. My aim is to shed light on functional interactions between LRP4 and LRP6 linked to the WNT pathway during forebrain development. Towards this aim, I applied molecular methods using LRP4- and LRP6-deficient mice as well as double mutants.

Abnormal development associated with abnormal activation of LRP4 is similar to WNT loss-of-function phenotypes in certain tissue (Ahn et al., 2010). Intriguingly, as shown by the laboratory of Rob Krumlauf, loss of LRP4 can partly rescue or compensate for developmental defects caused by loss of LRP6. These studies focused on mammary gland, tooth and limb development but there were hitherto no studies on the role of LRP4 in early forebrain development. Therefore, I intended to test whether LRP4 modulates the WNT pathway in early neuronal progenitors by checking the stem cell marker and proliferation marker at E9.5 embryo forebrain. Furthermore, the WNT pathway activation and downstream targets were detected in developing forebrain at E9.5.

Moreover, I aim to recapitulate the contribution of LRP4 and LRP6 to balance and titrate WNT signaling strength in cell culture models to test if the interaction between LRP4 and LRP6 is present beyond the context of the neuroepithelium.

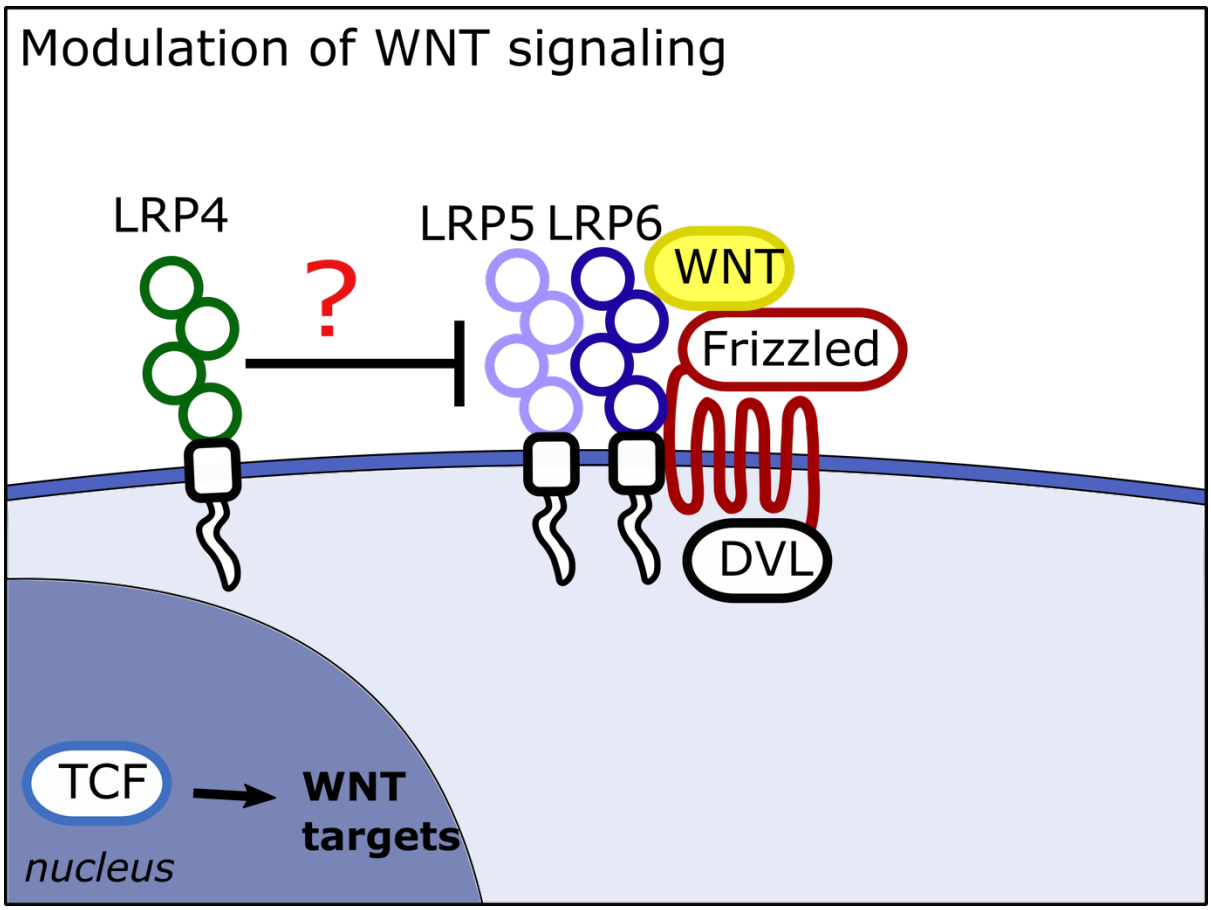


Figure 6: How LRP4 modulates WNT signaling pathway during early forebrain development is unknown

Besides LRP5 and LRP6 also LRP4 is expressed in the early forebrain as shown by our lab. LRP4 has been connected to the WNT signaling pathway in the mammary gland and limb(Ahn et al., 2017), however there is no information on the receptors function in early forebrain development and little is known about the detailed mechanisms on how this receptor modulates the WNT pathway. Note: the schematic presenting LRP5 and LRP6 next to each other indicates their role in binding WNT as Frizzled co-receptors but does not imply heterodimer formation.

## 2.2 Hypothesis

LRP4 and LRP6 as well as LRP5 play an important role in WNT signaling pathway during early forebrain development. LRP4 and LRP6 both functionally interact with each other during this process to titrate WNT signaling strength and ultimately regulate

proliferative capacity of neuronal precursors and the balance between proliferation and differentiation.

# 3. Material and Methods

## 3.1 Material

### 3.1.1 Chemicals and regent

| Chemicals and regent | Supplier and catalog number |
|---|---|
| Bovine serum albumin (BSA) | Sigma-Aldrich; A9647 |
| Dako fluorescence mounting medium | Agilent; S302380-2 |
| Roti Mix PCR 3 (dNTP) | Carl Roth; 0179.2 |
| Donkey serum | Biowest; S2170-500 |
| GeneRuler DNA Ladder Mix | Thermo scientific; SM0331 |
| Glycerol | Carl Roth; 3783.1 |
| Methanol | Carl Roth; KK44.1 |
| Paraformaldehyde (PFA) | Sigma Aldrich; 16005-1KG-R |
| O.C.T.™ Compound Tissue-Tek | Sakura Finetek; sa-4583 |
| PageRuler Plus Prestained Protein Ladder | LIFE Technologies; 26619 |
| Cresol red sodium salt | Sigma; 114480 |
| Taq Polymerase | NewEngland Biolabs; M0267L |
| ThermoPol® Buffer | NewEngland Biolabs; B9004S |
| Midori Green Advance DNA Stain | Nippon Genetics Europe GmbH; MG 04 |
| HpyCH4V | BioLabs; R0620L |
| Tris-HCl | Carl Roth; 9090.5 |
| Triton X-100 | Carl Roth; 3051.2 |
| Tween-20 | Carl Roth; 9127.2 |
| TaqMan Gene Expression Master Mix | life technologies; 4369016 |
| Lipofectamine RNAiMAX | Thermofisher; 13778-150 |
| Dimethyl sulfoxide (DMSO) | Roth; 4720.4 |
| Novex 10% Tris-Glycine Mini Gels, WedgeWell format, 15-well | life technologies; XP00105BOX |
| Tris-Glycine SDS Running Buffer | life technologies; LC2675 |
| High Capacity RNA-to-cDNA Kit | Thermo fisher scientific; 4387406 |
| Chloroform | Honeywell; C2432-500mL |
| Sodium chloride | Roth; HN00.2 |
| Ethylenediaminetetraacetic acid (EDTA) | Roth; 8043.2 |
| Skim milk powder | Sigma; 70166-500g |
| D (+)-Sucrose | Roth; 4621.1 |
| IGEPAL®CA-630 | Sigma; 18896-50mL |
| Taqman™ Gene expression master mix | Thermo Fisher Scientific; 4369016 |
| Potassium hexacyanoferrate (II) trihydrate | Sigma; P9387-100g |
| Potassium hexacyanoferrate (III) | Sigma; 244023-100g |

Table 3: List of Chemicals and reagents

### 3.1.2 Chemicals and reagents used in cell culture

| | |
|---|---|
| DMEM/F12 (1:1) (1X) HEPES | life technologies; 31330038 |
| Trypan Blue Dye | Bio-Rad; 1450021 |
| Dual-Chamber cell counting slides | Bio-Rad; 1450011 |
| Opti-MEM, reduced Serum Medium | life technologies; 31985-062 |
| Fetal Bovine Serum (FBS) | PAN-Biotech GmbH; P40-37500 |
| Trypsin-EDTA (1X) 0.05% | Gibco; 25300-054 |
| Hank's Balanced Salt Solution (HBSS) | BioWhiiaker, BE10-547F |
| RIPA buffer (10X) | Cell signaling technology; 9806S |
| Hygromycin B (100mg/mL) | ChemCruz; sc-506168 |
| Microscope cover glasses | Paul Marlenfeld Gmbh; 0111520 |
| Trizol reagent | Life techonoliges; 15596018 |
| *LRP4* siRNA | Ambion; 4392420 |
| *LRP6* siRNA | Ambion; 4390824 |

Table 4: List of chemicals and regent used in cell culture

### 3.1.2 Solutions and buffers

| **Name** | **Recipe** |
|---|---|
| PBS 10X (1L) | NaCl 80g<br>KCl 2g<br>$Na_2HPO_4$ 18,8g<br>$KH_2PO_4$ 2.4g<br><br>adjust pH 7.4 with NaOH, add water to 1L<br>filter & autoclave |
| TAE (50x) 1L | 242g Tris (MW = 121.14)<br>57,1 ml acidic acid pure<br>100 ml 0.5M EDTA pH=8 |
| EDTA 0.5M | EDTA 73,02 g<br>add NaOH pellets to help with dissolve<br>adjust pH=8 |
| Hot shot buffer | 0.5 mM NaOH<br>0.2 mM EDTA |
| Neutralization buffer | 1 M Tris-HCl<br><br>pH=6.8 |

| | |
|---|---|
| 4xSDS loading buffer | 40% glycerol<br>240mM Tris, pH=6.8<br>8% SDS<br>0.04% Bromphenolblue<br>5% beta-mercaptoethanol |
| 10x transfer buffer | Tris base 30.39g<br>Glycine 144 g<br>Add 1L MQ water |
| 10x TBS | 25g Tris<br>88g NaCl<br>add MQ water to 1L |
| 4% PFA | 40 g Paraformaldehyde in 1L PBS<br>pH=7.4 |
| X-gal washing Buffer | 500 µL of Igepal Ca-30, 0.25mL of 10% deoxycholate solution, 500mL PBS |
| X-gal staining solution (50 mL) | 1.25mL 200mM Potassium hexacyanoferrate (II) trihydrate solution<br>1.25mL 200mM Potassium hexacyanoferrate (III) solution<br>45.8mL X-gal washing buffer<br>1.2mL X-gal substrate (40mg X-gal/ 1mL DMF) |

Table 5: List of solutions and buffers

### 3.1.3 Antibodies

| **Antigen** | **Host** | **Supplier and catalog number** | **working dilution** |
|---|---|---|---|
| LRP6 | rabbit | Abcam, ab134146 | WB - 1:1000 |
| Axin2 | rabbit | Abcam, ab109307 | WB - 1:1000 |
| cyclin D1 | rabbit | Abcam, ab16663 | WB - 1:2500<br>IHC - 1:100 |
| a-TUBULIN | mouse | Merck Millipore, CP06 | WB - 1:10000 |
| HSP90 | rabbit | Cell signaling technology, #4874 | WB - 1:1000 |
| GAPDH | mouse | Santa Cruz biotechnology, sc-32233 | WB - 1:10000 |
| Phospho-Histone H3 | mouse | Invitrogen, # MA5-15220, | IHC – 1:250 |
| MPM-2 | mouse | Millipore, 05-368, | IHC – 1:1500 |

| | | | |
|---|---|---|---|
| SOX2 | rabbit | Abcam, ab97959 | IHC - 1:100 |
| GFP | chicken | Abcam, ab13970 | IHC - 1:200 |

Table 6: List of primary antibodies

| **Antigen** | **Supplier and catalog number** | **working dilution** |
|---|---|---|
| DAPI | Invitrogen | 1:1000 |
| Donkey anti-mouse Alexa 488 | Abcam, ab150109 | 1:500 |
| Donkey anti-rabbit Alexa 555 | Abcam, ab150074 | 1:500 |
| Donkey anti-chicken Alexa 488 | Abcam, | 1:500 |
| Goat anti-mouse IgG (HRP) | Abcam, ab97265 | 1:10000 |
| Goat anti-rabbit IgG (HRP) | Abcam, ab6721 | 1:10000 |

Table 7: List of secondary antibodies

### 3.1.4 Technical equipment and software for data analysis

| **Technical equipment** | **Supplier** |
|---|---|
| Cryostat CM1950 | Leica |
| Leica DM 5000C microscope | Leica |
| Leica SP8 confocal microscope | Leica |
| Nanodrop spectrometer 2000 | Thermo Fisher |
| Zeiss 700 confocal microscope | Zeiss |
| GraphPad Prism 7 | GraphPad Software, Inc |
| Image J | |
| Affinity photo | Serif Ltd |

Table 8: List of Technical equipment and software for data analysis

## 3.2 Animal experiments

### 3.2.1 Mouse husbandry and breeding

The mice were kept under conditions suitable for the species and treated in accordance with the provisions of the German animal protection act **(**Tierschutzgesetz: TierSchG §1-11). Mice were exposed to artificial light from 6 a.m. to 6 p.m. in a fixed day-and-night cycle. Timed mating was established before the end of the day cycle (approximately 6 p.m.) to obtain embryos at a defined stage of development. The vaginal plug was detected in the morning, indicating conception during the dark cycle (active phase of mice), referring as day E0.5 (embryo day 0.5). All dissections were

performed at a given time to collect embryos at around noon. Dissections were carried out regarding to German animal protection act. All genetically modified mouse line were maintained on C57BL/6N (black6) inbreeding background. C57BL/6N mice that do not carry any genetically modified alleles are referred as the wild type.

### 3.2.2 *Lrp4$^{mitt}$* functional null mouse line

The *Lrp4$^{mitt}$* mouse line was created by the laboratory of Lee Niswander and was a courtesy of Scott Weatherbee and Robert Krumlauf. The *Lrp4$^{mitt}$* mouse line was generated by ENU-induced point mutations(Russell et al., 1979). The *Lrp4$^{mitt}$* allele contains two different point mutations in coding region. A terminal mutation at the end of the C terminal of the LDLR type A (LA) domain, causing premature termination of the codon. The second splice site mutation can introduce a second premature stop(Weatherbee et al., 2006). This resulted in the loss of most of the *Lrp4*-coding gene region. Another early termination codon is caused by a mutation at the splicing site. In this study, *Lrp4$^{mitt}$* heterozygotes are referred to as *Lrp4$^{+/-}$* and likewise *Lrp4$^{mitt}$* homozygotes are termed *Lrp4$^{-/-}$* mice.

### 3.2.3 *Lrp6$^{Gt(Ex187)Byg}$* functional null mouse line

The *Lrp6$^{Gt(Ex187)Byg}$* functional null mouse line was created by William Skarnes(Pinson et al., 2000) and obtained from Jackson Laboratories. The *Lrp6$^{Gt(Ex187)Byg}$* functional null mutation was generated by inserting the first 321 amino acid sequences of the LRP6 gene trap vector with a β-Galactosidase-Neomycin cassette. In this study, mice that carried one *Lrp6$^{Gt(Ex187)Byg}$* allele (heterozygotes) are termed *Lrp6$^{+/-}$* mice, while embryos that had both alleles with the *Lrp6$^{Gt(Ex187)Byg}$* mutation (homozygotes) are referred to as *Lrp6$^{-/-}$* embryos.

### 3.2.4 *TCF/Lef:H2B/GFP* transgenic reporter mouse line

The *Tg(TCF/Lef1-HIST1H2BB/EGFP)$^{61Hadj}$* transgenic reporter mouse line was created by Anna-Katerina Hadjantonakis (Ferrer-Vaquer et al., 2010) and was obtained from the Jackson Laboratories (MGI:4881498). In this study, mice that carry one allele of the *TCF/Lef:H2B-GFP* reporter are referred to as *GFP$^{+/-}$* (e.g. *Lrp4$^{-/-}$; GFP$^{+/-}$)*

### 3.2.5 *Lrp4$^{mitt}$; Lrp6$^{Gt(Ex187)Byg}$* double mutant mouse line

*Lrp4$^{mitt}$; Lrp6$^{Gt(Ex187)Byg}$* double mutant embryos were generated by combing two *Lrp4$^{+/-}$; Lrp6$^{+/-}$* adult mice in timed mating. Different genotypes were obtained. *Lrp4$^{mitt}$; Lrp6$^{Gt(Ex187)Byg}$* double null mutants are referred to as *Lrp4$^{-/-}$; Lrp6$^{-/-}$* embryos.

### 3.2.6 Dissection of mice and fixation of specimen

The pregnant females from timed matings were sacrificed and dissected according to the detected plug date to obtain the embryos of the required embryonic stage. The uterus was removed and immediately transferred to cold (4°C) PBS to anesthetize the embryo and preserve tissue integrity. The embryos were dissected from the uterus, and the somites were counted to match the developmental stage. Subsequently, embryos were transferred to a 4% paraformaldehyde solution (PFA) and fixed overnight at 4 °C. After fixation, the embryos were washed in 25%, 50%, 75% MetOH, 25 minutes of each step, and stored in 100% MetOH at -20℃.

## 3.3 Molecular biology methods

### 3.3.1 Genotyping

#### 3.3.1.1 Isolation of genomic DNA from tissue

For detection of mouse embryos, the yolk sac of each embryo was collected during preparation. For adult mice which were kept in animal facility, the ear punch or toe cut was collected for genotyping. Both embryonic and adult tissue were to extract DNA as fellows. The samples were transferred to 90-150µL Hotshot buffer (depending on sample size), boiling at 95°C for 20minutes (for yolk sac) or 25 minutes (for adult tissue). Subsequently, 7.5 - 12.5µL neutralization buffer containing 1 M Tris-HCl (pH = 6.8) was added to the samples and samples were centrifuged to neutralize. Isolated genomic DNA was stored at 4°C and ready for genotyping.

### 3.3.1.2 Genotyping by PCR

In this study, Polymerase chain reaction (PCR) was used for genotyping of mouse tissue or yolk sac. The genome sequence was designed to specifically amplify to distinguish the oligonucleotide pairs of the modified alleles from the wild-type alleles. Specific primers were set for different genetically modified mouse lines, as well as PCR cycling conditions.

| Name of primer | Sequence (5' to 3') |
|---|---|
| Lrp4-G-P27 | GGT GAG GAG AAC TGC AAT GT |
| Lpr4-G-pp9-rev | TGA GTC AAG GTC ACA CCC ATC |
| beta-geo F | CAA ATG GCG ATT ACC GTT GA |
| GP-Lrp6-R (beta-geo R) | TGC CCA GTC ATA GCC GAA TA |
| GP-TCFgfp-F-P130 (Hadj_F) | ACA ACA AGC GCT CGA CCA TCA C |
| GP-TCFgfp-F-P130 (Hadj_R) | AGT CGA TGC CCT TCA GCT CGA T |

Table 9: List of primers

### 3.3.1.3 Digest of DNA with restriction enzymes

Enzymatic digestion is a method to cut at specific sites within the genomic sequence with restriction enzymes. Restriction digestion is established by mixing and incubation of the target DNA molecule with restriction enzyme, which can recognize and bind specific DNA sequences and cleave at specific nucleotides of the recognition sequence. In order to fully digest the DNA fragment, the amount of restriction enzyme is determined by applying the following formula. The DNA-enzyme mixture solution (including the corresponding enzyme buffer) was set up according to the manufacturing instructions. The DNA-enzyme mixture was then continuously digested for 3 hours at 37°C. In this study, restriction enzyme HpyCH4V (BioLabs, R0620L), of which the cut site is CG/TA, was used to digest the amplified products of *Lrp4* genotyping PCR. The enzyme was diluted as 1:5 dilution, and 2µL of this mix was added into PCR-product.

### 3.3.1.4 Genotyping by X-gal staining

Homozygotic *Lrp6*$^{Gt(Ex187)Byg}$ were identified by X-gal staining of the yolk sac. Yolk sacs were collected and quickly washed in cold PBS. Then the yolk sacs were transferred to X-gal washing buffer and washed for 10 minutes, shaking at 4°C. Subsequently, the yolk sacs were incubated in X-gal staining solution (seen in Table 5) at 37 ° C. After 15-30 minutes, the staining intensity was sufficient to discriminate between heterozygous and homozygous samples. Yolk sacs were transferred to X-gal washing buffer to stop the staining process.

### 3.3.1.5 PCR programs for *Lrp4*, *Lrp6* and *TCF/Lef1-GFP* genotyping

| **PCR protocol for *Lrp4* genotyping** | |
|---|---|
| 95°C | 3 min. |
| 95°C | 20 sec. |
| 60°C | 20 sec. |
| 68°C | 30 sec. |
| 68°C | 5 min. |
| 10°C | ∞ |
| cycles | 40 |
| Digestion with HpyCH4V at 37 °C for 2 hours | |
| *WT* band at 150 bp; *KO* band at 200 bp; *HET* band at 200 bp +150 bp | |

| **PCR protocol for *Lrp6* genotyping** | |
|---|---|
| 95°C | 3 min. |
| 95°C | 45 sec. |
| 60°C | 45 sec. |
| 72°C | 1 min. |
| 72°C | 3 min. |
| 10°C | ∞ |
| cycles | 35 |
| *HET* and *KO* band at 160 bp; *WT* no band | |

| **PCR protocol for TCF/GFP genotyping** | |
|---|---|
| 95°C | 3 min. |
| 95°C | 25 sec. |
| 57°C | 25 sec. |
| 72°C | 35 sec. |
| 72°C | 3 min. |
| 10°C | ∞ |
| cycles | 32 |
| Positive band at 530 bp; negative no band | |

Table 10: program of LRP4, LRP6 and TCF/GFP genotyping

### 3.3.1.6 DNA/RNA gel electrophoresis

Gel electrophoresis can be used to separate DNA of different sizes by applying an electric field to the gel matrix. In this study, gel electrophoresis was performed to separate DNA from PCR products. 2.5-3.0% agarose gel (in TAE buffer) was used as

a matrix. Midori Green Advance DNA Stain (5µ in 100µL Agarose) was added to the gel to ensure that DNA fragments could be visualized under ultraviolet light. The voltage was set to 130V, and the gel was run 40 minutes to 1 hour. DNA/RNA bands were detected by exposure to UV light.

## 3.4 Immunohistochemistry

### 3.4.1 Cryo embedding of tissue and sectioning

The embryo was embedded in TissueTek OCT mounting medium (Sakura) as follows. The embryos were dehydrated in 75%, 50%, 25% MetOH and washed 2 times in PBS, 20 minutes for each step. The samples were then transferred to a 15% sucrose/PBS solution and washed on a shaker until completely immersed. Then the samples were transferred to 30% sucrose/PBS solution and incubated until they sank to the bottom of the test tube. Subsequently, the specimens were transferred to an embedding mold and OCT mounting medium was added. After the embryos were aligned, the mold was transferred to cold pure methanol on dry ice to rapidly freeze the sample. Cryo blocks were kept in -20°C until further processing. Before cutting the frozen sample, the OCT block was placed in a constant temperature chamber to balance to -20°C. The samples were sliced at 10µm with the HM 560M cryogenic thermostat (Microm). All cryosections were stored at -20°C until further processing.

### 3.4.2 Fluorescent immunohistochemistry on cryosections

Immunohistochemistry (IHC) is the most common application of immunostaining, which involves the process of selectively recognizing antigens in cells on slices of tissue using the principle of antibodies that specifically bind to antigens in tissue. First, frozen sections were removed from -20°C and dried in air for 1h. Then the slides were transferred to a Coplin jar and washed in PBS+0.1 % Triton-X100 (PBTr) for 5 times, 7 minutes each. Subsequently, the solution was replaced by PBTr with 10% goat serum and 1%BSA and the slides were blocked inside for 1h. Subsequently, the sections were incubated with primary antibody at 4 °C overnight. Antibodies were used in a dilution as listed in the Table 6 (see section 3.1.3). The next day, the primary antibody was discarded, and the sections were washed in PBTr for 7 minutes, 5 times

each. The slides were incubated with secondary antibody and Dapi in a dilution as listed in the Table 6 (see section 3.1.3) at RT in the dark for 1h. Subsequently, the slides were transferred to PBTr and washed for 5 x 7 minutes at RT avoiding light. In the next step, the sections were quickly washed in water and mounted with fluorescent mounting medium (Dako). The slides were dried in a hood for 3-4 h and stored at 4 °C to minimize fading of the fluorophores.

### 3.4.3 Whole mount fluorescent immunohistochemistry

In this study, whole mount fluorescent immunohistochemistry was used to visualize target protein expression in E9.5 embryos. The embryos were rehydrated by washing in 75%, 50%, 25% MetOH and 3 times in PBS, 20 minutes for each step. Then the samples were transferred to PBS with 1% heat-inactivated donkey serum, 2% BSA and 0.1% Triton-X100 (PHBT) and blocked on shaker at 4°C overnight. In the next day, the PHBT was discarded, and samples were incubated with primary antibody at 4°C for 3 days. The embryos were transferred to PBS+0.1 % Triton-X100 (PBTr) and washed at RT for 1h, 6 times in total. After that, specimen was incubated with secondary antibody and Dapi overnight at 4°C on shaker, avoiding light. On the following day, the samples were washed in PBTr for 6 x 1 h in dark at RT. Subsequently, the embryos were washed with 10%, 25%, 50%, and 100% TDE (2,2′-thiodiethanol) solution, which is a clearing reagent, in RT shaker. After that, the samples were washed in 100% TDE solution overnight at 4°C shaking in the dark. Then the specimens were mounted with 100% TDE and store at 4°C to minimize fading of the fluorophores.

### 3.4.4 Confocal microscopy image acquisition

Image acquisitions of tissue sections were carried out using either a Leica SPE or Leica TCS SP8 confocal microscope using a HC Pl Apo 20× NA 0.75 MultiIMM and HC Pl Apo 63× NA 1.3 oil immersion objective. All samples that were compared for either qualitative or quantitative analysis were imaged under identical settings for laser power, detector, and pixel size.

## 3.5 Cell culture experiments

### 3.5.1 Cell culture maintenance

To investigate how LRP4 and LRP6 balance WNT signaling pathway in vitro, the hTERT RPE-1 cell line is used as an ideal model. Cells were cultured in DMEM: F12 Medium (ATCC® 302006™) with 10% Fetal Bovine Serum (FCS) in a 10 cm dish. When the cells reach a certain confluency, cells were washed with HBSS and incubated with 0.05% Trypsin-EDTA at 37°C for 3 min. Then the cells were passaged with a 1:10 dilution for maintenance.

### 3.5.2 Cryopreservation

Cells were detached and collected in a 50 ml flacon tube. Then the cells were centrifuged at 1000 rpm at RT for 5 minutes. The supernatant was discarded. The cells were diluted in the DMEM with 20% FCS and 10% DMSO (1mL/10 cm dish). Cells were stored at -80°C overnight in cryo-vials filled with isopropanol. The next day, frozen cells were transferred to liquid nitrogen containers.

### 3.5.3 Transfection with siRNA for gene silencing experiments

Cells were split and seeded to a 12-well plate with a concentration of $5x10^4$ cells per well and $4x10^4$ cells/well in 24-well plate with coverslip. At the next day, cells were washed with HBSS before changing to DMEM medium with 10% FSC and without hygromycin B. LRP4, and LRP6 silencing was achieved by siRNA transfection. hTERT RPE-1 cells were transfected using Lipofectamine™ RNAiMAX (Thermo Fisher, Cat. #13778-150) for the Western blotting and/or qPCR experiments. For 12-well plate, the prepared mix is enough to have triplicates transfections. The siRNA was diluted in 1:10 dilution beforehand. Then 150 µL reduced-serum Opti-MEM Medium (life technologies; 31985-062) and 15 µL Lipofectamine™ RNAiMAX were mixed up at RT. Next, 150 µL Opti-MEM Medium and 3 µL siRNA (seen in the Table 4, section 3.1.2) was mixed up at RT. Afterwards, the diluted siRNA in Opti-MEM Medium and diluted Lipofectamine RNAiMAX Reagent was mixed up as 1:1 and incubated at RT for 5 min. The mixture was distributed equally to the cells. As the final concentration, 10 pmol siRNA was used each well, and 3 µL Lipo RNAiMAX was applied in each well. The

technical replicates were three for each experiment, experimental replicates were three.

48 h after transfection, cells were harvested for protein and RNA isolation. After 24 h transfection, cells were quickly washed with cold PBS and then fixed with 4% PFA at RT for 15 min, then cells were applied with Immunofluorescence.

### 3.5.4 Western blotting

The protein was diluted with 4x SDS buffer and loaded in the same amount to an SDS-PAGE using 10% Tris-Glycine gel. Protein samples were run at 80V and then separated. Then, proteins were transferred to a nitrocellulose membrane (Amersham Protran 0.2 µm) using a wet electroblotting system (Bio-Rad Mini Protean II Cell) with 1x transfer buffer, which contained 20% MetOH. Next, samples were transferred at 100V for 1.5 hours. Next, the membrane was moved off and blocked with 5% slim milk in 1x TBST at RT for 1 h. Then the membrane was incubated in primary diluted TBST in a dilution as listed in the Table 6 (see section 3.1.3) overnight at 4°C on a roller.

The next day, the membrane was washed in TBST for 3x10 min. Secondary antibodies were diluted in 1x TBST (1:10000) and the membrane was incubated in secondary antibodies (seen in the Table 6, section 3.1.3) for 2h at RT on a roller. After incubation, the membrane was washed in TBST for 3x10min, then developed with components of the enhanced chemiluminescence (ECL) kit, which is the reagent detecting picogram amounts of antigen and is based on the emission of light during the horse radish peroxides (HRP).

The result was quantified with ImageJ. The bands were selected with rectangle tool, and the measurement of signal intensity was performed, followed with the subtraction of measured background signal. The signal intensity of target gene signal was normalized to housekeeping gene that used on the plot. The p value was based on One-way ANOVA.

### 3.5.5 Immunofluorescence on cells

Cells were split and seeded into a 24 well plate coated with coverslip, as a final concentration $4x10^4$ cells/ml. After 48 hours of transfection, cells were quickly washed with cold PBS (1mL/well) then fixed with 4% PFA (500 µL/well) for 15 min at RT. Cells

were permeabilized by PBS with 0.25% Triton X-100 (500 µL/well) at RT for 20 minutes. Next, the cells were blocked with 10% donkey Serum in PBS-Triton 0.25% (500 µL/ well) for 1h at RT. Primary antibodies were diluted in a dilution as listed in the Table 6 (see section 3.1.3) in 0.25% PBS-Triton and dropped to a parafilm as 80µL/ drop. Then the coverslips were taken out from plate and put on the drops with cell facing down. The cells were incubated with primary antibodies for 1h at RT. After that, the coverslips were placed back on the 24 well plate and the cells were washed with 0.25% Triton X-100 for 3x10 min. Secondary antibodies were diluted (1:500) and applied in the same way as primary antibodies. Cells were incubated with secondary antibodies in the dark for 1h at RT. Subsequently, cells were washed with 0.25% Triton X-100 for 3x10 min in a 24 well plate. Afterwards, the coverslips were mounted with DAKO.

### 3.5.6 RNA Isolation and reverse transcription

After transfection with siRNA for 48h, the medium was discarded, and cells were added 0.5mL TRIzol™ Reagent (Life Technology, Catalog Numbers 15596018). After incubation for 3-5 min, cell lysate was pipetted for several time and transferred to a 1.5 ml Eppendorf tube and centrifuged for 15 minutes at 12000 × g at 4°C. The mixture was separated into a lower red phenol-chloroform and a colorless upper aqueous phase. Then the aqueous phase containing the RNA was transferred to a new tube by pipetting the solution out. Subsequently, the aqueous solution was added 0.25 mL isopropanol and incubated for 10 min and then centrifuged for 15 minutes at 12000 × g at 4°C. After centrifuge, the supernatant was discarded with a micro pipettor. The pellet was added 0.5 mL 75% ethanol and vortexed briefly, then centrifuged for 5 min at 7500 × g at 4°C. Afterwards, the supernatant was discarded with a micro pipettor. The pellet was resuspended with 20 µL of RNase-free water and incubated in the heat block at 60°C for 10 min. After the measurement of RNA concentration, the cDNA was prepared according to High-Capacity RNA-to-cDNA™ Kit protocol (appliedbiosystems, Catalog Number 4387406). The mixture component was prepared according to the protocol and incubated for 37°C for 60 minutes. The reaction was stopped by heating to 95°C for 5 minutes and hold at 4°C.

### 3.5.7 quantitative RT-PCR (qPCR) with Taqman assay

The cDNA was diluted in RNAse-free $H_2O$ as a 1:20 dilution and pipetted into the PCR stripes. 10 µL of each sample was taken and mixed up in PCR stripes to make S1 standard. Then S1 standard was made into a 1:2 dilution as S2 standard. S3 and S4 standard was made from S2 and S3 standard as 1:2 dilution, respectively. The mastermix was prepared with Taqman™ Gene Expression Master Mix (appliedbiosystem, ref. 4369016) and taqman probe mix (life technologies; LRP4: Hs00391006_m1, Gapdh: Hs99999905_m1) in the tube as the table below and then vortexed.

| | Stock concentration | Final concentration | Volume per reaction (µL) |
|---|---|---|---|
| $H_2O$ | | | 0.5 |
| Pol mix | 2X | 1X | 5.0 |
| Primer probe mix | 20X | 1X | 0.5 |

Table 11: protocol of master mix of qPCR

Then the triplicate mix was prepared in PCR stripes as the table below and vortexed. Then the mixture was spined down with microcentrifuge and directly pipetted into a 384-well plate.

| For three reactions | |
|---|---|
| Master mix | 19.35 µL |
| DNA (sample or standard) | 12.90 µL |
| Total | 32.25 µL |

Table 12: protocol of triplicate mix of qPCR

### 3.6 Statistical analysis

Statistical analysis was performed with GrapdPad. The standard error of mean (SEM) is provided. The p value was based on One-way ANOVA, and the term significant was used if p value was less than 0.05 ($p<0.05$).

# 4. Results

## 4.1 *Lrp4* is a genetic modifier for neuroepithelial hypoplasia phenotypes in *Lrp6*$^{-/-}$ mutants but not for neural tube closure defects

To analyze the impact of LRP4 and LRP6 deficiency on the fate of early neural progenitors I used mutant mice deficient for either LRP4 or LRP6. In addition, to investigate the potential gene interaction of *Lrp4* and *Lrp6* during forebrain development, I also analyzed *Lrp4*$^{-/-}$; *Lrp6*$^{-/-}$ double mutant embryos, herein referred to as *Lrp4*$^{-/-}$; *Lrp6*$^{-/-}$ double mutants. By stereomicroscopic analysis of embryos at E9.5, I found that most of *Lrp6*$^{-/-}$ mutant embryos showed an obvious tailbud defect, which is called caudal truncation, compared with wild types (WT). The caudal truncation phenotype was described previously as open caudal neuropore (spina bifida) and axis truncation(Gray et al., 2010). *Lrp6* null mutants also showed abnormal head development since they showed a smaller head size compared to the wild types (Figure 7). However, all these phenotypes were described before (Pinson et al., 2000; Song et al., 2009), but needed to be confirmed in our present breeding colony where all mice were kept on a pure C57BL6/N background, since strain background differences and genetic drifts can cause changes in phenotype penetrance and expressivity. After comparing the somite numbers between wild-type and *Lrp6*$^{-/-}$ embryos, I found that in *Lrp6* null mutants, the somite number is lower compared to age matched wild-type embryos (Figure 9A). Besides that, a cranial open neural tube was observed in 16 out of 65 *Lrp6* null mutants. However, *Lrp4*$^{-/-}$ embryos showed no obvious anomalies at this stage of development compared to wild types when analyzed under the stereomicroscope. Surprisingly, the *Lrp4*$^{-/-}$*; Lrp6*$^{-/-}$ double mutants showed a milder phenotype compared to the *Lrp6*$^{-/-}$ single mutants regarding body size at the given stage of development (Figure 9C).

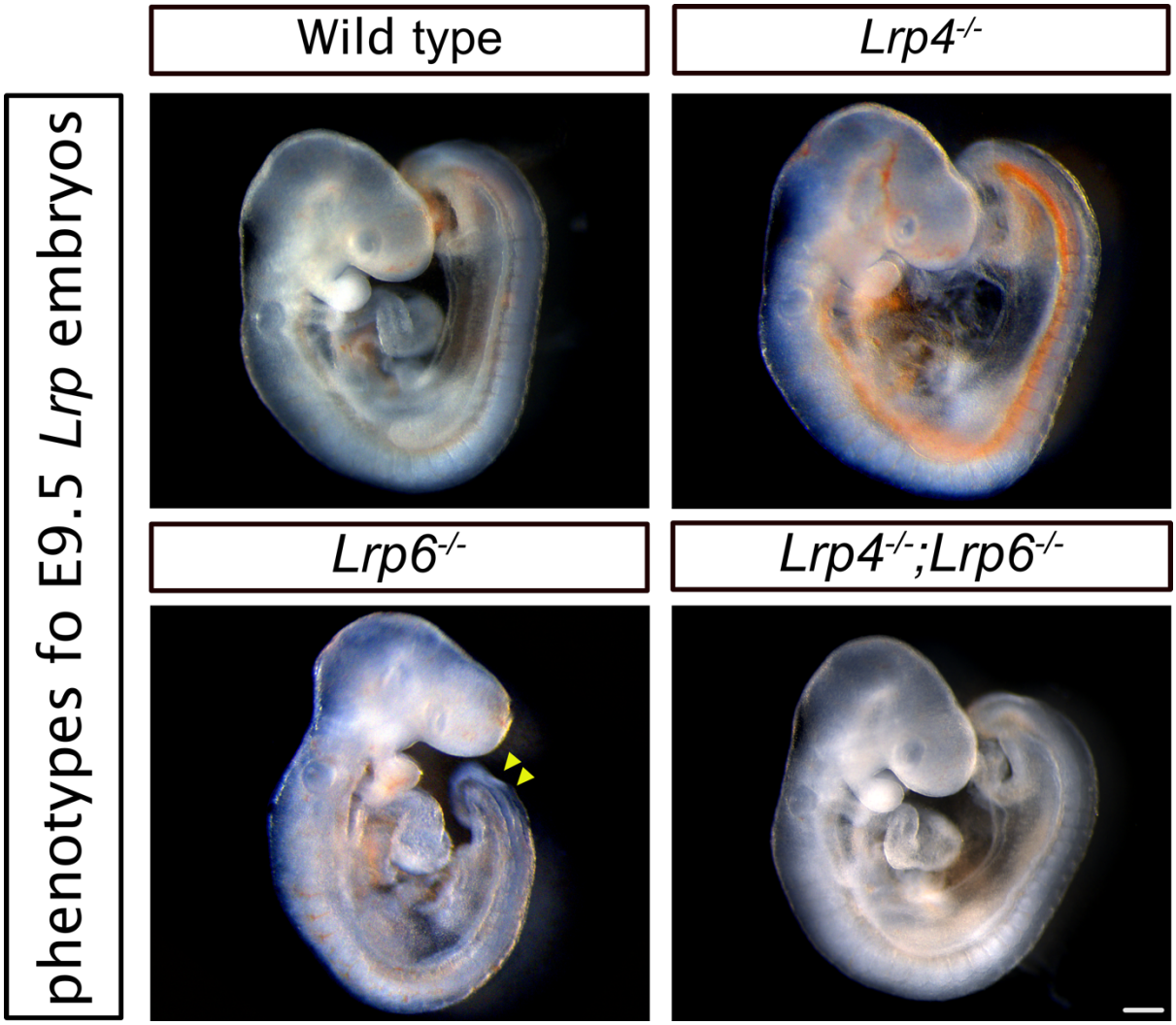


Figure 7: Body size differences between embryos of different *Lrp* genotypes at E9.5

Representative images of mouse embryos at embryonic stage E9.5. *Lrp6*$^{-/-}$ embryos showed a typical caudal truncation phenotype as well as a smaller body size comparing to wild types, whereas *Lrp4*$^{-/-}$ and *Lrp4*$^{-/-}$*; Lrp6*$^{-/-}$ mutants showed no significant difference compared with wild types. However, *Lrp4*$^{-/-}$ *; Lrp6*$^{-/-}$ double mutants showed a normal body size and tail bud compared to *Lrp6* null mutants. *Lrp4*$^{-/-}$ n=43, *Lrp6*$^{-/-}$ n=40, *Lrp4*$^{-/-}$*; Lrp6*$^{-/-}$ n=10. Scale bar =300 µm

In addition, it was observed that LRP6-deficient embryos also exhibited neural tube closure defects, including caudal truncation and neural tube defects (Figure 8A, B), further highlighting the important role of LRP6 in early forebrain development. However, concerning the neural tube closure phenotype, three out of ten *Lrp4; Lrp6* double mutants exhibited an open anterior neural tube even if the body size and tail defect were rescued (Figure 8E, F), which revealed that the loss of LRP4 might not rescue the neural tube defect that was caused by loss of LRP6.

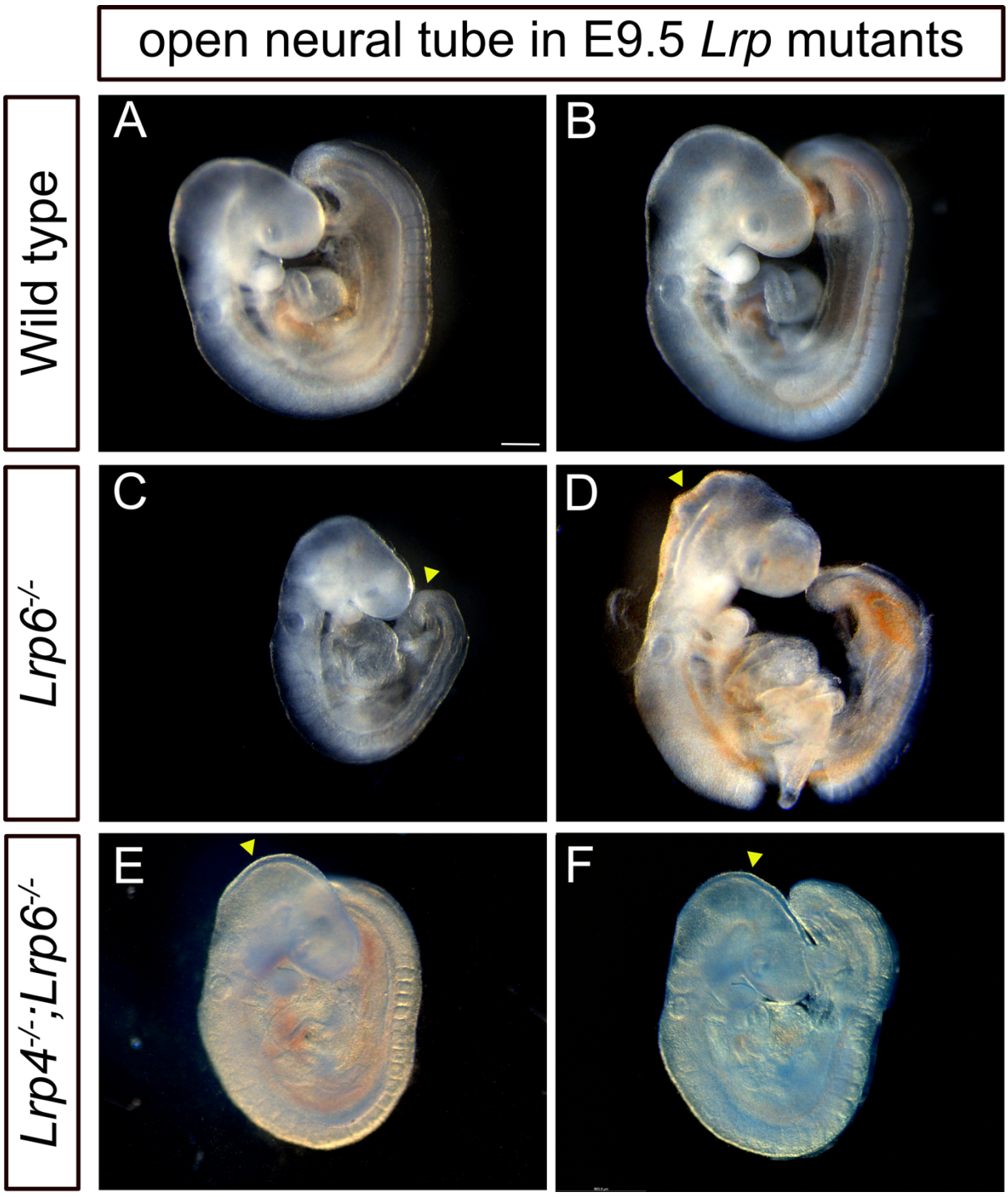


Figure 8: Open anterior neural tube of *Lrp6*$^{-/-}$ and *Lrp4*$^{-/-}$*; Lrp6*$^{-/-}$ mice embryos at E9.5

The open anterior neural tube could be observed in the *Lrp6*$^{-/-}$ mutants (C+D), whereas the neural tube closes at this stage. Most *Lrp4*$^{-/-}$*; Lrp6*$^{-/-}$ mutants showed a normal phenotype concerning the macroscopic appearance, which is similar to wild types (A+B). However, three out of ten *Lrp4; Lrp6* double mutants showed open neural tube (E+F), indicating that loss of LRP4 may not save the deficient

anterior neural tube closure in *Lrp6* null embryos. Neural tube closure defects were indicated by arrowheads. Scale bar =300 μm

Figure 9 presents the numbers mice with caudal truncation (Figure 9D) and open neural tube (Figure 9E), respectively in *Lrp6*$^{-/-}$ versus *Lrp4*$^{-/-}$*; Lrp6*$^{-/-}$ mutants. From the collected embryos, I demonstrated that there is a higher rate of caudal truncation in *Lrp6*$^{-/-}$ (47 out of 49) compared to *Lrp4*$^{-/-}$*; Lrp6*$^{-/-}$ double mutants. *Lrp4*$^{-/-}$*; Lrp6*$^{-/-}$ mutants showed no caudal truncation (six out of ten) or very mild (three out of ten) caudal truncation. Only one *Lrp4*$^{-/-}$*; Lrp6*$^{-/-}$ still displayed a sever tail defects. As for the open neural tube, there were 25% of *Lrp6* mutants showed an open neural tube defect (Figure 9E). However, loss of LRP4 cannot rescue this defect in *Lrp6*$^{-/-}$ embryos completely, three out of ten *Lrp4*$^{-/-}$*; Lrp6*$^{-/-}$ mutants still showed the open neural tube. No caudal truncation or open neural tube was observed in wild types or *Lrp4* mutants.

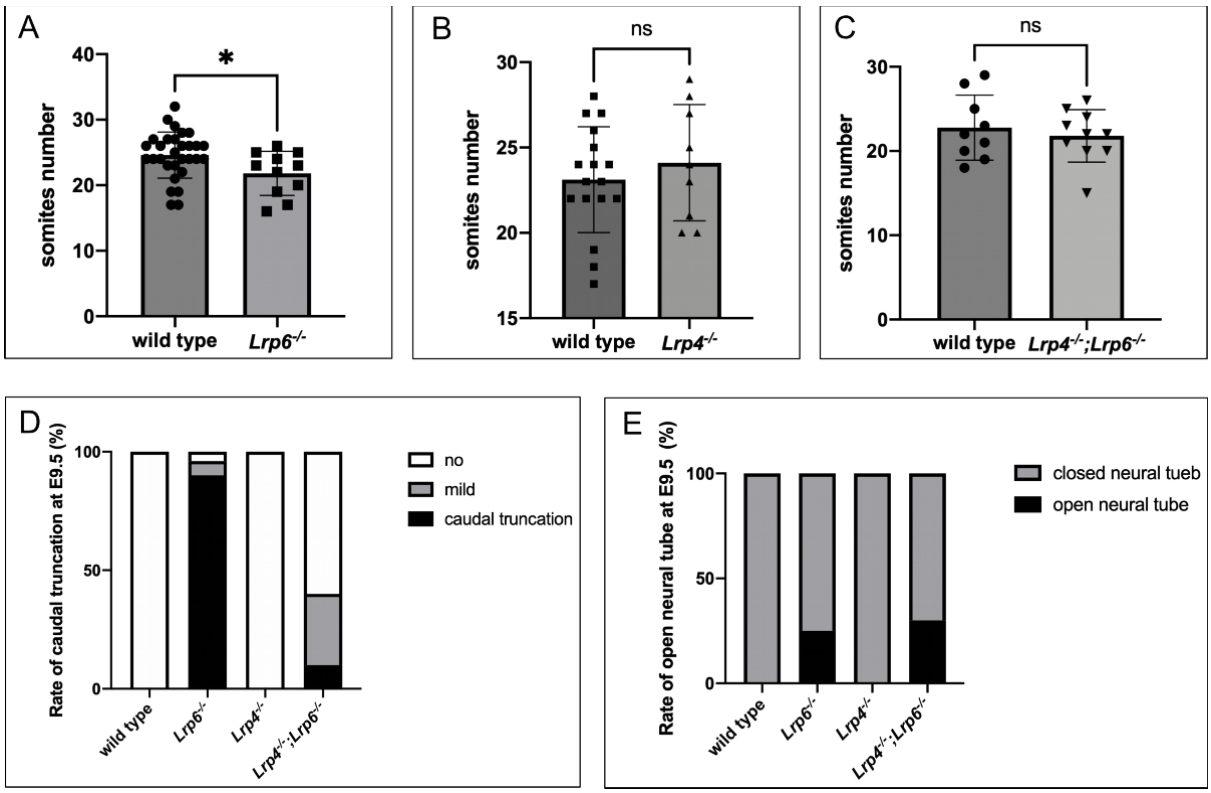


Figure 9: Evaluation of caudal truncation and neural tube defects in *Lrp4*$^{-/-}$, *Lrp6*$^{-/-}$ and *Lrp4*$^{-/-}$*; Lrp6*$^{-/-}$ embryos

(A-C): Somite numbers in mouse embryos of *Lrp4*$^{-/-}$, *Lrp6*$^{-/-}$ and *Lrp4*$^{-/-}$*; Lrp6*$^{-/-}$ mutants genotype at embryonic stage E9.5. (A): *Lrp6*$^{-/-}$ embryos showed a significant reduction in body size compared to

wild-type littermates, (B): *Lrp4*$^{-/-}$ mutants showed no significant difference compared to wild types, (C): interestingly, the somites count of *Lrp4; Lrp6* double mutants was similar to that in wild types. P values based on Student's *t*-test. *P<0.05

(D+E): The rate of caudal truncation (Left) and open neural tube (Right). (D): The caudal truncation in *Lrp6*$^{-/-}$ mutants was partially rescued by loss of LRP4. In *Lrp4*$^{-/-}$*; Lrp6*$^{-/-}$ mutants, the caudal truncation was either milder than that in *Lrp6*$^{-/-}$ embryos (three out of ten), or even not present (six out of ten). Only one out of ten *Lrp4*$^{-/-}$*; Lrp6*$^{-/-}$ still displayed a severe tail defect. (E): While open neural tube defects occurred in similar rates in both *Lrp6*$^{-/-}$ and *Lrp4*$^{-/-}$*; Lrp6*$^{-/-}$ mutants at around 30%. Loss of LRP4 could not rescue the open neural tube caused by loss of LRP6. All wild types and *Lrp4* mutants displayed a completely closed neural tube.

Furthermore, we also detected the thickness of the neuroepithelia (NE) layer in different genotypes and found that there is a clear decrease of NE thickness in *Lrp6*$^{-/-}$ mutants comparing to wild types. There is no difference between the thickness of wild type and *Lrp4* null mice. Interestingly, when comparing the *Lrp4; Lrp6* double embryos and wild types there is no difference (Figure 10). This decrease in NE thickness in *Lrp6*$^{-/-}$ mutants may contribute to the smaller size of the forebrain observed in these mutants, while the similar NE thickness in *Lrp4*$^{-/-}$*; Lrp6*$^{-/-}$ double mutants may explain why the forebrain size is rescued in these mutants.

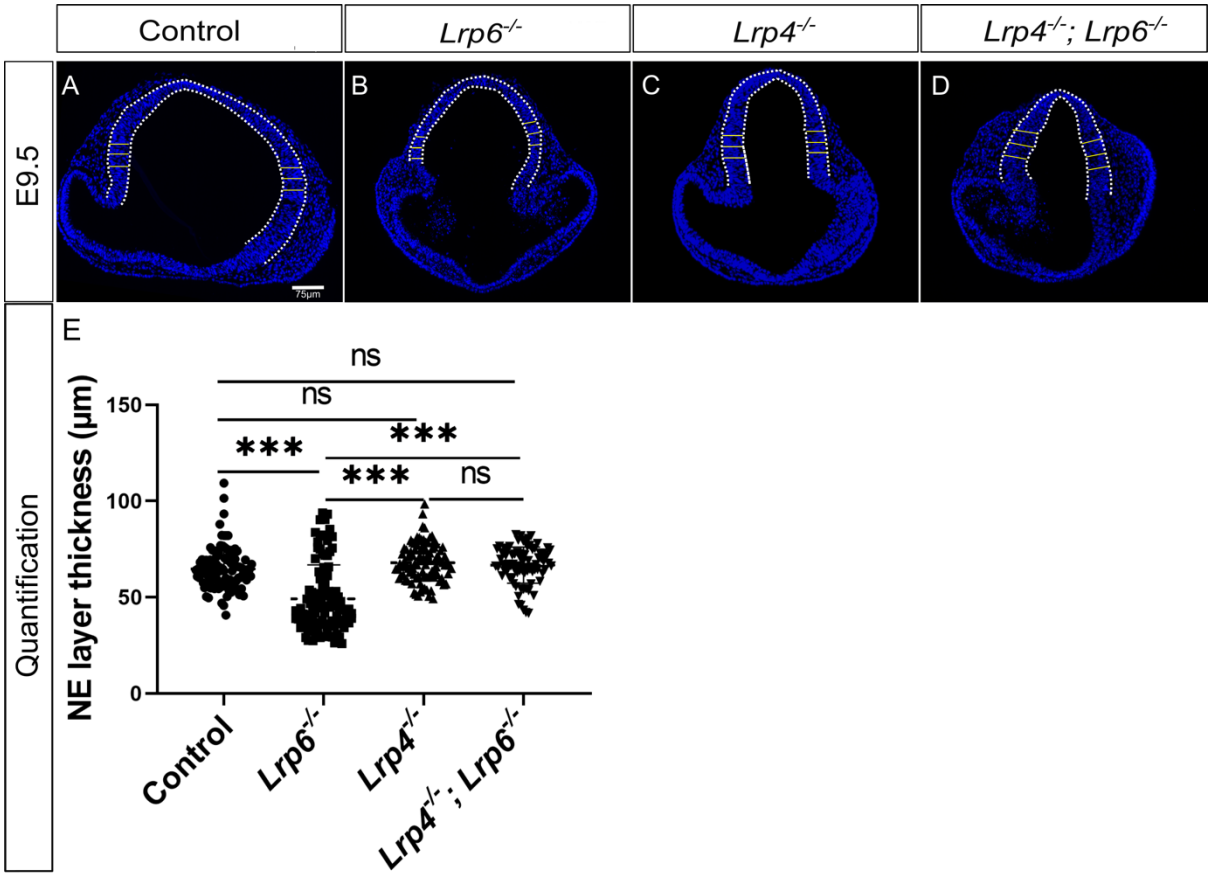


Figure 10: Representative images of coronal sections from E9.5 embryos stained with DAPI.

*Lrp6*$^{-/-}$ mutants (B) displayed in average a significantly thinner neuroepithelium compared to embryonic stage-matched wild-type controls (A**)** and *Lrp4*$^{-/-}$ mutants (C), which had normal neuroepithelial morphology comparable to controls. *Lrp4*$^{-/-}$; *Lrp6*$^{-/-}$ double mutants (D) showed a rescue of neuroepithelium thickness compared to *Lrp6*$^{-/-}$ single mutants and had a neuroepithelial morphology comparable to controls. Scale bar=75µm. (E) The quantification of the measurements of the forebrain neuroepithelium thickness. The bars indicating the thickness of the forebrain neuroepithelium at E9.5 measured along the dorsolateral domain indicated by the dotted line. For each sample 5 to 15 sections were examined; wild types n = 4, n = 3 *Lrp6*$^{-/-}$ mutants n=3, *Lrp4*$^{-/-}$ mutants n = 3, *Lrp4*$^{-/-}$; *Lrp6*$^{-/-}$ double mutants n = 4. P values based on One-way ANOVA. ***P<0.005

From the results above we can conclude that *Lrp4* can be a genetic modifier for the growth retardation and forebrain hypoplasia phenotypes caused by loss of LRP6 at E9.5 developing forebrain, but not for the neural tube closure defects.

## 4.2 LRP4 is modulating LRP6 mediated functions in the neuroepithelium of the early forebrain

### 4.2.1 Loss of LRP4 can rescue abnormal SOX2 pattern in *Lrp6*$^{-/-}$ mutants

Next, to gain further insights into how LRP4 modulates LRP6 during early forebrain development, detailed analysis of forebrain structures was performed for all mutants at E9.5. I analyzed the forebrain structures of all mutants in more detail at E9.5. First, I analyzed the expression pattern SRY-box 2 (SOX2). SOX2 encodes a highly conserved transcription factor and is a marker of neural progenitor and stem cells throughout the vertebrate CNS, expressed in embryonic proliferating neural stem cells (Graham et al., 2003; B. Lee et al., 2013). In mouse embryos, SOX2 starts to be expressed in the neural plate, which is the earliest stage of CNS development and will fold to form the neural tube in later stages (Zappone et al., 2000).

I applied whole mount immunofluorescence staining with an antibody against SOX2. With this method, I can get an overview of the forebrain neural tube structure without sectioning and investigate the morphology of the pseudostratified neuroepithelium in all genotypes. The aim was also to detect possible differences in the pattern for SOX2 in *Lrp4*$^{-/-}$, *Lrp6*$^{-/-}$, and double mutants. With the help of the Advanced light microscopy technology platform at the MDC, I obtained images of the whole embryonic head. In the wild type, SOX2 is mainly expressed in the anterior forebrain and in the dorsolateral domain of the diencephalon and mesencephalon. Whole-mount immunofluorescence results showed that there is more signal for SOX2 in the *Lrp4*$^{-/-}$ mutant, compared to that in wild types, especially in the dorsal brain. However, in *Lrp6*$^{-/-}$ mutant there was less SOX2 signal compared to wild type. Interestingly, the SOX2 signal in *Lrp4*$^{-/-}$*; Lrp6*$^{-/-}$ embryo forebrain was rescued and similar to that in the wild type (Figure 11). Interestingly, in *Lrp4*$^{-/-}$*; Lrp6*$^{-/-}$ embryo, a stronger SOX2 signal could be also detected in the dorsal telencephalon compared to wild type.

The result showed that loss of LRP6 leads to an aberrant SOX2 pattern, suggesting patterning defects of the neural tube that might be caused by reduced proliferation. Loss of LRP4 can rescue the abnormal SOX2 pattern in *Lrp6* mutants (Figure 11).

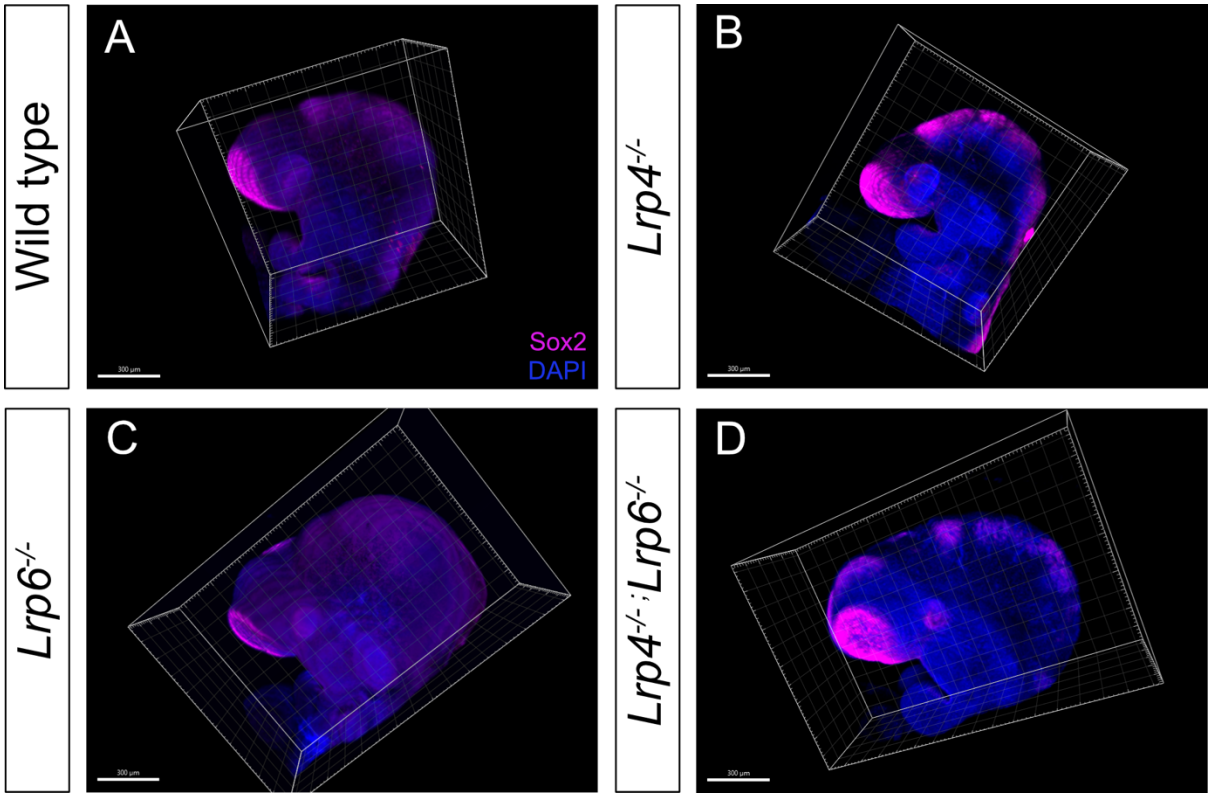


Figure 11: SOX2 pattern in the embryonic brain detected by whole mount immunohistochemistry.

The immunofluorescence analysis of SOX2 expression in the developing forebrain at E9.5 revealed that the *Lrp4*$^{-/-}$ embryos (B) displayed a stronger signal for SOX2 in the dorsal and anterior part of the forebrain compared to the wild type (A) (n=1). In contrast, the loss of LRP6 (C) resulted in a significant decrease in SOX2 signal in the forebrain (n=1). Interestingly, the abnormal SOX2 pattern observed in *Lrp6*$^{-/-}$ mutants was rescued by the loss of LRP4 (D) (n=1). Scale bar =300 µm

### 4.2.2 Loss of LRP4 can rescue decreased proliferation in the neuroepithelium of *Lrp6*$^{-/-}$ mutants

Mitosis is critical to cell fate determination during development. Neural progenitors divide specifically to enrich a certain cell population or generate a differentiated progeny (Molina & Pituello, 2017). During CNS development, precise control of cell proliferation, cell death, and cell differentiation happens during the expansion of the neural progenitor cell population in the neuroepithelium, resulting in the formation of complex neural structures (brain and spinal cord) (Pai et al., 2015). The neural tube development is under the control of complex regulatory mechanisms that coordinate proliferation, fate specification, and differentiation. A crucial transition, which is from

proliferation to differentiation, happens during the G1 phase of the cell cycle (Lukaszewicza & Anderson, 2011).

Next, to analyze the proliferation status in the forebrain of the various *Lrp* mutants, I performed immunohistochemistry on coronal forebrain sections of various planes along the anterior-posterior axis as indicated in Figure 4.3. Phosphorylation of histone H3 at serine 10 occurs in mitotic cells of various specifies and organs (M. Huang et al., 2022). Immunofluorescence labelling for the proliferation marker phospho-histone-H3 (pHH3) was used to visualize and quantify mitotic cells within the neuroepithelium (Figure 12). pHH3 visualizes late G2 and the four phases of mitosis (prophase, metaphase, anaphase and telophase) (Nielsen et al., 2013).

*Lrp6*$^{-/-}$ embryos showed a markedly reduced number of mitotic cells in the neuroepithelium at E9.5 compared to the rate of pHH3 positive cells in wild-type embryos. No difference regarding the count of mitotic cells within the neuroepithelium was detected in *Lrp4*$^{-/-}$ *embryos* compared with wild types. There was a tendency that the rate of mitotic cells in *Lrp4*$^{-/-}$*; Lrp6*$^{-/-}$ double mutants was similar to levels in wild types at E9.5. (Figure 12). The quantification was done within the neuroepithelium. Four areas of the same size were chosen for quantification, two were in the dorsal part of the forebrain and the other two were in the ventral forebrain. The pHH3 and DAPI-labelled cells were counted separately in each box. The average rate of pHH3 positive cells compared to DAPI was taken for quantification. Positive cells labelled with pHH3 and nuclei labelled with DAPI were counted with Fiji, respectively. The rate of pHH3 positive cell was calculated according to the count of DAPI divided with the count of pHH3 positive cells. Then average was taken with the rate of the four areas chosen in dorsal and ventral of neuroepithelium.

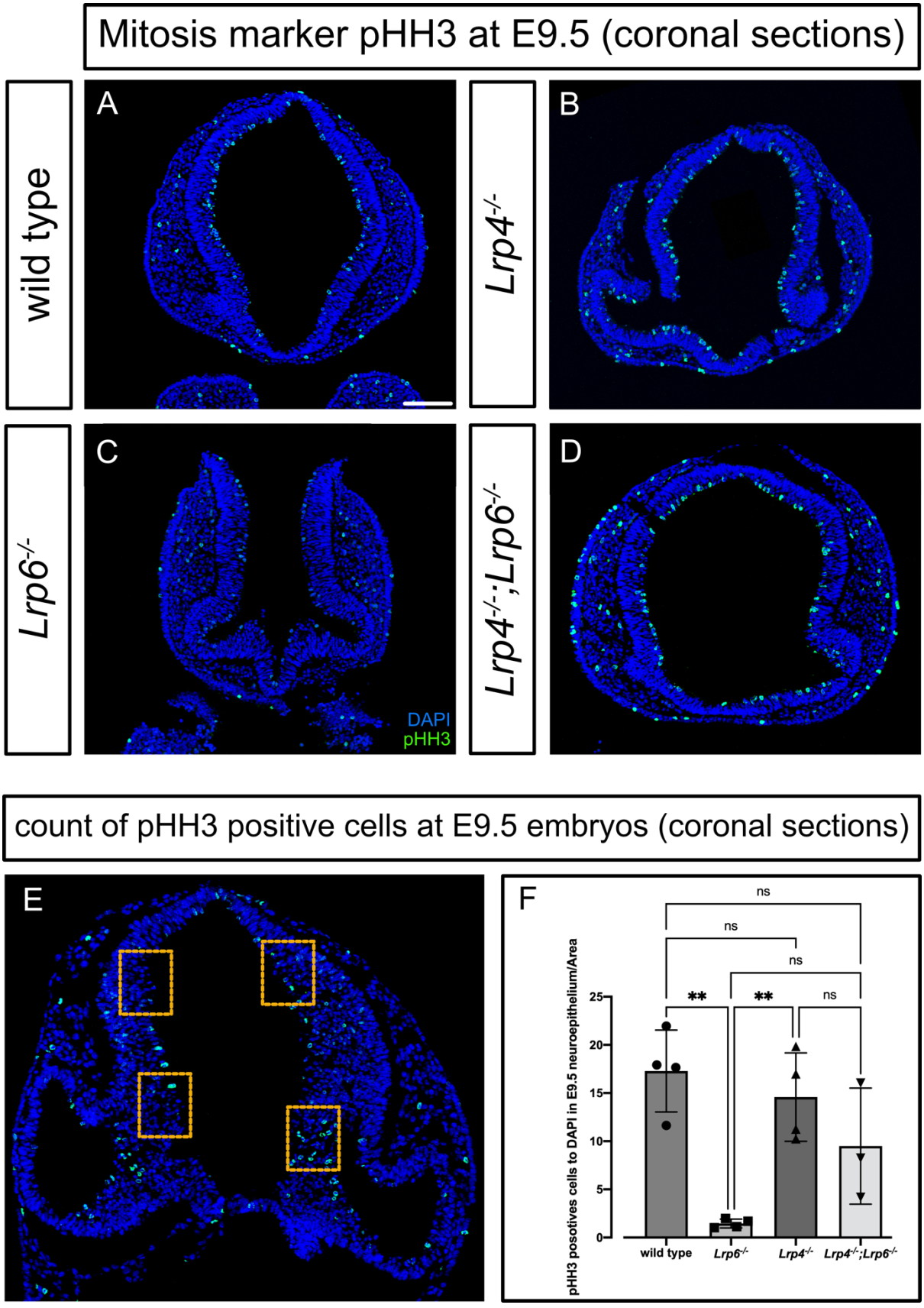


Figure 12: Loss of LRP4 can partially rescue decreased proliferation in the neuroepithelium of *Lrp6*$^{-/-}$ mutants.

(A-D): pHH3 positive cell bodies are detected at the apical side of the neuroepithelium in the wild type (A) (n=3) and *Lrp4*$^{-/-}$ (B) (n=4) embryos. Less mitotic cells were observed in *Lrp6*$^{-/-}$ (C) (n=6) at E9.5 comparing to wild type. A tendency of the rescue of pHH3 positive cells could be visualized in neuroepithelial excrescences of E9.5 *Lrp4*$^{-/-}$*; Lrp6*$^{-/-}$ embryos (D) (n=3) comparing to *Lrp6*$^{-/-}$ embryos. Scale bar =100 µm

(E+F): Rate of pHH3 cells to DAPI positive cells in the neuroepithelium of *Lrp* mutant embryos. Four areas were chosen as the orange rectangular shown in panel E. Loss of LRP6 leads to a decrease in mitotic activity in the developing forebrain. Quantification was normalized with DAPI. P values based on One-way ANOVA. *P<0.05

Furthermore, aberrant localization of the cell body positive for pHH3 could be observed in *Lrp6* mutants (Figure 13B). During the cell cycle, the nucleus migrates from apical to basal at the G1 phase stage, where the cell is preparing to divide, and from basal towards apical at the G2 phase, during which the cells are prepared themselves for mitosis (Kosodo & Huttner, 2009). The mitotic nuclei can usually be detected apically within the cell of the neuroepithelium, facing the lumen. However, in some *Lrp6*$^{-/-}$ embryos, the pHH3 positive nuclei appeared in the more basal part of the neuroepithelium, as shown in Figure 13.

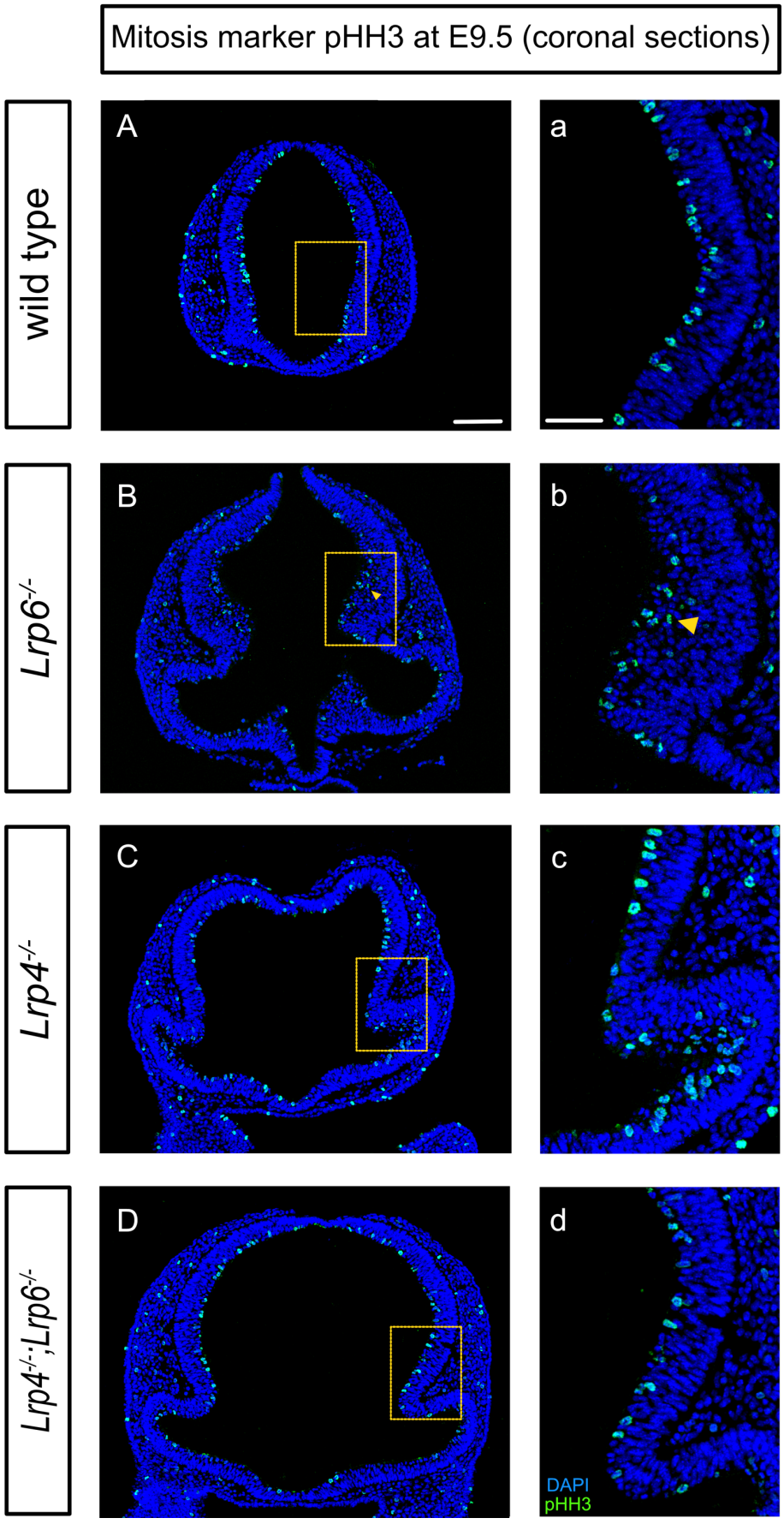


Figure 13: Loss of LRP6 can cause the dislocation of mitotic nuclei in the neuroepithelium.

In *Lrp6*$^{-/-}$ embryos (B), a dislocation of pHH3 positive nuclei can be seen as shown in this figure in the yellow box. The arrowheads in the images indicate the abnormal positioning of pHH3-positive cell bodies in the neuroepithelium. In the wild types (A), *Lrp4* null (C) and *Lrp4; Lrp6* double mutants (D), the mitotic nuclei were located properly at the apical surface of the neuroepithelium. Scale bar =100 μm

(a-d): Zoom-in images of the boxed areas in (A-D). Scale bar = 50 μm

In previous work from our lab another mitotic marker, mitotic protein monoclonal 2 (MPM-2), which marks all cells in M-phase was analyzed in all *Lrp* mutants. These studies also confirmed that *Lrp6*$^{-/-}$ embryos showed a markedly reduced number of mitotic cells in the neuroepithelium at E9.5 compared to the rate of M-phase cells in wild-type embryos (Geng et al., 2023). *Lrp4*$^{-/-}$; *Lrp6*$^{-/-}$ double mutant embryos showed a rescue of the impaired mitotic activity in *Lrp6*$^{-/-}$ mutants. The results on MPM-2 also support my result of pHH3 signals in the forebrain of all *Lrp* genotypes. Unfortunately, due to the low sample number for the double mutants, we could not perform rigorous quantification.

Together with the result on SOX2 whole mount staining, we can draw the conclusion that loss of LRP6 leads to a decrease in the neuronal progenitor pool; furthermore, loss of LRP4 in *Lrp6* mutants rescues the loss of SOX2 positive progenitors and might lead even to sporadic hyperproliferation.

These results support the hypothesis that loss of proliferative neuronal progenitors caused by decreased WNT signaling activity in *Lrp6*$^{-/-}$ mutants, can be rescued in *Lrp4*$^{-/-}$*; Lrp6*$^{-/-}$ double mutants.

## 4.3 Loss of LRP4 can rescue WNT activity and WNT target gene expression in the neuroepithelium of *Lrp6* mutants

### 4.3.1 Loss of LRP4 can rescue WNT signaling activity in the neuroepithelium of *Lrp6* mutants

To further test our hypothesis, that altered WNT signaling is the underlying cause of changes in the pool of proliferating neuronal precursors and to address the question of how WNT signaling is balanced by LRP family members and how LRP4 and LRP6

functionally interact with each other during early forebrain development we crossed the WNT activity reporter mouse line *Tg(TCF/Lef1-HIST1H2BB/EGFP)*$^{61Hadj}$ transgenic reporter mouse line (here referred to as *TCF/Lef:H2B-GFP* reporter line) with all *Lrp* mutants (Ferrer-Vaquer et al., 2010). In this mouse line, the H2B-GFP cassette was placed under the control of six *TCF/Lef* response elements hsp68 minimal promoter to generate a strain of mice that can be used to visualize WNT/ß-catenin signaling activity (Ferrer-Vaquer et al., 2010). *TCF/Lef:H2B-GFP* transgenic mice express GFP protein under the control of TCF/LEF promoter. This reporter line serves as a genetic tool to visualize WNT responsiveness in cells that activated TCF/LEF gene expression.

First, it was confirmed that most GFP-positive neural progenitors were located in the dorsolateral part of the neural tube, which overlapped with the domains that are underlying WNT-dependent patterning. Then I demonstrated that GFP signal intensity was markedly reduced in *Lrp6*$^{-/-}$ mutants compared to wild types. This result showed that there was reduced WNT activity in the E9.5 embryonic anterior neural tube of *Lrp6*$^{-/-}$ mutants compared to wild types (Figure 14C, G). In contrast, in *Lrp4*$^{-/-}$ mutants (Figure 14B, F), GFP signals were significantly stronger than that in wild types, especially at the dorsal neural tube, where the *Lrp4* expression is mainly observed in the forebrain at E9.5 (Geng et al., 2023). Markedly, the GFP signals in *Lrp4; Lrp6* double mutant samples were increased compared to *Lrp6* null mutants and similar to that in wild types (Figure 14D, H). Analyses were performed in a more posterior area (section plane 2) and anterior area (section plane 1) of the forebrain (Figures 14). Interestingly, the GFP positive cells in the *Lrp4*$^{-/-}$*; Lrp6*$^{-/-}$ double mutants extended towards the dorsal midline of the neural tube, the domain that normally shows expression for *Lrp4* at E9.5 in forebrain.

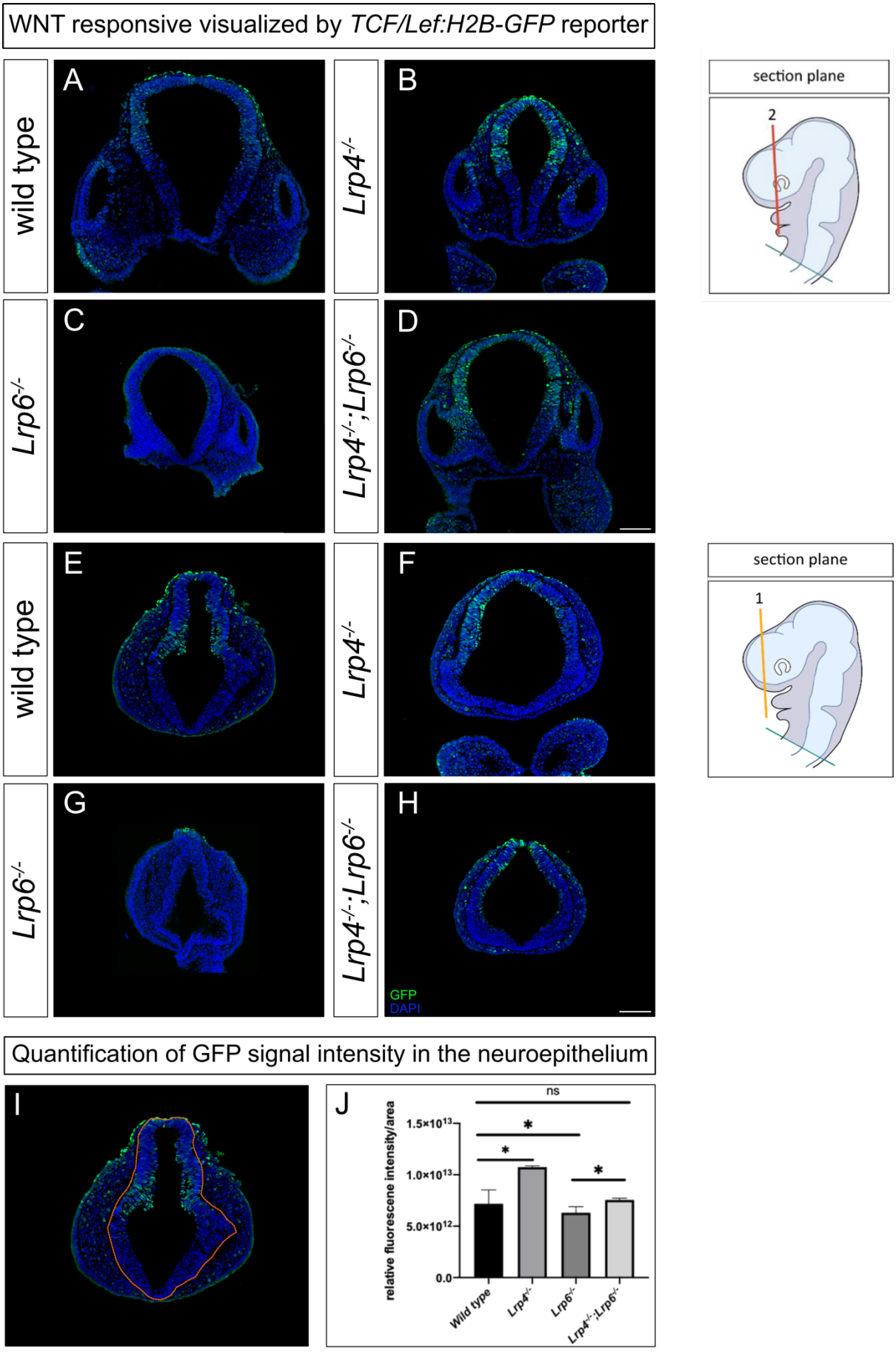
WNT responsive visualized by TCF/Lef:H2B-GFP reporter
wild type
A
Lrp4-/-
B
Lrp6-/-
C
Lrp4-/-;Lrp6-/-
D
section plane
2
wild type
E
Lrp4-/-
F
Lrp6-/-
G
Lrp4-/-;Lrp6-/-
H
section plane
1
GFP
DAPI
Quantification of GFP signal intensity in the neuroepithelium
I
J
ns
*
*
*
relative fluorescene intensity/area
1.5×10^13
1.0×10^13
5.0×10^12
0.0
Wild type
Lrp4-/-
Lrp6-/-
Lrp4-/-;Lrp6-/-

Figure 14: Loss of LRP4 can rescue impaired WNT signaling in the telencephalic neuroepithelium of *Lrp6*$^{-/-}$ mutants.

(A-H): To visualize WNT-responsive ß-catenin signaling in neural progenitor cells in the forebrain we crossed *Lrp* mutants onto a *TCF/Lef:H2B-GFP* reporter line. (B+F): Immunohistochemistry, detecting GFP signals as a readout for WNT signaling strength, confirmed that there were obvious differences in GFP levels between *Lrp4*$^{-/-}$ embryos (n=3) and wild type controls with higher levels in *Lrp4*$^{-/-}$ samples. (C+G): *Lrp6*$^{-/-}$ embryos (n=3) showed a greatly reduced of GFP expression in the developing forebrain. (H+G): In contrast, more GFP signals were detected in dorsal regions of the neural tube of E9.5 *Lrp4*$^{-/-}$ *; Lrp6*$^{-/-}$ embryos (n=3). Quantification was done in the planes between the telencephalon and the area of the developing eye. Scale bar = 100 µm.

(I+J): (I) The outer circumference of the neural tube (dotted line) was measured. (J) Quantification of GFP signal intensity in the forebrain of the different genotypes. P values based on One-way ANOVA. *P<0.05

My results from the analysis of *TCF/Lef:H2B-GFP* reporter activity in *Lrp4*$^{-/-}$*; Lrp6*$^{-/-}$ forebrain indicate a rescue of WNT signaling in *Lrp6*$^{-/-}$ mutants upon loss of LRP4. We can further conclude that LRP4 acts as an inhibitor of LRP6 mediated WNT signaling in the developing forebrain.

### 4.3.2 Loss of LRP4 can rescue WNT downstream targets in the neuroepithelium of *Lrp6* mutants

To test whether LRP4 and LRP6 can functionally interact and thereby influence the activity of WNT downstream targets, I also tested levels of cyclin D1, a key downstream target of WNT/ß-catenin signaling that is activated by the WNT pathway transcription factor LEF1. Cyclin D1 influences cell proliferation in G1 phase and survival during neural tube development (Lukaszewicza & Anderson, 2011). In the developing telencephalon, cyclin D1 is expressed in the ventrolateral region of the neural tube but not in the dorsal midline (Lukaszewicza & Anderson, 2011).

Immunohistochemistry results indicated that there were no changes in cyclin D1 levels in *Lrp4*$^{-/-}$ embryos compared to wild type controls, but an extension of the signals for cyclinD1 towards the dorsal midline of the neural tube could been observed. Interestingly the dorsal midline is the domain that normally shows prominent Lrp4

expression. *Lrp6*$^{-/-}$ mutant embryos showed markedly reduced signals for cyclin D1 at the dorsal neural tube (Figure 15C). The loss of cyclin D1 signals that was observed in the forebrain of *Lrp6* single mutants was partially rescued in *Lrp4*$^{-/-}$*; Lrp6*$^{-/-}$ double mutant embryos that showed stronger signals for cyclin D1 levels in the dorsolateral domain of the forebrain compared to *Lrp6*$^{-/-}$ single mutants (Figure 15D). In combination with existing data from the lab (from Fabian Paul), we quantified the cyclin D1 signal intensity within the neuroepithelium and confirmed the differences as statistically significant. The quantification was done with the help by my colleague Tamrat Mamo.

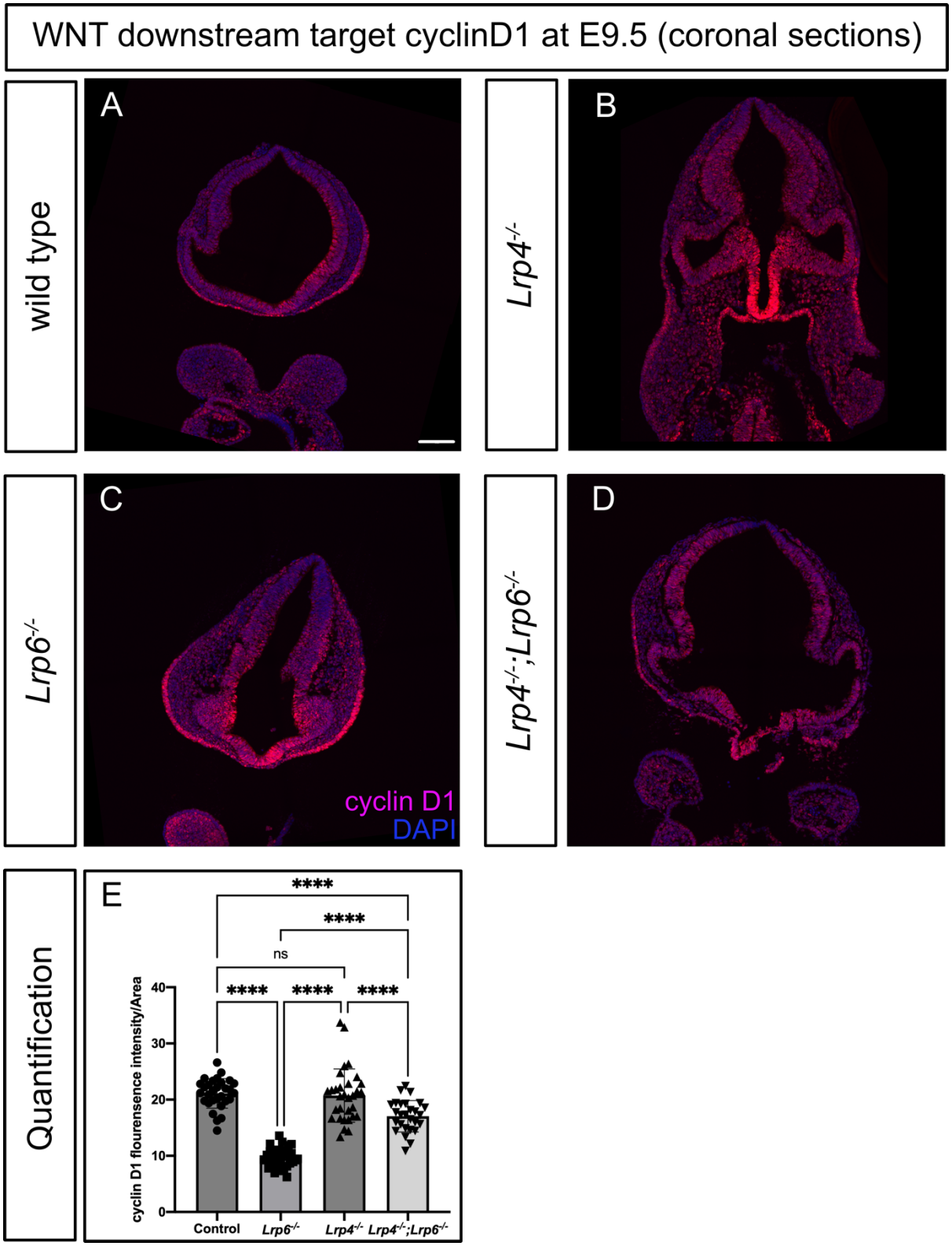


Figure 15: WNT/ß-catenin downstream target cyclin D1 signal intensity is reduced in the forebrain of *Lrp6*$^{-/-}$ mutants but not in *Lrp4*$^{-/-}$*; Lrp6*$^{-/-}$ embryos at E9.5 compared with wild types.

(A-D): Immunostaining on E9.5 coronal forebrain sections showed broad localization of cyclin D1 within the forebrain neuroepithelium. Loss of LRP4 did not affect levels of cyclin D1 in the neuroepithelium (B). *Lrp6*$^{-/-}$ embryos (C) showed a great reduction of cyclin D1 protein in neural progenitors comparing

to wild type (A). However, compared to *Lrp6*$^{-/-}$ single mutants *Lrp4*$^{-/-}$*; Lrp6*$^{-/-}$ double mutant embryos (D) showed a rescue of cyclin D1 levels in the dorsolateral domain of the telencephalon at E9.5. Scalebar = 100 µm.

(E): Quantification of cyclin D1 signals in the neuroepithelium at E9.5 of the different genotypes. Cyclin D1 signals were increased in *Lrp4*$^{-/-}$ embryos (n = 3) compared to wild types (n = 3) at E9.5. In contrast, cyclin D1 signals were significantly lower in *Lrp6*$^{-/-}$ mutant mice (n = 4) compared to wild types (n=3). However, signal intensity levels for cyclin D1 in *Lrp4*$^{-/-}$*; Lrp6*$^{-/-}$ samples (n = 3) were similar to that in wild types (n=3). P values based on One-way ANOVA. ****P<0.0001

This result showed that loss of LRP4 can rescue the decrease of WNT downstream target activity caused by loss of LRP6.

Now we can confirm that brain developmental disorders caused by loss of *Lrp6* can be partially rescued by loss of LRP4. Loss of LRP4 can rescue WNT signaling in the forebrain of LRP6-deficient embryos. We hypothesize that LRP4 acts as a negative modulator of WNT activity counteracting the function of LRP6. Mouse genetics combined with our functional analyses identified *Lrp4* as a genetic modifier for *Lrp6* in forebrain development.

## 4.4 LRP4 is a central modulator of the WNT signaling pathway in a more general context beyond forebrain development

### 4.4.1 Human TERT RPE-1 cells as a model system to study how WNT signaling is balanced

Our results in the mouse model suggested that LRP4 acts as an antagonist to LRP5/6 function in WNT signaling. Next, I wanted to test whether the functional interaction between LRP4 and LRP6 is not only relevant in the mouse neuroepithelium but whether this is a systems wide overarching mechanism. In addition, we aimed at elucidating the molecular mechanism underlying the interaction between these LRP family members. Towards this aim we tested our hypothesis using cell culture models. The hTERT RPE-1 cell line, a human retinal pigmented epithelial cell line, is a commonly used *in vitro* model for analyzing WNT signaling (Emons et al., 2017).

I confirmed expression of *LRP4* and *LRP6* in this cell line at RNA level by RT-PCR (Figure 16C) and at protein level by Western blotting analyses (Figure 16A, B). I performed siRNA silencing experiments to reduce *LRP4* and *LRP6* expression. Thereby I was able to test whether WNT signaling strength can be fine-tuned by modulating expression levels of *Lrp4* and *Lrp6*, respectively.

As a proof of concept for my approach I could demonstrate that siRNA mediated knockdown resulted in significant reduction of RNA or protein levels of LRP4 and LRP6, respectively, compared to controls. Moreover, knockdown of LRP4 and LRP6, respectively in hTERT RPE-1 cells did not affect the expression of each other.

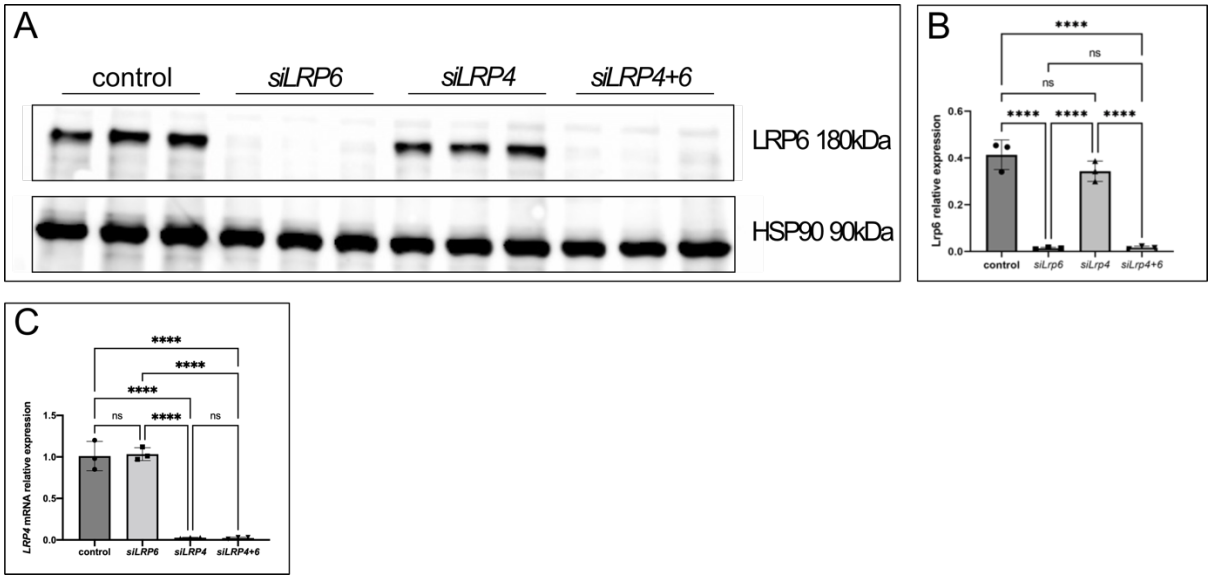


Figure 16: Western blotting analysis and quantitative RT-PCR confirmed reduction of *LRP6* RNA and LRP6 protein level, respectively after siRNA mediated silencing in hTERT RPE-1 cells.

(A+B): Western blotting analyses revealed that LRP6 protein levels were significantly reduced in hTERT RPE-1 cells after siRNA mediated silencing compared to controls treated with scrambled siRNA. *LRP4* expression was not influenced when *LRP6* was downregulated. P values based on One-way ANOVA. ****p≤ 0.0001

(C): qPCR result showed that LRP4 expression was decreased in *siLRP4* treated cells but not in siLrp6 treated cells. P values based on One-way ANOVA. ***p≤ 0.001, ****p≤ 0.0001

### 4.4.2 Silencing of *LRP4* can rescue the reduced proliferation in *LRP6* knocked down cells.

It has been reported that ß-catenin interacts with TCF to form the complex that induces gene transcription, leading to the activation of cyclin-dependent kinases responsible of cell cycle progression from G1 to S phase (Kuznetsova et al., 2014).

To evaluate whether LRP4 can balance WNT signaling and influence proliferation of hTERT RPE-1 cells, as shown *in vivo*, the proliferation markers MPM-2 (Figure 17) and pHH3 (Figure 18) were tested in siRNA treated cells. Our previous work in mice showed that cell cultures with *LRP6* knockdown had a significantly decreased number of mitotic cells compared to that of the control cultures.

Consistent with our in vivo findings, knockdown of LRP6 resulted in a significant decrease in the number of MPM-2-positive cells compared to control siRNA treated cells (Figure 17B). No difference in the number of mitotic cells was observed in cells with *Lrp4* silencing compared to the control siRNA treated cells (Figure 17C). Interestingly, a higher rate of mitotic cells, which was comparable to the control, was detected in *LRP4* and *LRP6* double knockdown cells (Figure 17D), suggesting that LRP4 can balance WNT signaling to regulate cell proliferation.

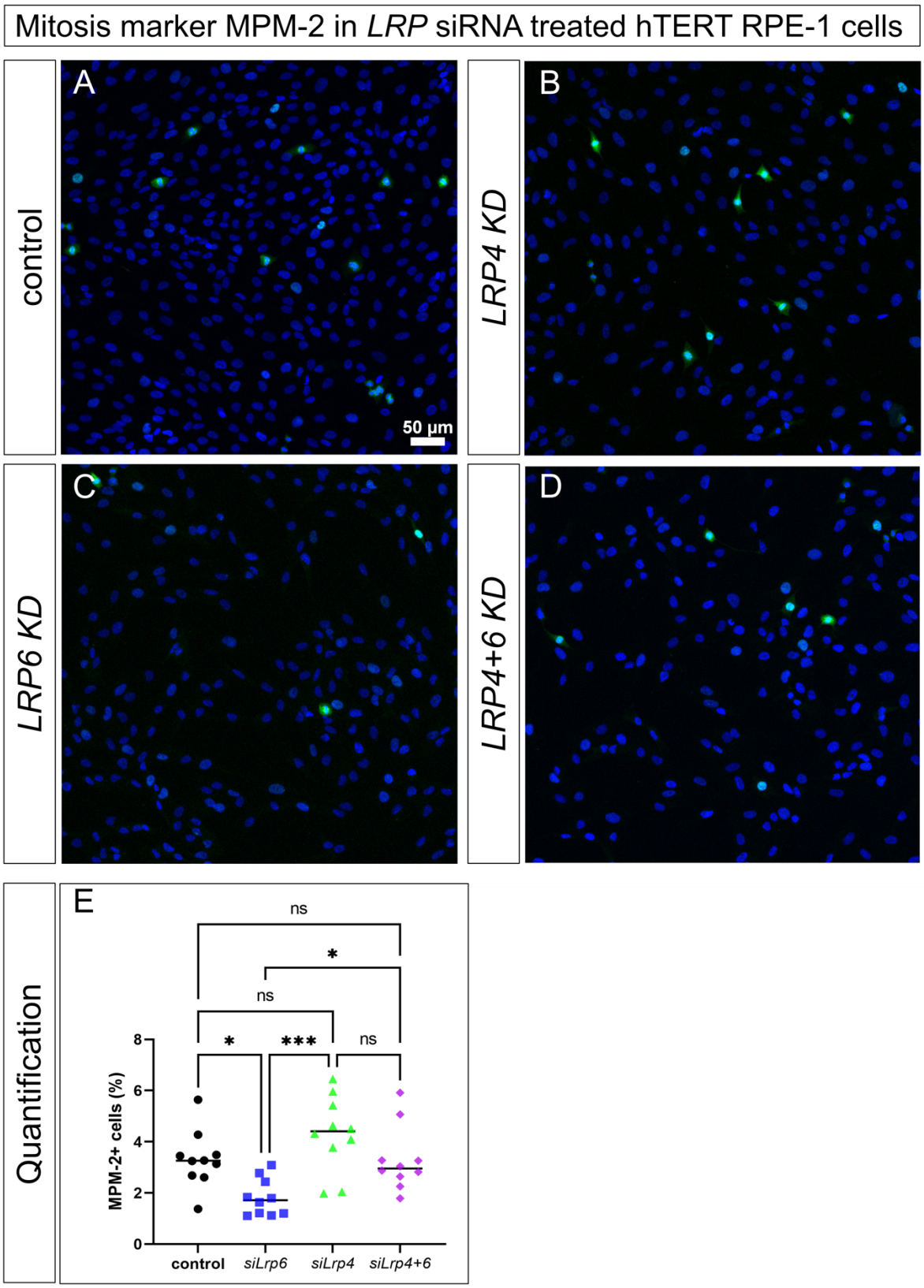


Figure 17: Mitosis marker MPM-2 in *LRP* siRNA treated RPE cells.

(A-D): MPM-2 positive cells are detected in hTERT RPE-1 cells. Less mitotic cells were observed in cells with siRNA mediated downregulation of LRP6 levels (C). An increased count of MPM-2 positive

cells could be visualized in *Lrp4*; *Lrp6* double knockdown cells (D). When LRP4 was decreased (B), the rate of MPM-2 signals was not changed compared to controls (A). Scalebars=50 µm.

(E): Quantification was normalized to DAPI positive cells. P values based on One-way ANOVA. **p<0,01, ***p≤ 0.001

The results of our study indicate that knockdown of *LRP6* in cultured cells led to a significant reduction in the number of pHH 3 positive cells as observed in MPM-2 staining results, indicating a decrease in mitotic activity (Figure 18B). This is consistent with previous findings in *Lrp6* null mice (Figure 12C), where impaired mitotic activity of forebrain neuronal precursors was observed. Moreover, we observed that concomitant knockdown of *LRP4* and *LRP6* led to a higher mitotic rate compared to cells with only *LRP6* knockdown (Figure 18D). Surprisingly, the mitotic rates in *LRP4* and *LRP6* double downregulated cells were comparable to those in the control group, suggesting that downregulation of LRP4 could rescue cell proliferation in the absence of LRP6 (Figure 18D).

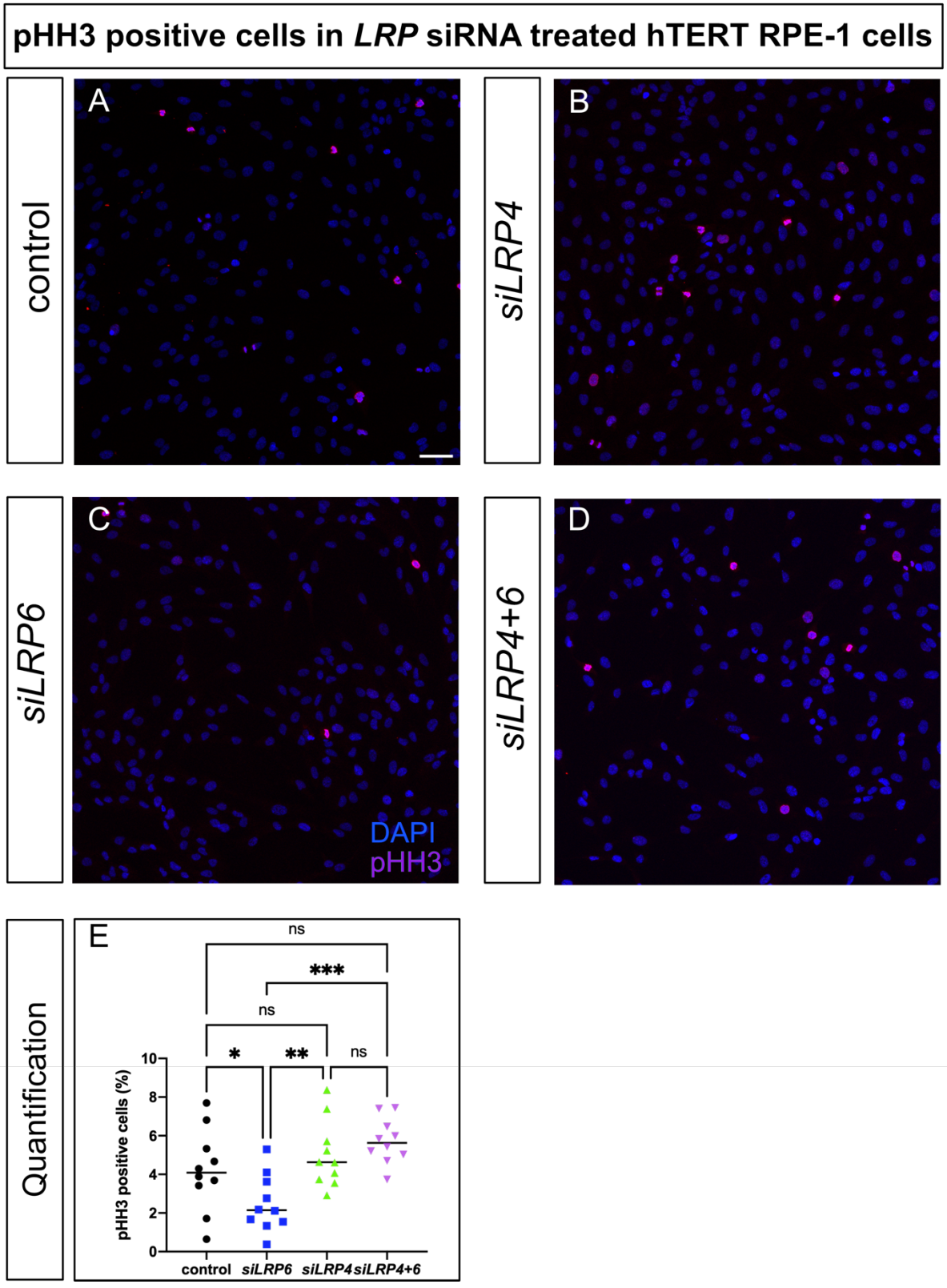


Figure 18: Mitosis marker pHH3 in *siRNA* treated hTERT RPE-1 cells silencing LRP4, LRP6 or both.

(A-D): pHH3 positive cells are detected in hTERT RPE-1 cells. Less pHH3 labelled cells were observed in *LRP6* knockdown cells (C). An increased count of pHH3 positive cells could be observed in *LRP4; LRP6* double knockdown cells (D) compared to single *siLRP6* treated cells. Specifically, the counts

were comparable to those in the control group (A), indicating that LRP4 knockdown can partially rescue the mitotic defect induced by *LRP6* knockdown. Additionally, there was no discernible difference between *LRP4* siRNA treated cells (B) and the control group, or between downregulated *LRP4* single and *LRP4; LRP6* double downregulated cells. Scale bar=50 µm.

(E): Quantification of pHH3 positive cells was normalized to DAPI counts. No significant changes in the rate of mitotic cells compared to controls were observed after knocking down *LRP4*. P values based on One-way ANOVA. *p<0.05, **p<0.01, ***p≤ 0.001

These results showed that loss of LRP6 not only decreased the proliferation of neuroepithelial cells *in vivo* but also caused a reduction of mitotic cell numbers *in vitro*; loss LRP4 on top of LRP6 silencing can rescue the impaired proliferative capacity caused by loss of LRP6 *in vitro*. Taken together, my results support the notion that LRP4 and LRP6 play important roles in regulating cell proliferation, consistent with their known roles in embryonic development. Moreover, our findings suggest that LRP4 may have compensatory functions in promoting cell proliferation in the absence of LRP6.

### 4.4.3 Functional interaction of LRP4 and LRP6 within the WNT signaling pathway in human TERT RPE-1 cells

The study aimed to investigate the potential modulation of WNT downstream targets by functional interaction of LRP4 and LRP6 beyond forebrain development. To achieve this, hTERT RPE-1 cells were utilized and LRP4 and LRP6 levels were manipulated through siRNA mediated knockdown. The levels of cyclin D1, a key downstream target of canonical WNT signaling and a cell cycle regulator, were then measured.

As anticipated, the results of the study demonstrated that *LRP6* knockdown led to a significant reduction in cyclin D1 levels in hTERT RPE-1 cells (Figure 19), consistent with previous findings in mouse embryos. Interestingly, the study also revealed a novel finding, that a reduction of LRP4 levels resulted in a significant increase in cyclin D1 levels above control levels in hTERT RPE1 cells. This was confirmed through both Western blotting experiments and immunofluorescence analysis, indicating a clear rescue of cyclin D1 levels by concomitant *LRP4; LRP6* double knockdown in comparison to *LRP6* single knockdown samples (Figure 19).

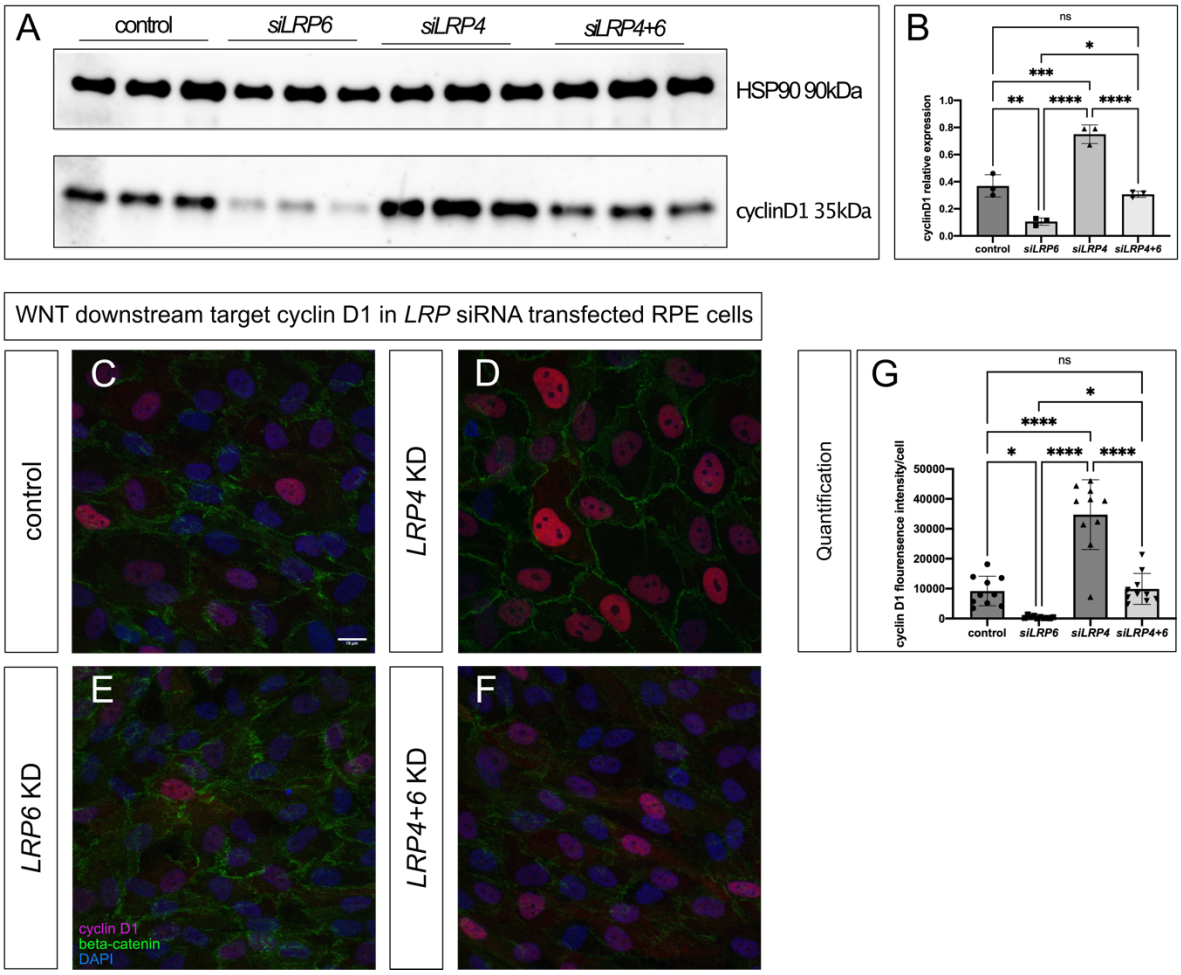


Figure 19: WNT signaling downstream target cyclin D1 expression in *LRP* siRNA treated RPE cells.

(A+B): Western blotting of cyclin D1 expression in *siLRP* treated hTERT RPE-1 cells and the quantification. When *Lrp4* was knocked down in hTERT RPE-1 cells, cyclin D1 protein levels increased (n=6). When *Lrp6* was downregulated, cyclin D1 levels significantly decreased. This effect, caused by loss of LRP6, was rescued by silencing LRP4. Cyclin D1 levels in hTERT RPE-1 cells treated with *LRP4* and *LRP6* siRNA were similar to that in control groups. Quantification was normalized with HSP90. P values based on One-way ANOVA. *p<0.05, **p<0.01, ***p≤ 0.001, ****p≤ 0.0001

(C-G): The immune staining on human RPE cells showed that when *LRP4* was reduced in RPE cells, cyclin D1 expression increased (B) compared to control (A). When *LRP6* was knocked down (C), cyclin D1 expression was markedly reduced. However, in *LRP4* and *LRP6* double knocked down cells (D), cyclin D1 expression was rescued. Beta-catenin labeled cell borders. Quantification was normalized with DAPI. P values based on One-way ANOVA. *p<0.05, ****p≤ 0.0001. Scale bar=15 µm

Interestingly, in five out of seven experiments, silencing of both LRP4 and LRP6 resulted in cyclin D1 levels that were even significantly higher in *LRP4* and *LRP6* siRNA treated cells compared to control siRNA treated cells (Figure 20). This can be observed not only in immunofluorescence experiments but also in Western blotting analyses (Figure 20).

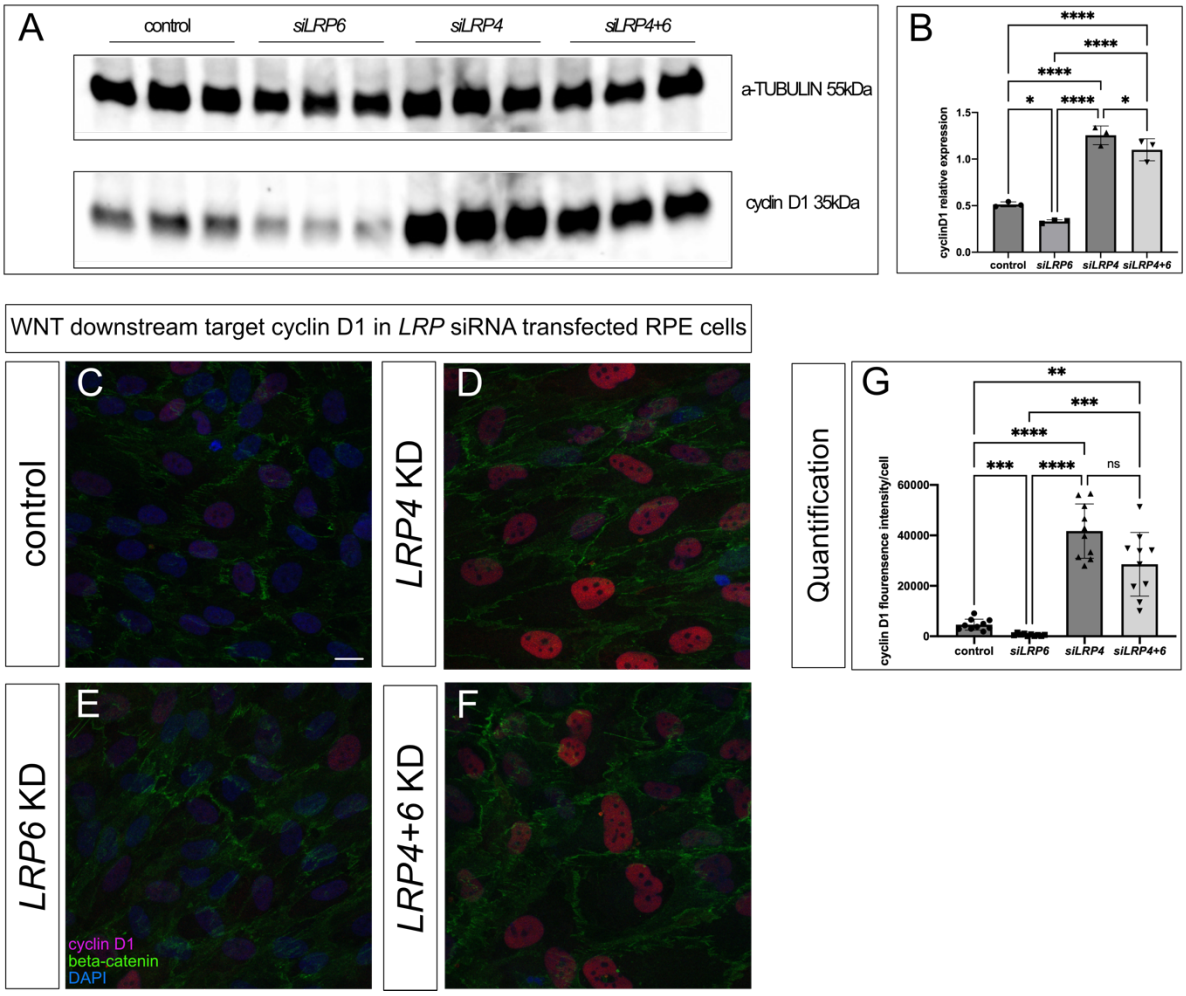


Figure 20: WNT signaling downstream target cyclin D1 expression in siRNA-treated hTERT RPE-1 cells.

(A+B): The Western blotting showed that when *LRP4* was knocked down in hTERT RPE-1 cells, cyclin D1 protein levels were increased (n=6). When *LRP6* was downregulated, cyclin D1 protein levels decreased significantly. However, in cells with downregulation of both, *LRP4* and *LRP6*, cyclin D1 protein levels were rescued and even significantly increased compared with controls. Quantification was normalized with a-Tubulin. P values based on Student's t-test. ***p≤ 0.001, ****p≤ 0.0001

(C-G): The ICC on RPE cell showed when *LRP4* was silenced in hTERT RPE-1 cells (D), signals for cyclin D1 increased compared with control (C). *LRP6* knockdown (E) resulted in decreased signals for

cyclin D1 comparing to control (C). However, in *LRP4* and *LRP6* silenced cells (F), cyclin D1 levels were not only rescued but also significantly increased compared to controls. beta-catenin labeled cell borders. (G) Quantification was normalized with DAPI. P values based on One-way ANOVA. *p<0.05, ****p≤ 0.0001. Scale bar=15 µm

To support the assumption that WNT signal transduction is impaired in *LRP6* downregulated cells and to provide further evidence that *LRP4; LRP6* double downregulation might display a divergent WNT target gene expression *in vitro*, I detected Ain2 in *LRP* siRNA treated cells. Among the various bona fide target genes of ß-catenin is Axin2, which is a component of the cytoplasmic destruction complex as well as the downstream target of WNT signaling pathway (Stolz et al., 2015). Axin2 protein levels were detected in hTERT RPE-1 cells treated with control and *LRP* siRNA by Western blotting analysis.

I found that when *LRP6* was knocked down, Axin2 protein levels were significantly reduced compared to controls. However, when *LRP4* was downregulated, there was no change in Axin2 expression compared to controls. Concomitant silencing of *LRP4* and *LRP6* resulted in Axin2 protein levels similar to controls, although there was a trend, the levels were not significantly increased compared to the levels in *LRP6* siRNA treated cells (Figure 21).

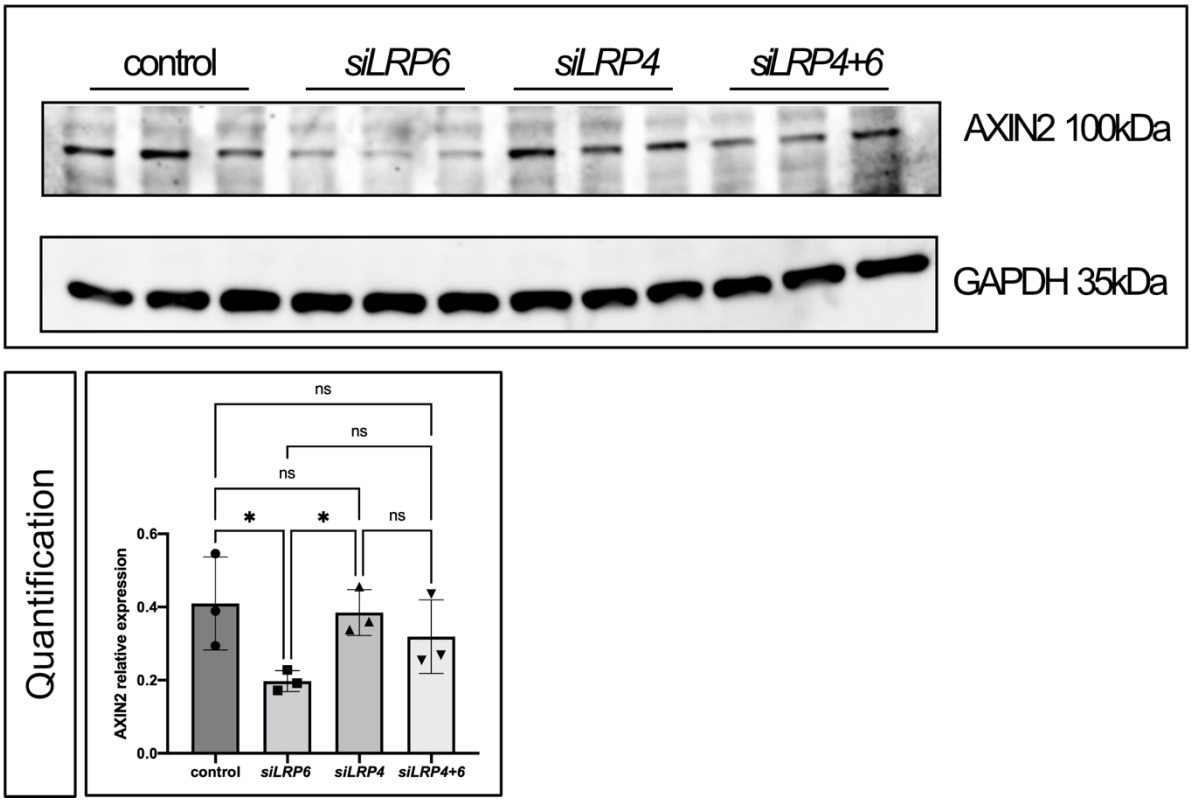


Figure 21: WNT signaling downstream target Axin2 protein levels in LRP downregulated hTERT RPE-1 cells.

When *LRP6* was knocked down in hTERT RPE-1 cells, Axin2 protein levels decreased compared to controls treated with scrambled siRNA (n=3). When *LRP4* was downregulated, there was no change of Axin2 protein levels. In *LRP4* and *LRP6* knockdown cells, Axin2 protein levels were similar to that in controls (n=3); However, Axin2 protein levels were not significantly higher than in *LRP6* single siRNA treated cells. Quantification was normalized with GAPDH. P values based on One-way ANOVA. *p<0.05.

In summary, I could draw the conclusion that down-regulation of LRP6 could also decrease WNT pathway signaling activity *in vitro*, whereas down regulation of *LRP4* could rescue the reduced WNT downstream activity caused by the silencing of *LRP6*.

The *in vitro* results suggested that loss of LRP4, as a WNT inhibitor, can cause a dramatic imbalance in WNT downstream signaling and lead to hyperproliferation, even in the absence of LRP6. From the present results, we conclude that in the absence of LRP4, the LRP5-FZD complex can compensate for the loss of LRP6 since the inhibitory impact by LRP4 is missing. Most importantly, these results confirm our findings in the animal model and suggested and the functional interaction of LRP4 and

LRP6 can modulate WNT signaling not only in mouse forebrain development but also *in vitro* in human cell lines.

**Conclusion**

In conclusion, my results showed that LRP4 is an inhibitor of the canonical WNT pathway and functionally interacts with LRP6 during early forebrain development. Loss of LRP4 can rescue the deficient WNT activity caused by loss of LRP6. LRP4 and LRP6 can not only balance WNT signaling during forebrain development but can also balance cell proliferation and WNT activity *in vitro* in human cells. The cooperation of LRP4- and LRP6-mediated function is essential for the delicate balance of WNT signaling.

## 5 Discussion

During forebrain development, the surface area of the mammalian neocortex undergoes a significant increase accompanied by a substantial increase in the number of projection neurons, which are essential for higher cognitive functions (Da Silva et al., 2021). The regulation of multiple early patterning events is mediated by WNT ligands, and specific WNT ligand expression occurs in distinct regions during brain development. For example, WNT-3a is expressed in discrete patterns in the developing forebrain. In E9.5 mouse embryo, WNT-3a is expressed at the dorsal midline of the neural tube (anterior segment, where the telencephalon is located and the neural tube has closed) and functions in controlling dorsolateral patterning (Harrison-Uy & Pleasure, 2012; Patapoutian & Reichardt, 2000).

Activation of WNT requires the interaction of FZD with its co-receptor LRP5/6, which can also bind with WNT ligands and activate canonical WNT pathway by inducing the degradation of Axin (Malaterre et al., 2007). LRP6 is involved in embryogenesis processes by mediating the biological activity of canonical WNT signaling; for example, LRP6 expression was detected in the developing lung and spinal cord tissues (Alrefaei & Abu-Elmagd, 2022). In addition to LRP6, LRP4 function is also required for the regulation of WNT signaling, which is important for normal limb and kidney development (Karner et al., 2010; Li et al., 2010).

However, unlike LRP6, previous work in the field suggests that LRP4 could be an inhibitor of the WNT pathway. Overexpression of *Lrp4* results in reduced WNT/β-catenin signaling activity *in vivo* (Karakatsani et al., 2017), suggesting that LRP4 may have a different effect on WNT signaling pathway compared with LRP5/6. Moreover, LRP4 also plays an important role in CNS development; downregulation of LRP4 in embryonic cortical neurons will reduce density of synapses and number of primary dendrites (Karakatsani et al., 2017). Intriguingly, as shown by the Lab of Rob Krumlauf, loss of LRP4 can partly rescue or compensate for developmental defects caused by loss of LRP6 (Ahn et al., 2013, 2017). These studies focused on mammary gland, tooth and limb development but there were hitherto no studies on the role of LRP4 in early forebrain development. Previous work in our lab has already confirmed that both *Lrp4* and *Lrp6* are expressed early on during forebrain development. The two LRP members are co-expressed in most of the neural progenitors (NPCs) within the developing forebrain from E9.5 onwards, indicating a potential interaction between

LRP4 and LRP6. Since WNT ligands are also expressed during forebrain development and localized at the dorsal part of neural tube, LRP4 and LRP6 could functionally interact and mediate early forebrain development by modulating WNT signaling pathway.

My data showed that LRP4 can act as a negative modulator of WNT signaling pathway counteracting the function of LRP5/6. Furthermore, I demonstrated that *Lrp4* is a genetic modifier for LRP6 loss-of-function phenotypes in forebrain development and in cell culture. In addition, in the absence of LRP4, the LRP5-FZD complex can compensate for the loss of LRP6 since the inhibitory impact by LRP4 is missing.

## 5.1 Loss of LRP4 can rescue the caudal truncation phenotype caused by loss of LRP6

It is widely known that LRP6 can mediate WNT signaling pathway. However, the potential modulation of the FZD-LRP5/6 receptor complex via WNT signaling by other LRP family members in the dorsolateral forebrain, such as LRP4, are not fully understood, especially in the context of forebrain development. To further explore the potential functional interaction between LRP4 and LRP6 during early forebrain development, single and double mutants of LRP4 and LRP6 were analyzed in mice.

Firstly, I confirmed that there was a decrease in the number of somites in *Lrp6*$^{-/-}$ compared to wild type, suggesting that LRP6 is required for proper axial elongation during embryonic development (Figure 9A). Besides, some *Lrp6* null embryos also showed an open cranial neural tube at E9.5 (Figure 8C+D), indicating neural tube defects (NTDs) - a group of defects that arise due to the improper closure of the neural tube during early neural development (Noelanders & Vleminckx, 2017). These findings suggest that LRP6 plays a critical role in the proper neural tube development. Consistent with these observations, previous work by Pinson and others has revealed the phenotype of *Lrp6* by loss-of-function in mice and they found that *Lrp6* null embryos displayed a decreased size in tailbud starting from at E8.5 onwards, as well as a reduction in somite number (Pinson et al., 2000). These phenotypes are likely to be caused by impaired WNT3a uptake as a consequences of LRP6 depletion, since WNT3a loss-of-function in mice also leads to a similar phenotype (Yoshikawa et al.,

1997). Therefore, it can be inferred that the loss of LRP6 may cause neural tube defects through the suppression of the WNT signaling pathway.

A previous study has reported that loss of LRP4 could rescue the teeth and limb defects caused by loss of LRP6 during development (Ahn et al., 2017). To investigate the potential interaction between LRP4 and LRP6 during early embryonic forebrain development, I generated *Lrp4*$^{-/-}$*; Lrp6*$^{-/-}$ double mouse embryos as the animal model. Surprisingly, when compared to the wild types, there was no obvious difference in *Lrp4*$^{-/-}$*; Lrp6*$^{-/-}$ embryos as well as *Lrp4*$^{-/-}$ embryos. The number of somites in *Lrp4*$^{-/-}$*; Lrp6*$^{-/-}$ embryos was similar to that in wild types. Consistently, the caudal truncation seen in *Lrp6*$^{-/-}$ embryos was either significantly milder or completely rescued in *Lrp4*$^{-/-}$*; Lrp6*$^{-/-}$ embryos, suggesting loss of LRP4 could rescue the improper axis elongation caused by loss of LRP6 in mouse embryos (Figure 9C).

Another phenotype observed in some *Lrp6* mutants is the occurrence of neural tube closure defects during anterior neural tube closure in E9.5 mouse embryos. This phenotype can be seen in in mice carrying either gain-of-function or loss-of-function mutations of *Lrp6* (Gray et al., 2010; Zhao et al., 2022). In contrast, no NTDs were observed in wild type or *Lrp4*$^{-/-}$ embryos. However, in some *Lrp4*$^{-/-}$*; Lrp6*$^{-/-}$ embryos, the open neural tube at the anterior forebrain was still present at the same frequency of approximately 30% as in *Lrp6*$^{-/-}$ single mutants, suggesting that loss of LRP4 on top of LRP6 is unable to rescue the neural tube closure defects (Figure 9E). These findings indicate that LRP4 and LRP6 may have distinct roles in forebrain development.

Recently, studies have demonstrated that LRP6 is not only necessary for canonical WNT signaling, but also associated with non-canonical WNT/planar cell polarity (WNT/PCP) signaling, which is critical in neural tube closure process (Nikolopoulou et al., 2017). WNT/PCP pathway was closely associated with severe neural tube defects in *Lrp6* hypermorphic mice, resulting in a partially or completely open cranial neural tube (Gray et al., 2013). Whereas, canonical WNT signaling pathway is important for neural tube closure processes through regulation of ß-catenin-TCF/LEF-dependent gene transcription, cell proliferation and apoptosis (Bilir et al., 2013). My data support the notion that interruption of LRP6 function, which is related to the non-canonical WNT/FZD-PCP pathway, can cause cranial NTDs in early developing forebrain. Notably, the absence of LRP4 in *Lrp6* null mutants cannot rescue this cranial NTDs, suggesting that LRP4 is not involved in WNT/PCP pathway modulation. Instead, loss

of LRP4 can only rescue neuroepithelial defects caused by loss of LRP6 via canonical WNT pathway.

Furthermore, we also detected the neuroepithelium thickness (NE) of different mutants at E9.5 embryo. Our results demonstrated that *Lrp6*$^{-/-}$ mutants exhibited a significantly thinner neuroepithelium compared to wild-type and *Lrp4*$^{-/-}$ mutants. Comparing to *Lrp6*$^{-/-}$ single mutants, *Lrp4*$^{-/-}$; *Lrp6*$^{-/-}$ double mutants showed a rescue of neuroepithelium thickness and had a neuroepithelial morphology comparable to wild types (Figure 10). This result indicated that LRP4 and LRP6 may participate in the neural progenitor cell proliferation during forebrain development via canonical WNT pathway, consistent with my hypothesis that loss of LRP4 could rescue the deficits that caused by loss of LRP6 during early forebrain development.

Despite these findings, the precise role of the interaction between LRP4/6 and canonical WNT signaling in neuroepithelial expansion and neural tube patterning, particularly during early embryonic development before the onset of neurogenesis, remains unclear. To address this, we next examined whether LRP4 modulates cell proliferation in *Lrp6*$^{-/-}$ mutants neural epithelium during forebrain development.

## 5.2 Loss of LRP4 can rescue the reduction of proliferation in the neuronal progenitor pool caused by loss of LRP6 function

Consequently, to determine whether the proliferation is also affected by loss of LRP4 and/or LRP6 function, I examined the proliferation rate using phospho-Histone H3 (pHH3) as a mitosis-specific marker at E9.5 in the forebrain. With immunostaining, I found that *Lrp6*$^{-/-}$ embryos have a significantly reduced rate of proliferating progenitor cells within the neuroepithelium of the developing forebrain (Figure 12C), consistent with the previous findings that there was a reduced rate of dividing neural tube cells in *Lrp6*$^{-/-}$ embryos compared to wild types (Gray et al., 2013).

At embryonic stages E9.5, the neural plate is composed of a single layer of neuroepithelial cells that form the neuroepithelium (Norden, 2017). The nuclear position determines the shape of neuroepithelial cell, varying from apical (during mitosis) to basal (during S-phase of the cell cycle) (Nikolopoulou et al., 2017). At E9.5 during the early forebrain development, in the wild type, immunostaining showed that the pHH3 positive nuclei are located at apical part of the neuroepithelial cells, whereas

in *Lrp6*$^{-/-}$ embryos, pHH3 signals could be detected at a more basal part of early neural tube. Furthermore, *Lrp6*$^{-/-}$ mice showed a significant decrease in the number of pHH3 positive cells compared to wild type, indicating impaired mitotic activity. The localization and number of pHH3 positive signals in *Lrp4*$^{-/-}$ embryos was comparable to wild types. Interestingly, there was a trend that *Lrp4*$^{-/-}$*; Lrp6*$^{-/-}$ double embryos showed a rescue of the number of pHH3 positive cells in forebrain comparing with *Lrp6*$^{-/-}$ mice and there was no aberrant localization of pHH3 signals in double mutants (Figure 13). These results suggest that LRP6, but not LRP4, is more crucial for promoting the proliferation of neural progenitor cells in the developing forebrain, and that LRP4 may play a modulatory role in this process.

Unfortunately, I did not have enough samples of *Lrp4; Lrp6* double mutants to include into pHH3 quantification. However, previous work from our lab has confirmed a reduced count of MPM-2 (mitotic cell marker) positive cells in *Lrp6*$^{-/-}$ embryonic forebrains at E9.5 compared. In addition, the rate of MPM-2 positive cells in *Lrp6*$^{-/-}$ embryos was rescued by genetic depletion of LRP4 function and mitotic activity in *Lrp4*$^{-/-}$*; Lrp6*$^{-/-}$ double mutants were similar to that in wild types. Previous research confirmed a thinner cortex in *Lrp6*$^{-/-}$ mice at late gestation (C. J. Zhou et al., 2006), supporting the hypothesis that loss of LRP6 causes a decrease in the number of proliferative neuronal progenitors.

Additionally, previous research demonstrated LRP4 is expressed in astrocytes and precursor cells and is required for NPCs proliferation (H. Zhang et al., 2019), indicating that LRP4 could influence progenitor proliferation. Furthermore, my findings indicate that genetic ablation of *Lrp4* partially rescued impaired neuroepithelial cell proliferation and forebrain hypoplasia in *Lrp6*$^{-/-}$ mutants, suggesting that loss of LRP4 function may counteract the negative effects of LRP6 deficiency on forebrain development through WNT signaling pathway.

To further validate the interaction of LRP4 and LRP5/6 with the WNT signaling pathway *in vitro* as a system overarching mechanism, I used human TERT RPE-1 cell line as a cell culture model. The canonical WNT/ß-catenin signaling is involved in human retinal pigment epithelium (RPE) development (Nadar et al., 2015), making hTERT RPE-1 cell line a suitable model for investigating the interaction of LRP4/6 with the WNT pathway. First, I confirmed expression of *LRP4* and *LRP6* in hTERT RPE-1 cell line, suggesting the LRP4/6 and WNT signaling could interact in hTERT RPE cells. Next, I established the knockdown model of LRP4 and LRP6 in the RPE cell line, using

*LRP4* and *LRP6* siRNA, respectively. With this cell line and knock down model, it allowed me to determine if the interaction between LRP4/6 and the WNT signaling pathway is not only relevant to murine embryonic development but also applicable to human cells.

To evaluate the impact of LRP4/6 knockdown on cell proliferation, I performed immunocytochemistry (ICC) on the cells treated with *LRP4* and *LRP6* siRNA. As observed in mouse model, the mitotic activity in hTERT RPE-1 cells was affected by *LRP4* and *LRP6* silencing, respectively. Immunostaining with pHH3 and MPM-2 both showed that when *LRP6* is knocked down, the count of proliferative cells is reduced compared to controls (Figure 17C, Figure 18C). However, when both *LRP4* and *LRP6* were both downregulated, the rate of proliferating cells was rescued when compared to *siLRP6* treated cells and was similar to that of controls (Figure 17D, Figure 18D). No obvious difference could be detected between *LRP4* siRNA treated cells and controls. This finding suggests that the effect of LRP4 ablation in ameliorating reduced mitosis in *Lrp6*$^{-/-}$ mutants was not restricted to the murine neuroepithelium but can be recapitulated in human cells.

Supporting my data, a pro-proliferative effect of LRP6 function in cells other than neuroepithelial cells was reported before. For instance, it was confirmed that up-regulation of LRP6 expression contributes to breast cancer tumorigenesis and down-regulation of LRP6 can inhibit breast cancer tumorigenesis (C. C. Liu et al., 2010). The evidence above shows that LRP6 plays a positive role in cell proliferation during development as well as *in vivo.*

Based on my findings on mice and cells, it could be inferred that interaction between LRP4 and LRP6 via WNT signaling, could also affect the early neural progenitor cells proliferation. Given the results of my study and the existing literature, I propose that the functional interaction between LRP4 and LRP6 may have relevance beyond forebrain development and is also relevant to human cells *in vitro*.

Overall, my results could demonstrate that LRP4 interaction with LRP6 is required to maintain the balance between proliferation and cell survival in the neuroepithelium of E9.5 embryos and human TERT RPE cells, suggesting LRP4/6 is important in maintaining the balance of proliferation and cell survival in various cell and tissue types.

### 5.3 Canonical WNT activity is suppressed by loss of LRP6 during forebrain development, whereas loss of LRP4 can rescue the reduced WNT signaling in *Lrp6*$^{-/-}$ embryos

To further investigate if the rescue in number of mitotic neuronal precursors is due to augmented canonical WNT signaling activity, I detected WNT activity by crossing *Lrp* mutants with the *TCF/Lef:H2B-GFP* reporter mouse line. This reporter line allows visualization of WNT responsiveness in cells that activate *TCF/Lef* gene expression. Immunostaining results revealed that GFP signal intensity was markedly reduced in *Lrp6*$^{-/-}$ mutants compared to wild types. Only few GFP-positive cells were observed within the dorsolateral forebrain neuroepithelium in *Lrp6*$^{-/-}$ mutants, regardless of whether anterior neural tube was open or closed at E9.5. In contrast, in *Lrp4*$^{-/-}$ mutants, GFP expression is significantly stronger than that in wild types, suggesting that LRP4 could be an inhibitor of the canonical WNT signaling pathway. Strikingly, the GFP expression in *Lrp4*$^{-/-}$*; Lrp6*$^{-/-}$ samples was rescued compared to *Lrp6*$^{-/-}$ mice and similar to that in wild types (Figure 14D, H), indicating a rescue of canonical WNT activity in *Lrp6*$^{-/-}$ mutants upon loss of LRP4.

Intriguingly, the Krumlauf lab has demonstrated that the limb and tooth defects can be partially rescued by reducing WNT co-receptor LRP5/6 or by inactivating β-catenin transduction (Ahn et al., 2013, 2017), strengthening our hypothesis that LRP4 could be an inhibitor of WNT pathway. Now my GFP staining data provides direct evidence that loss of LRP4 can rescue the reduced WNT signaling caused by loss of LRP6 during forebrain development, further supporting the idea that LRP4 could be a genetic modifier of LRP6 not only during limb development but also in early forebrain development. Moreover, previous research also indicated that LRP4 is important for control and modification of WNT signaling by effecting on LRP5/6 signaling in an antagonistic way (Li et al., 2010), providing additional evidence supporting this hypothesis.

Importantly, we found that depletion of LRP4 in *Lrp6*$^{-/-}$ mutants can rescue decreased WNT activity that ß-catenin-dependent gene transcription in embryos with closed and open neural tube at E9.5. This result suggests that LRP4 activity can significantly influence canonical WNT signaling in the forebrain neuroepithelium and thereby mitotic activity/proliferation of neuronal precursors, but not the morphogenesis of neural tube closure. Recent work demonstrated that enhanced LRP6 can be detected

in neurogenesis (Chow et al., 2021); besides, researches also confirmed that LRP4 plays a critical role CNS development (Gomez et al., 2014; Yan et al., 2020), strengthening the idea that the interaction of LRP4 and LRP6 via WNT signaling pathway plays an important part in stem cell activity and cell fate during early forebrain development.

In summary, the above findings demonstrate the crucial role of LRP4/6 in regulating WNT activity during early forebrain development. These results suggest that LRP4/6 modulation could potentially influence the proliferation and differentiation of neural progenitor cells, ultimately affecting the formation of the CNS.

### 5.4 LRP4 is a central modulator of the canonical WNT signaling pathway

To further support the idea that LRP4/6 modulate WNT downstream activity in the developing forebrain, I evaluated the expression level of cyclin D1 in E9.5 embryo forebrain via immunofluorescence. cyclin D1 is a key downstream target of WNT/β-catenin signaling, which is known to be activated by WNT downstream transcription factor LEF1 and is well-established as a central regulator of cellular proliferation (Lukaszewicza & Anderson, 2011; Qiu et al., 2014; Shtutman et al., 1999; Tetsu & McCormick, 1999). cyclin D1 is reported to be expressed in the ventrolateral region of the neural tube except for the dorsal midline in the developing telencephalon (Ortiz-Álvarez & Spassky, 2021; Santiago et al., 2017). In E9.5 *Lrp4*$^{-/-}$ embryos, cyclin D1 expression was identical as wild type controls. Interestingly, in contrast of *Lrp4*$^{-/-}$ embryos, *Lrp6*$^{-/-}$ mutant embryos showed markedly reduced levels of cyclin D1, which was partially rescued in the *Lrp4*$^{-/-}$*; Lrp6*$^{-/-}$ double mutant embryos (Figure 15D). Considering that cyclin D1 expression was mainly altered in the dorsal part of the forebrain in *Lrp4*$^{-/-}$; Lrp6$^{-/-}$ double mutant embryos, my results provide further evidence that LRP4/6 play an important role in regulating WNT signaling and its downstream targets in the developing forebrain.

To further investigate whether simultaneous downregulation of LRP4 and LRP6 would affect the downstream targets of WNT signaling pathway not only in early forebrain but also *in vitro*, I analyzed cyclin D1 expression in *LRP4/6* siRNA treated human hTERT RPE cells. Similar to the observation in mice, both immunofluorescence and Western blotting results showed that cyclin D1 expression was significantly decreased

in *LRP6* knockdown cells. Conversely, the expression of cyclin D1 in *LRP4* knockdown cells was significantly increased (Figure 19A, D), suggesting that in hTERT RPE-1 cells, unlike in the forebrain, downregulation of LRP4 can actually lead to an increase in cyclin D1 expression levels above control levels. Interestingly, when both *LRP4* and *LRP6* were downregulated, cyclin D1 expression was rescued (Figure 19F). Notably, in one Western blotting and immunostaining of cells, the cyclin D1 levels were elevated when both *LRP4* and *LRP6* were knocked down (Figure 20A, F). These results suggests that inhibition of LRP4 can activate WNT signaling pathway in a very effective way, indicating that there may be an unknown compensatory effect from LRP5.

Previous study has shown that overactive WNT signaling pathway induced by the β-catenin/LEF1 complex could lead to elevated cyclin D1 transcription, which is detected in various types of human cancer (Shtutman et al., 1999). Inhibition of ß-catenin will lead to a reduction in cyclin D1 expression and cell proliferation (Umazume et al., 2014). These findings are also consistent with my results of the downregulation of the proliferation markers pHH3 and MPM-2 in *siLRP6* treated cells, suggesting the suppression of LRP6 may affect the cell proliferation via canonical WNT signaling pathway.

The alteration of LRP4 caused by WNT activation could be partially rescued by decreasing the expression of WNT co-receptors *Lrp5* and *Lrp6*, or by suppressing of β-catenin expression in *in vitro* models (Ahn et al., 2013; S. P. Kim et al., 2019), supporting the hypothesis that LRP4 could act as an inhibitor of WNT pathway. Loss of LRP4, in the absence of LRP6, can cause a dramatic imbalance of WNT downstream targets expression. When LRP4 and LRP6 are both absent, LRP5, another important initiator of WNT signal transduction (Ren et al., 2021), can partially compensate the function of LRP6. The cell proliferation deficits during corticogenesis in *Lrp6* mutants are less severe in later gestation (C. J. Zhou et al., 2006), strengthening the idea of the partial compensation by LRP5 during early development. Supporting this hypothesis, the Western blotting revealed that when *LRP6* was downregulated, the expression of Axin2 in human RPE cells was also reduced (Figure 21). Axin2 is a direct target of canonical WNT signaling pathway and its inhibition can suppress over-proliferation of stem cells in mice (J. Gao et al., 2021). Therefore, my results suggest that LRP4 and LRP6 can affect progenitor cell proliferation via WNT signaling pathway. Additionally, my findings suggest that LRP4 is essential for

balancing the WNT signaling pathway by interacting with LRP6. Thus, LRP4 could be a genetic modifier of LRP6 via WNT signaling pathway.

Collectively, we found that in the absence of LRP4, the WNT signaling is activated due to the inhibitory impact by LRP4 is missing. Importantly, these results confirm our findings in the animal model.

### 5.5 Functional interaction between LRP4 and LRP6 is crucial for balancing WNT activity during early embryonic forebrain development

It is well-known that LRP5/6 are related to the canonical WNT pathway activation by preventing β-catenin degradation during central nervous system (Y. Huang et al., 2016). LRP4 has a different intracellular domain compared to LRP5/6 and is also considered to be a co-receptor for Wise and sclerostin (Sost), which are the WNT antagonists. The alteration of WNT signaling can be found in LRP4 mutants (Ahn et al., 2017; Li et al., 2010). Here, based on all evidence I have shown, LRP4 is an inhibitor of WNT pathway and functionally interacts with LRP6. The integration of LRP4 and LRP6 functions is critical for the delicate balance of the WNT signaling. For the first time, I confirmed the interaction between LRP4 and LRP6 in the developing forebrain. My data showed that (1) loss of LRP6 reduces the number of proliferating cells in the neural progenitor pool, which was rescued by ablation of LRP4; (2) loss of LRP4 alone can activate the WNT pathway; (3) the interaction of LRP4 and LRP6 in a human cell line.

In summary, the data on WNT reporter activity and analysis of WNT downstream targets in double *Lrp4*$^{-/-}$; *Lrp6*$^{-/-}$ mutants suggest that loss of LRP4 on an *Lrp6*$^{-/-}$ background can ameliorate impaired canonical WNT/ß-catenin/LEF pathway activation in the early mouse forebrain, supporting the hypothesis that LRP4 counteracts LRP6-mediated canonical WNT signaling and that *Lrp4* is a genetic modifier of proliferation phenotype caused by loss of LRP6. Furthermore, gene silencing experiments in a human RPE cell line could recapitulate the functional interaction of LRP4 and LRP6 in regulating mitotic activity. The results provide insight into the essential role of LRP4 in regulating mitotic activity and suggest that targeting LRP4 may be a potential therapeutic approach for diseases associated with aberrant canonical WNT and proliferative activities.

Taken together, I conclude that LRP4 acts as an inhibitor of the LRP-FZD receptor complex together with the WNT antagonists (Figure 22). Particularly, LRP5/6 binding

capacity for WNT is decreased by LRP4, which consequently modulates and balances WNT downstream target expression. When LRP4 is absent, WNT antagonists can still bind to the LRP5/6-FZD receptor complex (at least to a certain extent) so the expression of WNT downstream targets is either stronger or not affected. When LRP6 function is lost, LRP5 cannot fully compensate the function of binding with WNT3a, resulting in decrease of WNT target gene expression. In addition, LRP4 inhibition in interplay with WNT antagonist can still act on the LRP5-FZD complex. Therefore, WNT signal transduction is markedly reduced. When LRP4 and LRP6 are both absent, LRP4 can no longer inhibit WNT LRP5/6-FZD complex, thus the WNT antagonists cannot bind to LRP5-complex without LRP4. Consequently, LRP5 can still bind with WNT3a to activate WNT downstream targets. Therefore, WNT downstream targets are expressed to a higher extent compared to the LRP6 loss-of-function situation.

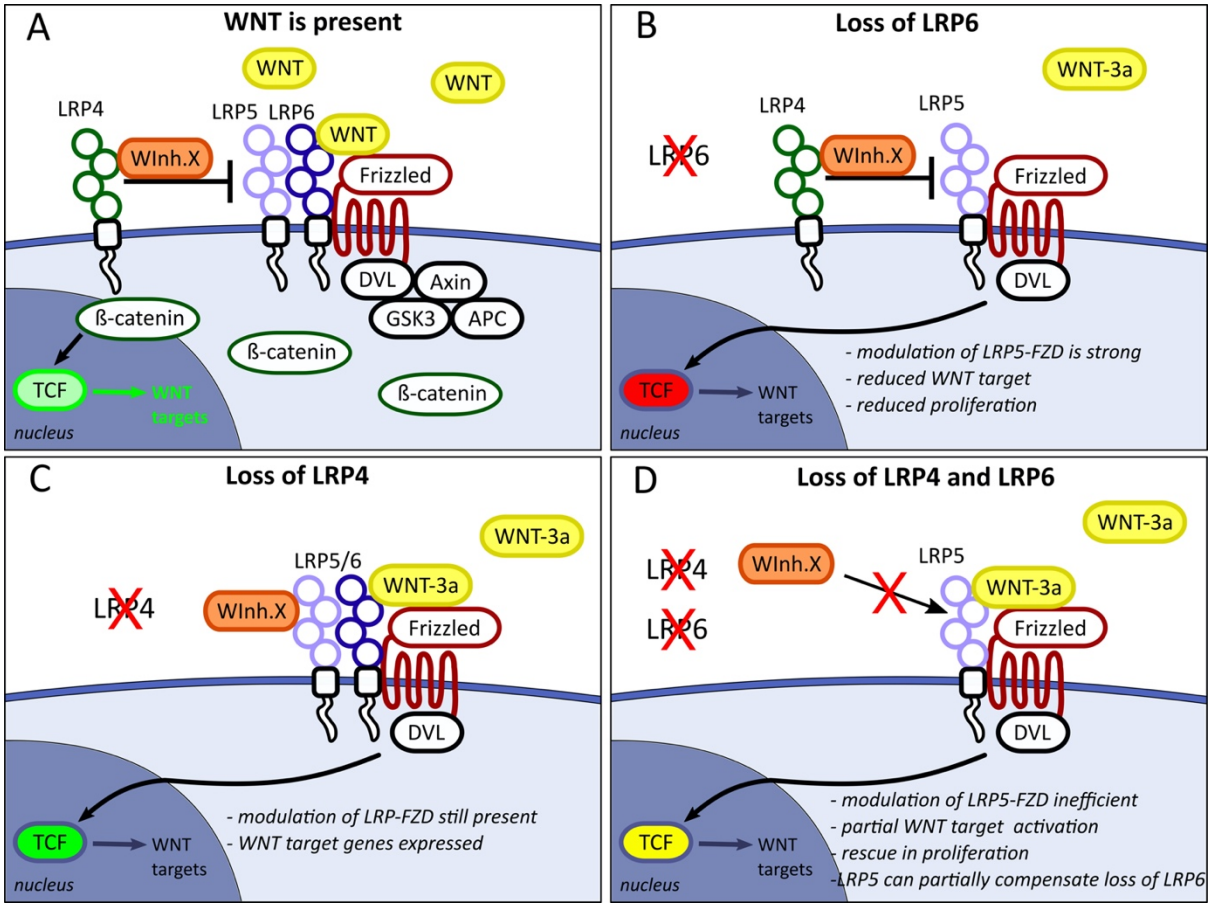


Figure 22: Hypothetical model of interaction between LRP4 and LEP5/6 via canonical WNT signaling pathway.

The co-operation between the WNT antagonist (for example: Wise and Dkk1) and LRP4 acts as an inhibitory on the LRP-FZD receptor complex. LRP5/6 binding capacity for WNT factors is decreased, which consequently modulates WNT downstream target expression.

**In absence of LRP4**, the WNT inhibitor X can still bind to the LRP-FZD receptor complex (at least to a certain extent) but cannot inhibit LRP5/6 at full function, so that expression of WNT downstream targets is not affected. It is why *Lrp4* single mutants show higher and partially ectopic WNT signaling in the neural tube.

**In absence of LRP6,** LRP4 inhibition in interplay with WNT inhibiting factor X acts on the LRP5-FZD complex and LRP5 cannot fully compensate the function of LRP6 and binding of WNT3a is impaired which result in a great reduction of WNT target gene expression, WNT signal transduction is markedly reduced.

**In absence of both LRP4 and LRP6:** LRP4 can no longer act as the co-operator of WNT inhibitor X binding to the LRP-FZD complex and WNT inhibitor X is too weak to have an inhibiting effect on binding of WNT3a. LRP5 can compensate for loss of LRP6 only in the absence of LRP4.Therefore, WNT downstream targets are expressed to a higher extent compared to LRP6 loss-of-function situation.

## 6. Outlook and future perspectives

From the present results we conclude that in the absence of LRP4, the LRP5-FZD complex can compensate for the loss of LRP6 since the inhibitory impact by LRP4 is missing. Most importantly, these results confirm our findings in the animal model. However, due to the limited number of *Lrp4; Lrp6* double mutants, some experiments cannot be performed, such as the SOX2 immunostaining on cryo sections. It is already published that LRP4 plays a key role in neuromuscular synapses formation and maintenance (Gomez et al., 2014). Therefore, neuron marker TUJ1 and proliferation marker BrdU could be also used to compare if loss of LRP4/6 would cause the difference of neuron development in forebrain. To provide more evidence, more WNT downstream targets could be detected in developing forebrain, such as LEF1, Gsk3 and Axin2, as well as in cell culture.

We can also assume that LRP5 can compensate for LRP6 function in the absence of LRP4 in further approaches and whether the effect is mediated by ß-catenin. To test the levels of activated and inactive ß-catenin we can further apply phospho-ß-catenin and unphosphorylated ß-catenin (active / inactivation form of ß-catenin) specific antibodies. To further confirm our hypotheses that LRP4 might interact with WNT antagonists and modulate LRP6 to balance WNT signaling, Dkk1 and Wise could be tested in *siLRP* treated RPE cells. Overexpression of LRP4 and LRP6 could be taken to deliver further evidence that LRP4 is an inhibitor of WNT pathway.

Dysregulation of WNT/β-catenin transcription is associated with CNS diseases, such as autism spectrum disorders (ASD) and Alzheimer's disease (Caracci et al., 2021; Palomer et al., 2019). The abnormal activity of WNT and its downstream targets is also found in different kind of cancers and knee osteoarthritis. More knowledge about WNT activity and how it is balanced will help with human health. My research revealed how LRP4 can balance WNT by modulating LRP6 function during forebrain development. However, to fully understand the mechanism how LRP4 modulates the LRP-FZD complex through WNT transduction during forebrain development, further experiments are required

## References

Acebron, S. P., & Niehrs, C. (2016). β-Catenin-Independent Roles of Wnt/LRP6 Signaling. *Trends in Cell Biology*, *26*(12), 956–967. https://doi.org/10.1016/j.tcb.2016.07.009

Ahn, Y., Sanderson, B. W., Klein, O. D., & Krumlauf, R. (2010). Inhibition of Wnt signaling by wise (Sostdc1) and negative feedback from Shh controls tooth number and patterning. *Development*, *137*(19), 3221–3231. https://doi.org/10.1242/dev.054668

Ahn, Y., Sims, C., Logue, J. M., Weatherbee, S. D., & Krumlauf, R. (2013). Lrp4 and Wise interplay controls the formation and patterning of mammary and other skin appendage placodes by modulating Wnt signaling. *Development (Cambridge)*, *140*(3), 583–593. https://doi.org/10.1242/dev.085118

Ahn, Y., Sims, C., Murray, M. J., Kuhlmann, P. K., Fuentes-Antrás, J., Weatherbee, S. D., & Krumlauf, R. (2017). Multiple modes of Lrp4 function in modulation of Wnt/β-catenin signaling during tooth development. *Development (Cambridge)*, *144*(15), 2824–2836. https://doi.org/10.1242/dev.150680

Akiri, G., Cherian, M. M., Vijayakumar, S., Liu, G., Bafico, A., & Aaronson, S. A. (2009). Wnt pathway aberrations including autocrine Wnt activation occur at high frequency in human non-small-cell lung carcinoma. *Oncogene*, *28*(21), 2163–2172. https://doi.org/10.1038/onc.2009.82

Albrecht, L. V., Tejeda-Muñoz, N., & De Robertis, E. M. (2021). Cell Biology of Canonical Wnt Signaling. *Annual Review of Cell and Developmental Biology*, *37*, 369–389. https://doi.org/10.1146/annurev-cellbio-120319-023657

Alrefaei, A. F., & Abu-Elmagd, M. (2022). LRP6 Receptor Plays Essential Functions in Development and Human Diseases. *Genes*, *13*(1). https://doi.org/10.3390/genes13010120

Avilés, E. C., & Stoeckli, E. T. (2016). Canonical wnt signaling is required for commissural axon guidance. *Developmental Neurobiology*, *76*(2), 190–208. https://doi.org/10.1002/dneu.22307

Bae, S. M., & Hong, J. Y. (2018). The wnt signaling pathway and related therapeutic drugs in autism spectrum disorder. *Clinical Psychopharmacology and Neuroscience*, *16*(2), 129–135. https://doi.org/10.9758/cpn.2018.16.2.129

Bengoa-Vergniory, N., Gorroño-Etxebarria, I., López-Sánchez, I., Marra, M., Di Chiaro, P., & Kypta, R. (2017). Identification of Noncanonical Wnt Receptors Required for Wnt-3a-Induced Early Differentiation of Human Neural Stem Cells. *Molecular Neurobiology*, *54*(8), 6213–6224. https://doi.org/10.1007/s12035-016-0151-5

Bilir, B., Kucuk, O., & Moreno, C. S. (2013). Wnt signaling blockage inhibits cell proliferation and migration, and induces apoptosis in triple-negative breast cancer cells. *Journal of Translational Medicine*, *11*(1), 1–12. https://doi.org/10.1186/1479-5876-11-280

Brady, M. V., & Vaccarino, F. M. (2021). Role of shh in patterning human pluripotent cells towards ventral forebrain fates. *Cells*, *10*(4). https://doi.org/10.3390/cells10040914

Caracci, M. O., Avila, M. E., Espinoza-Cavieres, F. A., López, H. R., Ugarte, G. D., & De Ferrari, G. V. (2021). Wnt/β-Catenin-Dependent Transcription in Autism Spectrum Disorders. *Frontiers in Molecular Neuroscience*, *14*(November), 1–16. https://doi.org/10.3389/fnmol.2021.764756

Chow, H. M., Sun, J. K. L., Hart, R. P., Cheng, K. K. Y., Hung, C. H. L., Lau, T. M., & Kwan, K. M. (2021). Low-Density Lipoprotein Receptor-Related Protein 6 Cell Surface Availability Regulates Fuel Metabolism in Astrocytes. In *Advanced Science* (Vol. 8, Issue 16). https://doi.org/10.1002/advs.202004993

Clevers, H. (2006). Wnt/β-Catenin Signaling in Development and Disease. *Cell*, *127*(3), 469–480. https://doi.org/10.1016/j.cell.2006.10.018

Clevers, H., & Nusse, R. (2012). Wnt/β-catenin signaling and disease. *Cell*, *149*(6), 1192–1205. https://doi.org/10.1016/j.cell.2012.05.012

Copp, A. J., & Greene, N. D. E. (2013). Neural tube defects-disorders of neurulation and related embryonic processes. *Wiley Interdisciplinary Reviews: Developmental Biology*, *2*(2), 213–227. https://doi.org/10.1002/wdev.71

Da Silva, F., Zhang, K., Pinson, A., Fatti, E., Wilsch-Bräuninger, M., Herbst, J., Vidal, V., Schedl, A., Huttner, W. B., & Niehrs, C. (2021). Mitotic WNT signalling orchestrates neurogenesis in the developing neocortex. *The EMBO Journal*, *40*(19), 1–23. https://doi.org/10.15252/embj.2021108041

de Almeida, G. C., Oliveira, L. F. S., Predes, D., Fokoue, H. H., Kuster, R. M., Oliveira, F. L., Mendes, F. A., & Abreu, J. G. (2020). Piperine suppresses the Wnt/β-catenin pathway and has anti-cancer effects on colorectal cancer cells. *Scientific Reports*, *10*(1), 1–12. https://doi.org/10.1038/s41598-020-68574-2

Dennis, D., Picketts, D., Slack, R. S., & Schuurmans, C. (2016). Forebrain neurogenesis: From embryo to adult. *Trends in Developmental Biology*, *9*(1), 77–90. http://www.ncbi.nlm.nih.gov/pubmed/28367004%0Ahttp://www.pubmedcentral.nih.gov/articlerender.fcgi?artid=PMC5373848

Depew, A. T., & Mosca, T. J. (2021). Conservation and innovation: Versatile roles for lrp4 in nervous system development. *Journal of Developmental Biology*, *9*(1). https://doi.org/10.3390/jdb9010009

*EMBO Reports - 2015 - Stolz - Wnt‐mediated protein stabilization ensures proper mitotic microtubule assembly and chromosome.pdf*. (n.d.).

Emons, G., Spitzner, M., Reineke, S., Möller, J., Auslander, N., Kramer, F., Hu, Y., Beissbarth, T., Wolff, H. A., Rave-Fränk, M., Heßmann, E., Gaedcke, J., Ghadimi, B. M., Johnsen, S. A., Ried, T., & Grade, M. (2017). Chemoradiotherapy resistance in colorectal cancer cells is mediated by Wnt/β-catenin signaling. *Molecular Cancer Research*, *15*(11), 1481–1490. https://doi.org/10.1158/1541-7786.MCR-17-0205

Falk, S., Wurdak, H., Ittner, L. M., Ille, F., Sumara, G., Schmid, M. T., Draganova, K.,

Lang, K. S., Paratore, C., Leveen, P., Suter, U., Karlsson, S., Born, W., Ricci, R., Götz, M., & Sommer, L. (2008). Brain Area-Specific Effect of TGF-β Signaling on Wnt-Dependent Neural Stem Cell Expansion. *Cell Stem Cell*, *2*(5), 472–483. https://doi.org/10.1016/j.stem.2008.03.006

Fernández-Torres, J., Zamudio-Cuevas, Y., López-Reyes, A., Garrido-Rodríguez, D., Martínez-Flores, K., Lozada, C. A., Muñóz-Valle, J. F., Oregon-Romero, E., & Martínez-Nava, G. A. (2018). Gene–gene interactions of the Wnt/β-catenin signaling pathway in knee osteoarthritis. *Molecular Biology Reports*, *45*(5), 1089–1098. https://doi.org/10.1007/s11033-018-4260-2

Ferrer-Vaquer, A., Piliszek, A., Tian, G., Aho, R. J., Dufort, D., & Hadjantonakis, A. K. (2010). A sensitive and bright single-cell resolution live imaging reporter of Wnt/-catenin signaling in the mouse. *BMC Developmental Biology*, *10*. https://doi.org/10.1186/1471-213X-10-121

Gao, C., Xiao, G., & Hu, J. (2014a). Gao_Regulation of Wntβcatenin signaling by modification_2014_cellbioscsience.pdf. *Cell & Bioscience*, 1–20.

Gao, C., Xiao, G., & Hu, J. (2014b). Regulation of Wnt/β-catenin signaling by posttranslational modifications. *Cell and Bioscience*, *4*(1), 1–20. https://doi.org/10.1186/2045-3701-4-13

Gao, J., Liao, Y., Qiu, M., & Shen, W. (2021). Wnt/β-Catenin Signaling in Neural Stem Cell Homeostasis and Neurological Diseases. *Neuroscientist*, *27*(1), 58–72. https://doi.org/10.1177/1073858420914509

Geng, S., Paul, F., Kowalczyk, I., Raimundo, S., Sporbert, A., Mamo, T. M., & Hammes, A. (2023). *Balancing WNT signalling in early forebrain development : The role of LRP4 as a modulator of LRP6 function*. *April*, 1–21. https://doi.org/10.3389/fcell.2023.1173688

Gomez, A. M., Froemke, R. C., & Burden, S. J. (2014). Synaptic plasticity and cognitive function are disrupted in the absence of Lrp4. *ELife*, *3*(November), 1–16. https://doi.org/10.7554/eLife.04287

Graham, V., Khudyakov, J., Ellis, P., & Pevny, L. (2003). SOX2 functions to maintain neural progenitor identity. *Neuron*, *39*(5), 749–765. https://doi.org/10.1016/S0896-6273(03)00497-5

Gray, J. D., Kholmanskikh, S., Castaldo, B. S., Hansler, A., Chung, H., Klotz, B., Singh, S., Brown, A. M. C., & Ross, M. E. (2013). LRP6 exerts non-canonical effects on Wnt signaling during neural tube closure. *Human Molecular Genetics*, *22*(21), 4267–4281. https://doi.org/10.1093/hmg/ddt277

Gray, J. D., Nakouzi, G., Slowinska-Castaldo, B., Dazard, J. E., Rao, J. S., Nadeau, J. H., & Elizabeth Ross, M. (2010). Functional interactions between the LRP6 WNT co-receptor and folate supplementation. *Human Molecular Genetics*, *19*(23), 4560–4572. https://doi.org/10.1093/hmg/ddq384

Greco, T. L., Takada, S., Newhouse, M. M., McMahon, J. A., McMahon, A. P., & Camper, S. A. (1996). Analysis of the vestigial tail mutation demonstrates that Wnt-3a gene dosage regulates mouse axial development. *Genes and Development*, *10*(3), 313–324. https://doi.org/10.1101/gad.10.3.313

Guo, R., & Xing, Q. S. (2022). Roles of Wnt Signaling Pathway and ROR2 Receptor in Embryonic Development: An Update Review Article. *Epigenetics Insights*, *15*. https://doi.org/10.1177/25168657211064232

Harrison-Uy, S. J., & Pleasure, S. J. (2012). Wnt signaling and forebrain development. *Cold Spring Harbor Perspectives in Biology*, *4*(7), 1–11. https://doi.org/10.1101/cshperspect.a008094

Hayat, R., Manzoor, M., & Hussain, A. (2022). Wnt signaling pathway: A comprehensive review. *Cell Biology International*, *46*(6), 863–877. https://doi.org/10.1002/cbin.11797

Ho, K. S., & Scott, M. P. (2002). Sonic hedgehog in the nervous system: Functions, modifications and mechanisms. *Current Opinion in Neurobiology*, *12*(1), 57–63. https://doi.org/10.1016/S0959-4388(02)00290-8

Houschyar, K. S., Tapking, C., Borrelli, M. R., Popp, D., Duscher, D., Maan, Z. N., Chelliah, M. P., Li, J., Harati, K., Wallner, C., Rein, S., Pförringer, D., Reumuth, G., Grieb, G., Mouraret, S., Dadras, M., Wagner, J. M., Cha, J. Y., Siemers, F., … Behr, B. (2019). Wnt Pathway in Bone Repair and Regeneration – What Do We Know So Far. *Frontiers in Cell and Developmental Biology*, *6*(January), 1–13. https://doi.org/10.3389/fcell.2018.00170

Huang, M., Xiao, X., Ji, G., & Wu, Q. (2022). Histone modifications in neurodifferentiation of embryonic stem cells. *Heliyon*, *8*(1), e08664. https://doi.org/10.1016/j.heliyon.2021.e08664

Huang, Y., Zhang, Q., Song, N. N., Zhang, L., Sun, Y. L., Hu, L., Chen, J. Y., Zhu, W., Li, J., & Ding, Y. Q. (2016). Lrp5/6 are required for cerebellar development and for suppressing TH expression in Purkinje cells via β-catenin. *Molecular Brain*, *9*(1), 1–13. https://doi.org/10.1186/s13041-015-0183-1

Jho, E., Zhang, T., Domon, C., Joo, C.-K., Freund, J.-N., & Costantini, F. (2002). Wnt/β-Catenin/Tcf Signaling Induces the Transcription of Axin2, a Negative Regulator of the Signaling Pathway. *Molecular and Cellular Biology*, *22*(4), 1172–1183. https://doi.org/10.1128/mcb.22.4.1172-1183.2002

Jia, L., Piña-Crespo, J., & Li, Y. (2019). Restoring Wnt/β-catenin signaling is a promising therapeutic strategy for Alzheimer's disease. In *Molecular Brain* (Vol. 12, Issue 1). https://doi.org/10.1186/s13041-019-0525-5

Jin, P., Qi, D., Cui, Y., Lenahan, C., Deng, S., & Tao, X. (2022). Activation of LRP6 with HLY78 Attenuates Oxidative Stress and Neuronal Apoptosis via GSK3 β /Sirt1/PGC-1 α Pathway after ICH. *Oxidative Medicine and Cellular Longevity*, *2022*. https://doi.org/10.1155/2022/7542468

Jing, H., Chen, P., Hui, T., Yu, Z., Zhou, J., Fei, E., Wang, S., Ren, D., Lai, X., & Li, B. (2021). Synapse-specific Lrp4 mRNA enrichment requires Lrp4/MuSK signaling, muscle activity and Wnt non-canonical pathway. *Cell and Bioscience*, *11*(1), 1–15. https://doi.org/10.1186/s13578-021-00619-z

Joiner, D. M., Ke, J., Zhong, Z., Xu, H. E., & Williams, B. O. (2013). LRP5 and LRP6 in development and disease. *Trends in Endocrinology and Metabolism*, *24*(1), 31–39. https://doi.org/10.1016/j.tem.2012.10.003

Kalkman, H. O. (2012). A review of the evidence for the canonical Wnt pathway in autism spectrum disorders. *Molecular Autism*, *3*(1), 1. https://doi.org/10.1186/2040-2392-3-10

Karakatsani, A., Marichal, N., Urban, S., Kalamakis, G., Ghanem, A., Schick, A., Zhang, Y., Conzelmann, K. K., Rüegg, M. A., Berninger, B., de Almodovar, C. R., Gascoón, S., & Kröger, S. (2017). Neuronal LRP4 regulates synapse formation in the developing CNS. *Development (Cambridge)*, *144*(24), 4604–4615. https://doi.org/10.1242/dev.150110

Karner, C. M., Dietrich, M. F., Johnson, E. B., Kappesser, N., Tennert, C., Percin, F., Wollnik, B., Carroll, T. J., & Herz, J. (2010). Lrp4 regulates initiation of ureteric budding and is crucial for kidney formation - a mouse model for cenani-lenz syndrome. *PLoS ONE*, *5*(4). https://doi.org/10.1371/journal.pone.0010418

Kim, H. J., Schleiffarth, J. R., Jessurun, J., Sumanas, S., Petryk, A., Lin, S., & Ekker, S. C. (2005). Wnt5 signaling in vertebrate pancreas development. *BMC Biology*, *3*, 1–21. https://doi.org/10.1186/1741-7007-3-23

Kim, S. P., Da, H., Li, Z., Kushwaha, P., Beil, C., Mei, L., Xiong, W. C., Wolfgang, M. J., Clemens, T. L., & Riddle, R. C. (2019). Lrp4 expression by adipocytes and osteoblasts differentially impacts sclerostin's endocrine effects on body composition and glucose metabolism. *Journal of Biological Chemistry*, *294*(17), 6899–6911. https://doi.org/10.1074/jbc.RA118.006769

Kosodo, Y., & Huttner, W. B. (2009). Basal process and cell divisions of neural progenitors in the developing brain. *Development Growth and Differentiation*, *51*(3), 251–261. https://doi.org/10.1111/j.1440-169X.2009.01101.x

Kucukefe, Y., & Kaypmaz, A. (2009). Delayed feedback control as applied to active suspension of a ground vehicle. *Ieee Eurocon 2009, Eurocon 2009*, 916–921. https://doi.org/10.1109/EURCON.2009.5167743

Kuznetsova, A. V., Kurinov, A. M., & Aleksandrova, M. A. (2014). Cell Models to Study Regulation of Cell Transformation in Pathologies of Retinal Pigment Epithelium. *Journal of Ophthalmology*, *2014*. https://doi.org/10.1155/2014/801787

Kwan, V., Unda, B. K., & Singh, K. K. (2016). Wnt signaling networks in autism spectrum disorder and intellectual disability. *Journal of Neurodevelopmental Disorders*, *8*(1), 1–10. https://doi.org/10.1186/s11689-016-9176-3

Lee, B., Song, H., Rizzoti, K., Son, Y., Yoon, J., Baek, K., & Jeong, Y. (2013). Genomic code for Sox2 binding uncovers its regulatory role in Six3 activation in the forebrain. *Developmental Biology*, *381*(2), 491–501. https://doi.org/10.1016/j.ydbio.2013.06.016

Lee, J. E., Wu, S. F., Goering, L. M., & Dorsky, R. I. (2006). Canonical Wnt signaling through Lef1 is required for hypothalamic neurogenesis. *Development*, *133*(22), 4451–4461. https://doi.org/10.1242/dev.02613

Li, Y., Pawlik, B., Elcioglu, N., Aglan, M., Kayserili, H., Yigit, G., Percin, F., Goodman, F., Nürnberg, G., Cenani, A., Urquhart, J., Chung, B. D., Ismail, S., Amr, K., Aslanger, A. D., Becker, C., Netzer, C., Scambler, P., Eyaid, W., … Wollnik, B. (2010). LRP4 Mutations Alter Wnt/β-Catenin Signaling and Cause

Limb and Kidney Malformations in Cenani-Lenz Syndrome. *American Journal of Human Genetics*, *86*(5), 696–706. https://doi.org/10.1016/j.ajhg.2010.03.004

Lian, G., Chenn, A., Ekuta, V., Kanaujia, S., & Sheen, V. (2019). Formin 2 Regulates Lysosomal Degradation of Wnt-Associated β-Catenin in Neural Progenitors. *Cerebral Cortex*, *29*(5), 1938–1952. https://doi.org/10.1093/cercor/bhy073

Liu, C. C., Prior, J., Piwnica-Worms, D., & Bu, G. (2010). LRP6 overexpression defines a class of breast cancer subtype and is a target for therapy. *Proceedings of the National Academy of Sciences of the United States of America*, *107*(11), 5136–5141. https://doi.org/10.1073/pnas.0911220107

Liu, Chengcheng, Yao, M., & Hogue, C. W. (2011). Near-membrane ensemble elongation in the proline-rich LRP6 intracellular domain may explain the mysterious initiation of the Wnt signaling pathway. *10th International Conference on Bioinformatics - 1st ISCB Asia Joint Conference 2011, InCoB 2011/ISCB-Asia 2011: Bioinformatics - Proceedings from Asia Pacific Bioinformatics Network (APBioNet)*, *12*(SUPPL. 13).

Liu, Chunming, Kato, Y., Zhang, Z., Do, V. M., Yankner, B. A., & He, X. (1999). β-Trcp couples β-catenin phosphorylation-degradation and regulates Xenopus axis formation. *Proceedings of the National Academy of Sciences of the United States of America*, *96*(11), 6273–6278. https://doi.org/10.1073/pnas.96.11.6273

Liu, Z., Kuna, V. K., Xu, B., & Sumitran-Holgersson, S. (2021). Wnt ligands 3a and 5a regulate proliferation and migration in human fetal liver progenitor cells. *Translational Gastroenterology and Hepatology*, *6*, 1–11. https://doi.org/10.21037/tgh.2020.01.12

Loh, N. Y., Neville, M. J., Marinou, K., Hardcastle, S. A., Fielding, B. A., Duncan, E. L., McCarthy, M. I., Tobias, J. H., Gregson, C. L., Karpe, F., & Christodoulides, C. (2015). LRP5 regulates human body fat distribution by modulating adipose progenitor biology in a dose- and depot-specific fashion. *Cell Metabolism*, *21*(2), 262–273. https://doi.org/10.1016/j.cmet.2015.01.009

Lukaszewicza, A. I., & Anderson, D. J. (2011). Cyclin D1 promotes neurogenesis in the developing spinal cord in a cell cycle-independent manner. *Proceedings of the National Academy of Sciences of the United States of America*, *108*(28), 11632–11637. https://doi.org/10.1073/pnas.1106230108

Lustig, B., Jerchow, B., Sachs, M., Weiler, S., Pietsch, T., Rarsten, U., Van De Wetering, M., Clevers, H., Schlag, P. M., Birchmeier, W., & Behrens, J. (2001). Negative feedback loop of Wnt signaling through upregulation of conductin/axin2 in colorectal and liver tumors. *Langenbeck's Archives of Surgery*, *386*(6), 466. https://doi.org/10.1128/mcb.22.4.1184-1193.2002

MacDonald, B. T., Tamai, K., & He, X. (2009). Wnt/β-Catenin Signaling: Components, Mechanisms, and Diseases. *Developmental Cell*, *17*(1), 9–26. https://doi.org/10.1016/j.devcel.2009.06.016

Machon, O., Van Den Bout, C. J., Backman, M., Kemler, R., & Krauss, S. (2003). Role of β-catenin in the developing cortical and hippocampal neuroepithelium. *Neuroscience*, *122*(1), 129–143. https://doi.org/10.1016/S0306-4522(03)00519-0

Makoto, I., Lee, S. M. K., Johnson, J. E., Mc Mahon, A. P., & Takada, S. (1997). Wnt signalling required for expansion of neural crest and cns progenitors. *Nature*, *389*(6654), 966–970. https://doi.org/10.1038/40146

Malaterre, J., Ramsay, R. G., & Mantamadiotis, T. (2007). Differentiation and Transcription Laboratory, Peter MacCallum Cancer Centre, St. Andrews Place, East Melbourne, 3002, VIC, Australia. *East*, 492–506.

Mao, J., McKean, D. M., Warrier, S., Corbin, J. G., Niswander, L., & Zohn, I. E. (2010). The iron exporter ferroportin 1 is essential for development of the mouse embryo, forebrain patterning and neural tube closure. *Development*, *137*(18), 3079–3088. https://doi.org/10.1242/dev.048744

Marchini, M., Hu, D., Lo Vercio, L., Young, N. M., Forkert, N. D., Hallgrímsson, B., & Marcucio, R. (2021). Wnt Signaling Drives Correlated Changes in Facial Morphology and Brain Shape. *Frontiers in Cell and Developmental Biology*, *9*(March), 1–16. https://doi.org/10.3389/fcell.2021.644099

Marzo, A., Galli, S., Lopes, D., McLeod, F., Podpolny, M., Segovia-Roldan, M., Ciani, L., Purro, S., Cacucci, F., Gibb, A., & Salinas, P. C. (2016). Reversal of Synapse Degeneration by Restoring Wnt Signaling in the Adult Hippocampus. *Current Biology*, *26*(19), 2551–2561. https://doi.org/10.1016/j.cub.2016.07.024

Mecklenburg, N., Kowalczyk, I., Witte, F., Görne, J., Laier, A., Mamo, T. M., Gonschior, H., Lehmann, M., Richter, M., Sporbert, A., Purfürst, B., Hübner, N., & Hammes, A. (2021). Identification of disease-relevant modulators of the SHH pathway in the developing brain. *Development (Cambridge)*, *148*(17), 1–17. https://doi.org/10.1242/DEV.199307

Mehta, S., Hingole, S., & Chaudhary, V. (2021). The Emerging Mechanisms of Wnt Secretion and Signaling in Development. *Frontiers in Cell and Developmental Biology*, *9*(August), 1–17. https://doi.org/10.3389/fcell.2021.714746

Molina, A., & Pituello, F. (2017). Playing with the cell cycle to build the spinal cord. *Developmental Biology*, *432*(1), 14–23. https://doi.org/10.1016/j.ydbio.2016.12.022

Nadar, V. P., Buchholz, D. E., Lowenstein, S. E., Clegg, D. O., & Clegg, D. O. (2015). Canonical/β-catenin wnt pathway activation improves retinal pigmented epithelium derivation from human embryonic stem cells. *Investigative Ophthalmology and Visual Science*, *56*(2), 1002–1013. https://doi.org/10.1167/iovs.14-15835

Narcisi, R., Cleary, M. A., Brama, P. A. J., Hoogduijn, M. J., Tüysüz, N., Ten Berge, D., & Van Osch, G. J. V. M. (2015). Long-term expansion, enhanced chondrogenic potential, and suppression of endochondral ossification of adult human MSCs via WNT signaling modulation. *Stem Cell Reports*, *4*(3), 459–472. https://doi.org/10.1016/j.stemcr.2015.01.017

Newmire, D., & Willoughby, D. (2015). Wnt and β-Catenin Signaling and Skeletal Muscle Myogenesis in Response to Muscle Damage and Resistance Exercise and Training. *International Journal of Kinesiology and Sports Science*, *3*(4), 39–50. https://doi.org/10.7575/aiac.ijkss.v.3n.4p.40

Nguyen, D. X., Chiang, A. C., Zhang, X. H. F., Kim, J. Y., Kris, M. G., Ladanyi, M.,

Gerald, W. L., & Massagué, J. (2009). WNT/TCF Signaling through LEF1 and HOXB9 Mediates Lung Adenocarcinoma Metastasis. *Cell*, *138*(1), 51–62. https://doi.org/10.1016/j.cell.2009.04.030

Nielsen, P. S., Riber-Hansen, R., Jensen, T. O., Schmidt, H., & Steiniche, T. (2013). Proliferation indices of phosphohistone H3 and Ki67: Strong prognostic markers in a consecutive cohort with stage I/II melanoma. *Modern Pathology*, *26*(3), 404–413. https://doi.org/10.1038/modpathol.2012.188

Nikolopoulou, E., Galea, G. L., Rolo, A., Greene, N. D. E., & Copp, A. J. (2017). Neural tube closure: Cellular, molecular and biomechanical mechanisms. *Development (Cambridge)*, *144*(4), 552–566. https://doi.org/10.1242/dev.145904

Noelanders, R., & Vleminckx, K. (2017). How Wnt Signaling Builds the Brain: Bridging Development and Disease. *Neuroscientist*, *23*(3), 314–329. https://doi.org/10.1177/1073858416667270

Norden, C. (2017). Pseudostratified epithelia - cell biology, diversity and roles in organ formation at a glance. *Journal of Cell Science*, *130*(11), 1859–1863. https://doi.org/10.1242/jcs.192997

Ohazama, A., Porntaveetus, T., Ota, M. S., Herz, J., & Sharpe, P. T. (2010). Lrp4: A novel modulator of extracellular signaling in craniofacial organogenesis. *American Journal of Medical Genetics, Part A*, *152 A*(12), 2974–2983. https://doi.org/10.1002/ajmg.a.33372

Ohkawara, B., Ito, M., & Ohno, K. (2021). Secreted signaling molecules at the neuromuscular junction in physiology and pathology. *International Journal of Molecular Sciences*, *22*(5), 1–16. https://doi.org/10.3390/ijms22052455

Ortiz-Álvarez, G., & Spassky, N. (2021). One progenitor to generate them all: new evidence for multi-fated neural progenitors. *Current Opinion in Neurobiology*, *66*, 186–194. https://doi.org/10.1016/j.conb.2020.10.013

Pacheco-Pinedo, E. C., Durham, A. C., Stewart, K. M., Goss, A. M., Lu, M. M., DeMayo, F. J., & Morrisey, E. E. (2011). Wnt/β-catenin signaling accelerates mouse lung tumorigenesis by imposing an embryonic distal progenitor phenotype on lung epithelium. *Journal of Clinical Investigation*, *121*(5), 1935–1945. https://doi.org/10.1172/JCI44871

Pai, V. P., Lemire, J. M., Chen, Y., Lin, G., & Levin, M. (2015). Local and long-range endogenous resting potential gradients antagonistically regulate apoptosis and proliferation in the embryonic cns. *International Journal of Developmental Biology*, *59*(7–9), 327–340. https://doi.org/10.1387/ijdb.150197ml

Palomer, E., Buechler, J., & Salinas, P. C. (2019). Wnt signaling deregulation in the aging and Alzheimer's brain. *Frontiers in Cellular Neuroscience*, *13*(May), 1–8. https://doi.org/10.3389/fncel.2019.00227

Patapoutian, A., & Reichardt, L. F. (2000). Roles of Wnt proteins in neural development and maintenance. *Current Opinion in Neurobiology*, *10*(3), 392–399. https://doi.org/10.1016/S0959-4388(00)00100-8

Pinson, K. I., Brennan, J., Monkley, S., Avery, B. J., & Skarnes, W. C. (2000). An

LDL-receptor-related protein mediates Wnt signalling in mice. *Nature*, *407*(6803), 535–538. https://doi.org/10.1038/35035124

Pohlkamp, T., Durakoglugil, M., Lane-Donovan, C., Xian, X., Johnson, E. B., Hammer, R. E., & Herz, J. (2015). Lrp4 domains differentially regulate limb/brain development and synaptic plasticity. *PLoS ONE*, *10*(2), 1–11. https://doi.org/10.1371/journal.pone.0116701

Qiu, C., Xie, Q., Zhang, D., Chen, Q., Hu, J., & Xu, L. (2014). GM-CSF induces cyclin D1 expression and proliferation of endothelial progenitor cells via PI3K and MAPK signaling. *Cellular Physiology and Biochemistry*, *33*(3), 784–795. https://doi.org/10.1159/000358652

Rattner, A., Wang, Y., & Nathans, J. (2022). *Signaling Pathways in Neurovascular Development*.

Ren, Q., Chen, J., & Liu, Y. (2021). LRP5 and LRP6 in Wnt Signaling: Similarity and Divergence. *Frontiers in Cell and Developmental Biology*, *9*(May), 1–11. https://doi.org/10.3389/fcell.2021.670960

Rifes, P., Isaksson, M., Rathore, G. S., Aldrin-Kirk, P., Møller, O. K., Barzaghi, G., Lee, J., Egerod, K. L., Rausch, D. M., Parmar, M., Pers, T. H., Laurell, T., & Kirkeby, A. (2020). Modeling neural tube development by differentiation of human embryonic stem cells in a microfluidic WNT gradient. *Nature Biotechnology*, *38*(11), 1265–1273. https://doi.org/10.1038/s41587-020-0525-0

Russell, W. L., Kelly, E. M., Hunsicker, P. R., Bangham, J. W., Maddux, S. C., & Phipps, E. L. (1979). Specific-locus test shows ethylnitrosourea to be the most potent mutagen in the mouse (gene mutation/spermatogonia/alkylating agent/temporary sterility). *Genetics*, *76*(11), 5818–5819.

Sadler, T. W. (2005). Embryology of neural tube development. *American Journal of Medical Genetics - Seminars in Medical Genetics*, *135 C*(1), 2–8. https://doi.org/10.1002/ajmg.c.30049

Santiago, L., Daniels, G., Wang, D., Deng, F. M., & Lee, P. (2017). Wnt signaling pathway protein LEF1 in cancer, as a biomarker for prognosis and a target for treatment. *American Journal of Cancer Research*, *7*(6), 1389–1406.

Sawakami, K., Robling, A. G., Ai, M., Pitner, N. D., Liu, D., Warden, S. J., Li, J., Maye, P., Rowe, D. W., Duncan, R. L., Warman, M. L., & Turner, C. H. (2006). The Wnt co-receptor LRP5 is essential for skeletal mechanotransduction but not for the anabolic bone response to parathyroid hormone treatment. *Journal of Biological Chemistry*, *281*(33), 23698–23711. https://doi.org/10.1074/jbc.M601000200

Shtutman, M., Zhurinsky, J., Simcha, I., Albanese, C., D'Amico, M., Pestell, R., & Ben-Ze'ev, A. (1999). The cyclin D1 gene is a target of the β-catenin/LEF-1 pathway. *Proceedings of the National Academy of Sciences of the United States of America*, *96*(10), 5522–5527. https://doi.org/10.1073/pnas.96.10.5522

Song, L., Li, Y., Wang, K., Wang, Y. Z., Molotkov, A., Gao, L., Zhao, T., Yamagami, T., Wang, Y., Gan, Q., Pleasure, D. E., & Zhou, C. J. (2009). Lrp6-mediated canonical Wnt signaling is required for lip formation and fusion. *Development*, *136*(18), 3161–3171. https://doi.org/10.1242/dev.037440

Sonnen, K. F., & Janda, C. Y. (2021). Signalling dynamics in embryonic development. *Biochemical Journal*, *478*(23), 4045–4070. https://doi.org/10.1042/BCJ20210043

Teo, S., & Salinas, P. C. (2021). Wnt-Frizzled Signaling Regulates Activity-Mediated Synapse Formation. *Frontiers in Molecular Neuroscience*, *14*(June), 1–9. https://doi.org/10.3389/fnmol.2021.683035

Tetsu, O., & McCormick, F. (1999). Beta-Catenin regulates expression of cyclinD1 in colon carcinomacells Osamu. *Nature*, *398*(April), 422.

Umazume, K., Tsukahara, R., Liu, L., Fernandez De Castro, J. P., McDonald, K., Kaplan, H. J., & Tamiya, S. (2014). Role of retinal pigment epithelial cell β-catenin signaling in experimental proliferative vitreoretinopathy. *American Journal of Pathology*, *184*(5), 1419–1428. https://doi.org/10.1016/j.ajpath.2014.01.022

Walker, L. J., Roque, R. A., Navarro, M. F., & Granato, M. (2021). Agrin/Lrp4 signal constrains MuSK-dependent neuromuscular synapse development in appendicular muscle. *Development (Cambridge)*, *148*(21). https://doi.org/10.1242/dev.199790

Wang, M., Marco, P. de, Capra, V., & Kibar, Z. (2019). Update on the Role of the Non-Canonical Wnt/Planar Cell Polarity Pathway in Neural Tube Defects. *Cells*, *8*(10), 1–21. https://doi.org/10.3390/cells8101198

Weatherbee, S. D., Anderson, K. V., & Niswander, L. A. (2006). LDL-receptor-related protein 4 is crucial for formation of the neuromuscular junction. *Development*, *133*(24), 4993–5000. https://doi.org/10.1242/dev.02696

Wei, W., Lu, Q., Chaudry, G. J., Leppla, S. H., & Cohen, S. N. (2006). The LDL Receptor-Related Protein LRP6 Mediates Internalization and Lethality of Anthrax Toxin. *Cell*, *124*(6), 1141–1154. https://doi.org/10.1016/j.cell.2005.12.045

Widelitz, R. (2005). Wnt signaling through canonical and non-canonical pathways: Recent progress. *Growth Factors*, *23*(2), 111–116. https://doi.org/10.1080/08977190500125746

Willnow, T. E., Christ, A., & Hammes, A. (2012). Endocytic receptor-mediated control of morphogen signaling. *Development (Cambridge)*, *139*(23), 4311–4319. https://doi.org/10.1242/dev.084467

Willnow, T. E., Hammes, A., & Eaton, S. (2007). Lipoproteins and their receptors in embryonic development: More than cholesterol clearance. *Development*, *134*(18), 3239–3249. https://doi.org/10.1242/dev.004408

Wilson, S. W., & Houart, C. (2004). Early steps in the development of the forebrain. *Developmental Cell*, *6*(2), 167–181. https://doi.org/10.1016/S1534-5807(04)00027-9

Wilson, S. W., & Houart, C. (2009). *Early Steps in the Development of the Forebrain The Structure, Origins, and Morphogenesis of the Forebrain*. *6*(2), 167–181.

*Wnt stabilization of β-catenin reveals principles for morphogen.pdf*. (n.d.).

*Wntβ-catenin signalling function.pdf*. (n.d.).

Wodarz, A., & Huttner, W. B. (2003). Asymmetric cell division during neurogenesis in Drosophila and vertebrates. *Mechanisms of Development*, *120*(11), 1297–1309. https://doi.org/10.1016/j.mod.2003.06.003

Wu, Y., Zhou, L., Liu, H., Duan, R., Zhou, H., Zhang, F., He, X., Lu, D., Xiong, K., Xiong, M., Zhuang, J., Liu, Y., Li, L., Liang, D., & Chen, Y. H. (2021). LRP6 downregulation promotes cardiomyocyte proliferation and heart regeneration. *Cell Research*, *31*(4), 450–462. https://doi.org/10.1038/s41422-020-00411-7

Xing, L., Wilsch-Bräuninger, M., & Huttner, W. B. (2021). How neural stem cells contribute to neocortex development. *Biochemical Society Transactions*, *49*(5), 1997–2006. https://doi.org/10.1042/BST20200923

Yan, M., Guo, A., Chen, P., Jing, H., Ren, D., Zhong, Y., Wu, Y., Fei, E., Lai, X., Zou, S., & Wang, S. (2020). LRP4 LDLα repeats of astrocyte enhance dendrite arborization of the neuron. *Molecular Brain*, *13*(1), 1–12. https://doi.org/10.1186/s13041-020-00708-z

Yang, S.-L., Yang, M., Herrlinger, S., Liang, C., Lai, F., Chen, J.-F., & Author, D. B. (2015). MiR-302/367 regulate neural progenitor proliferation, differentiation, and survival in neurulation HHS Public Access Author manuscript. *Dev Biol*, *408*(1), 140–150. https://doi.org/10.1016/j.ydbio.2015.09.020.MiR-302/367

Yang, T., & Williams, B. O. (2017). Low-density lipoprotein receptor-related proteins in skeletal development and disease. *Physiological Reviews*, *97*(3), 1211–1288. https://doi.org/10.1152/physrev.00013.2016

Yoshikawa, Y., Fujimori, T., McMahon, A. P., & Takada, S. (1997). Evidence that absence of Wnt-3a signaling promotes neuralization instead of paraxial mesoderm development in the mouse. *Developmental Biology*, *183*(2), 234–242. https://doi.org/10.1006/dbio.1997.8502

You, L., He, B., Xu, Z., Uematsu, K., Mazieres, J., Mikami, I., Reguart, N., Moody, T. W., Kitajewski, J., McCormick, F., & Jablons, D. M. (2004). Inhibition of Wnt-2-mediated signaling induces programmed cell death in non-small-cell lung cancer cells. *Oncogene*, *23*(36), 6170–6174. https://doi.org/10.1038/sj.onc.1207844

Yu, F., Yu, C., Li, F., Zuo, Y., Wang, Y., Yao, L., Wu, C., Wang, C., & Ye, L. (2021). Wnt/β-catenin signaling in cancers and targeted therapies. *Signal Transduction and Targeted Therapy*, *6*(1), 1–24. https://doi.org/10.1038/s41392-021-00701-5

Zappone, M. V., Galli, R., Catena, R., Meani, N., De Biasi, S., Mattei, E., Tiveron, C., Vescovi, A. L., Lovell-Badge, R., Ottolenghi, S., & Nicolis, S. K. (2000). Sox2 regulatory sequences direct expression of a β-geo transgene to telencephalic neural stem cells and precursors of the mouse embryo, revealing regionalization of gene expression in CNS stem cells. *Development*, *127*(11), 2367–2382. https://doi.org/10.1242/dev.127.11.2367

Zhang, B., Luo, S., Wang, Q., Suzuki, T., Xiong, W. C., & Mei, L. (2008). LRP4 Serves as a Coreceptor of Agrin. *Neuron*, *60*(2), 285–297. https://doi.org/10.1016/j.neuron.2008.10.006

Zhang, H., Sathyamurthy, A., Liu, F., Li, L., Zhang, L., Dong, Z., Cui, W., Sun, X.,

Zhao, K., Wang, H., Ho, H. Y. H., Xiong, W. C., & Mei, L. (2019). Agrin-Lrp4-Ror2 signaling regulates adult hippocampal neurogenesis in mice. *ELife*, *8*, 1–24. https://doi.org/10.7554/eLife.45303

Zhao, T., McMahon, M., Reynolds, K., Saha, S. K., Stokes, A., & Zhou, C. J. (2022). The role of Lrp6-mediated Wnt/β-catenin signaling in the development and intervention of spinal neural tube defects in mice. *DMM Disease Models and Mechanisms*, *15*(6). https://doi.org/10.1242/dmm.049517

Zhou, C. J., Borello, U., Rubenstein, J. L. R., & Pleasure, S. J. (2006). Neuronal production and precursor proliferation defects in the neocortex of mice with loss of function in the canonical Wnt signaling pathway. *Neuroscience*, *142*(4), 1119–1131. https://doi.org/10.1016/j.neuroscience.2006.07.007

Zhou, Cheng Ji, Pinson, K. I., & Pleasure, S. J. (2004). Severe defects in dorsal thalamic development in low-density lipoprotein receptor-related protein-6 mutants. *Journal of Neuroscience*, *24*(35), 7632–7639. https://doi.org/10.1523/JNEUROSCI.2123-04.2004

Zong, Y., Zhang, B., Gu, S., Lee, K., Zhou, J., Yao, G., Figueiredo, D., Perry, K., Mei, L., & Jin, R. (2012). *Structural basis of agrin – LRP4 – MuSK signaling*. *1*, 247–258. https://doi.org/10.1101/gad.180885.111.synapse

## Appendix

### 1. List of tables

## 2. List of figures